



# Seamless Navigation in Indoor and Outdoor based on 3D Spaces

**Author:**

Yan, Jinjin

**Publication Date:**

2020

**DOI:**

<https://doi.org/10.26190/unsworks/22210>

**License:**

<https://creativecommons.org/licenses/by-nc-nd/3.0/au/>

Link to license to see what you are allowed to do with this resource.

Downloaded from <http://hdl.handle.net/1959.4/70456> in <https://unsworks.unsw.edu.au> on 2024-04-29

# Seamless Navigation in Indoor and Outdoor based on 3D Spaces

Jinjin YAN

A thesis submitted in fulfillment of the requirements for the degree of  
**Doctor of Philosophy**



Geospatial Research Innovation Development (GRID)

Faculty of Built Environment

November 6, 2020



Australia's  
Global  
University

# Thesis/Dissertation Sheet

Surname/Family Name	: Yan
Given Name/s	: Jinjin
Abbreviation for degree as give in the University calendar	: Doctor of Philosophy (PHD)
Faculty	: Faculty of Built Environment
School	: Built Environment
Thesis Title	: Seamless Navigation in Indoor and Outdoor based on 3D Spaces

**Abstract 350 words maximum: (PLEASE TYPE)**

Contemporary living environments are getting more and more complex, combining structures in indoor and outdoor. These structures can be broadly subdivided into entirely bounded (indoor), partially bounded (semi-bounded), and unbounded (outdoor). Normally, agents (e.g., pedestrians) wish to have seamless navigation when seamlessly transferring from one kind of environment to another and back. Seamless here means human operations or interventions are not required when transitions happen between different navigation modes and environments.

In the past decades, seamless navigation has attracted a lot of attention and many approaches have been reported in the literature or made available as commercial applications. Most of them rely on integrating indoor navigation networks to outdoor road/street-based networks via specific structures (e.g., anchor node). Yet, navigation paths from such approaches are not seamless, which can be partly explained by the fact that navigation networks in indoor and outdoor used for integration are currently built differently; due to semi-bounded spaces have unclear definitions thus such spaces are often omitted from navigation maps.

Therefore, this thesis developed new theories, models, and approaches to support seamless navigation in all kinds of environments, which include a novel generic space definition framework, a unified 3D space-based navigation model, approaches for automatically reconstructing 3D spaces, and two new path options (MTC-path and NSI-path). This research brings in four contributions to seamless navigation: (i) living environments (spaces) are systematically categorised and defined as indoor (I-space), semi-indoor (sl-space), semi-outdoor (sO-space), and outdoor (O-space); (ii) all types of spaces are uniformly modelled and managed as 3D spaces, thereby sharing the same approaches for deriving navigation networks; (iii) sl-spaces and sO-spaces are included in navigation maps, which allows developing new path options based on them; and (iv) on the basis of 3D spaces, vertical constraints are considered in navigation path planning.

**Declaration relating to disposition of project thesis/dissertation**

I hereby grant to the University of New South Wales or its agents a non-exclusive licence to archive and to make available (including to members of the public) my thesis or dissertation in whole or in part in the University libraries in all forms of media, now or here after known. I acknowledge that I retain all intellectual property rights which subsist in my thesis or dissertation, such as copyright and patent rights, subject to applicable law. I also retain the right to use all or part of my thesis or dissertation in future works (such as articles or books).

.....  
Signature

.....  
Date

The University recognises that there may be exceptional circumstances requiring restrictions on copying or conditions on use. Requests for restriction for a period of up to 2 years can be made when submitting the final copies of your thesis to the UNSW Library. Requests for a longer period of restriction may be considered in exceptional circumstances and require the approval of the Dean of Graduate Research.

## Originality Statement

I hereby declare that this submission is my own work and to the best of my knowledge it contains no materials previously published or written by another person, or substantial proportions of material which have been accepted for the award of any other degree or diploma at UNSW or any other educational institution, except where due acknowledgement is made in the thesis. Any contribution made to the research by others, with whom I have worked at UNSW or elsewhere, is explicitly acknowledged in the thesis. I also declare that the intellectual content of this thesis is the product of my own work, except to the extent that assistance from others in the project's design and conception or in style, presentation and linguistic expression is acknowledged.'

Signed .....

Date .....

**COPYRIGHT STATEMENT**

'I hereby grant the University of New South Wales or its agents a non-exclusive licence to archive and to make available (including to members of the public) my thesis or dissertation in whole or part in the University libraries in all forms of media, now or here after known. I acknowledge that I retain all intellectual property rights which subsist in my thesis or dissertation, such as copyright and patent rights, subject to applicable law. I also retain the right to use all or part of my thesis or dissertation in future works (such as articles or books).'

'For any substantial portions of copyright material used in this thesis, written permission for use has been obtained, or the copyright material is removed from the final public version of the thesis.'

Signed .....

Date .....

**AUTHENTICITY STATEMENT**

'I certify that the Library deposit digital copy is a direct equivalent of the final officially approved version of my thesis.'

Signed .....

Date .....

## INCLUSION OF PUBLICATIONS STATEMENT

UNSW is supportive of candidates publishing their research results during their candidature as detailed in the UNSW Thesis Examination Procedure.

**Publications can be used in their thesis in lieu of a Chapter if:**

- The candidate contributed greater than 50% of the content in the publication and is the “primary author”, ie. the candidate was responsible primarily for the planning, execution and preparation of the work for publication
- The candidate has approval to include the publication in their thesis in lieu of a Chapter from their supervisor and Postgraduate Coordinator.
- The publication is not subject to any obligations or contractual agreements with a third party that would constrain its inclusion in the thesis

Please indicate whether this thesis contains published material or not:

This thesis contains no publications, either published or submitted for publication  
*(if this box is checked, you may delete all the material on page 2)*

Some of the work described in this thesis has been published and it has been documented in the relevant Chapters with acknowledgement  
*(if this box is checked, you may delete all the material on page 2)*

This thesis has publications (either published or submitted for publication) incorporated into it in lieu of a chapter and the details are presented below

**CANDIDATE'S DECLARATION**

I declare that:

- I have complied with the UNSW Thesis Examination Procedure
- where I have used a publication in lieu of a Chapter, the listed publication(s) below meet(s) the requirements to be included in the thesis.

Candidate's Name	Signature	Date (dd/mm/yy)

*"Life was like a box of chocolates, you never know what you're gonna get."*

Forrest Gump

*"If everything was perfect, you would never learn and you would never grow."*

Beyonce Knowles



THE UNIVERSITY OF NEW SOUTH WALES

## *Abstract*

Faculty of Built Environment

Doctor of Philosophy

### **Seamless Navigation in Indoor and Outdoor based on 3D Spaces**

by Jinjin YAN

Contemporary living environments are getting more and more complex, combining structures in indoor and outdoor. These structures can be broadly subdivided into entirely bounded (indoor), partially bounded (semi-bounded), and unbounded (outdoor). Normally, agents (e.g., pedestrians) wish to have seamless navigation when seamlessly transferring from one kind of environment to another and back. Seamless here means human operations or interventions are not required when transitions happen between different navigation modes and environments.

In the past decades, seamless navigation has attracted a lot of attention and many approaches have been reported in the literature or made available as commercial applications. Most of them rely on integrating indoor navigation networks to outdoor road/street-based networks via specific structures (e.g., anchor node). Yet, navigation paths from such approaches are not seamless, which can be partly explained by the fact that navigation networks in indoor and outdoor used for integration are currently built differently; due to semi-bounded spaces have unclear definitions thus such spaces are often omitted from navigation maps.

Therefore, this thesis developed new theories, models, and approaches to support seamless navigation in all kinds of environments, which include a novel generic space definition framework, a unified 3D space-based navigation model, approaches for automatically reconstructing 3D spaces, and two new path options (MTC-path and NSI-path). This research brings in four contributions to seamless navigation: (i) living environments (spaces) are systematically categorised and defined as indoor (I-space), semi-indoor (sI-space), semi-outdoor (sO-space), and outdoor (O-space); (ii) all types of spaces are uniformly modelled and managed as 3D spaces, thereby sharing the same approaches for deriving navigation networks; (iii) sI-spaces and sO-spaces are included in navigation maps, which allows developing new path options based on them; and (iv) on the basis of 3D spaces, vertical constraints are considered in navigation path planning.



## Acknowledgements

My PhD research journey is coming to the end. At this moment, there are many feelings up-well in my mind. First of all, I gratefully acknowledge the *China Scholarship Council* (CSC) for funding this PhD project (No. 201606410054). The picture of my PhD life can be described by a classical line from *Forrest Gump*, “Life was like a box of chocolates, you never know what you’re gonna get”.

I started this journey in the *3D Geoinformation in Delft University of Technology* (TU Delft). During the first year, I suffered a lot from English, new-built family, new culture, and new research mode. In details, the first time to express everything in English, to learn to live with my wife (during that period, she was my girlfriend), to adapt to Dutch styles, as well as to carry out research in a brand new mode (which is entirely different from Master’s life). When I finally got used to everything and had a four-year research plan, a new and vital issue found me. Stay in Delft or move to Sydney. After all-round considerations, I decided to transfer to *University of New South Wales* (UNSW) in Sydney. With this decision, the most important stuff became transferring my CSC scholarship from the Netherlands to Australia. Unfortunately, I got thousands of “negative” replies from the staffs who were working on the transfer stuffs. With the help of my friends and staffs from the China embassy, I finally addressed all the transfer-related issues. Before successfully moving to *Geospatial Research Innovation and Development* (GRID) in UNSW, I fought with the visa application around one hundred days.

Fortunately, as the old saying that “*If everything was perfect, you would never learn and you would never grow.*”, because of those tough issues, I gained a lot, not only the knowledge and skills but also friendships. Eventually, everything became smooth after arriving in Sydney. It has been three and half years, I am really grateful to all the people who helped me during the whole journey, including my supervisors, GRID family members, colleagues, my wife, parents, and friends.

It is super lucky for me to have Prof. Sisi Zlatanova and Dr. Abdoulaye Diakité as my supervisors. I still remember the first email from Sisi five years ago, in which she said “You are a lucky boy!!! I have a PhD position for you.” That was the greatest message at that time. She is a perfect supervisor, friend and family member, because she is rigorous, careful, persistent, innovative, casual, enthusiastic, cheerful, humour and friendly. My joint supervisor, friend and brother is the gentleman, Dr. Abdoulaye Diakité. He is handsome, humours and kind. Thanks for their thousands of constructive suggestions on my research as well as on my life and thought.

I had a great time in carrying out this work with GRID family members, including Dr. Ben Gorte, Dr. Mitko Aleksandrov, Dr. Jack Barton, and Dr. Wei Li. All of members in our group are friendly, kind and helpful to each other. I am sure that even many years later, I will still remember the lunchtime and absurd but funny chats with all of you.

Thinking back, I would like to say that moving to Australia is a crucial and a hundred percent right decision in my life.

Thanks a million of my previous colleagues in UNSW: Abdullah Alattas (TU Delft), Yijing Wang (Southeast University), Yuxuan Liu (Wuhan University), Kaixuan Zhou (TU Delft), Elyta Widyaningrum (TU Delft) and Shayan Nikoohemat (University of Twente). All the best to their PhD research and life. Furthermore, I also appreciate my previous colleagues in TU Delft: Prof. Jantien Stoter, Prof. Hugo Ledoux, Prof. Liangliang Nan, Dr. Ken Arroyo Ohori, Dr. Filip Biljecki, Dr. Sangmin Kim, Tom Commandeur, Kavisha Kumar, Anna Labetski, Ravi Peters, Stelios Vitalis, Weixiao Gao, Margo van der Helm, and Daniëlle Karakuza. I hope they are in good health and happy life. I especially appreciate all the help from my friend Rusnė Šilerytė (TU Delft). She is very smart and kind. I was lucky to attend the Master's course - *3D Modelling*, where I knew her. Thanks for her help, from Rhinoceros (and Grasshopper) to English writing and speaking. I wish her a successful PhD research. Long live our friendship.

Thanks for the two reviewers, Prof. Christophe Claramunt, the Research Chair of Naval Academy Research Institute, and Prof.dr.ir. P.H.A.J.M. van Gelder, from Faculty of Technology, Policy, and Management in Delft University of Technology. Thanks for their time and helpful reviews of this thesis. Their valuable and constructive remarks are of great importance for improving the presentation of this research.

I would like to be grateful to my wife (Wei Ling) and our parents. Thanks for their continued supports. With her company, I started this PhD research journey four years ago. Although we suffered a series of changes, from China to the Netherlands, from the Netherlands to China, and from China to Australia, she never complains but insists on supporting and helping me. I would like to thank our parents (my parents and parents in law), who are always supporting me to confidently and boldly pursue my dream.

Last but not least the people I would like to thank are all the friends who helped me with my CSC scholarship application and transfer. Thanks the supports from the following teachers: Prof. Jianga Shang (China University of Geosciences (Wuhan)) and Prof. Gang Chen (China University of Geosciences (Wuhan)), Yiwei Wang (Education Office, Embassy of the People's Republic of China in the Kingdom of the Netherlands) and Yongfeng Hou (Education Office, the Consulate General of the People's Republic of China in Australia).

In addition, I would like to express my deep gratitude to those friends who have helped me but have not been listed. I wish you a happy life and a great future.

Jinjin Yan (闫金金)

November 6, 2020





## *List of Publications*

The following lists are the publications during my PhD research.

- Papers finished/under review:
  1. **Yan, J.**, Brian Lee \*, Zlatanova, S., Diakit , A.A. Indoor Pedestrian Navigation Path Planning Using QR Codes. 2020 (Finished).
  2. **Yan, J.\***, Zlatanova, S., Diakit , A.A. A Unified 3D Space-based Model for Seamless Navigation in Indoor and Outdoor. *Environment and Planning B: Urban Analytics and City Science*. 2020. (Under review)
  
- Published international journal papers:
  1. **Yan, J.\***, Diakit , A.A., Zlatanova, S., Aleksandrov, M. Finding Boundaries of Outdoor for 3D Space-based Navigation. *Transactions in GIS*. 2020, 24, 371–389. DOI: <https://doi.org/10.1111/tgis.12613>
  2. Zlatanova, S., **Yan, J.\***, Wang, Y., Diakit , A., Isikdag, U., Sithole, G., Barton, J. Spaces in Spatial Science and Urban Applications – State of the Art Review. *ISPRS Int. J. Geo-Inf.* 2020, 9, 58. DOI: <https://doi.org/10.3390/ijgi9010058>
  3. **Yan, J.\***, Diakit , A.A., Zlatanova, S. A Generic Space Definition Framework to Support Seamless Indoor/outdoor Navigation Systems. *Transactions in GIS*. 2019, 23(6), 1273-1295. DOI: <https://doi.org/10.1111/tgis.12574>
  4. **Yan, J.\***, Diakit , A.A., Zlatanova, S., Aleksandrov, M. Top-Bounded Spaces Formed by the Built Environment for Navigation Systems. *ISPRS Int. J. Geo-Inf.* 2019, 8, 224. DOI: <https://doi.org/10.3390/ijgi8050224>
  
- Published international refereed conference papers:
  1. **Yan, J.\***, Zlatanova, S., Diakit , A.A. Two New Pedestrian Navigation Path Options based on Semi-indoor Space. *ISPRS Annals of Photogrammetry, Remote Sensing & Spatial Information Sciences*, VI-4/W1-2020, 175–182. DOI: <https://doi.org/10.5194/isprs-annals-VI-4-W1-2020-175-2020>.
  2. **Yan, J.\***, Zlatanova, S., Aleksandrov, M., Diakit , A.A., Pettit, C. Integration of 3D objects and Terrain for 3D Modelling Supporting the Digital Twin. *ISPRS Annals of Photogrammetry, Remote Sensing & Spatial Information Sciences*, IV-4/W8, 2019, 147-154. DOI: <https://doi.org/10.5194/isprs-annals-IV-4-W8-147-2019>

3. **Yan, J.**, Diakit , A.A. \*, Zlatanova, S. An Extraction Approach of the Top-Bounded Space Formed by Buildings for Pedestrian Navigation. *ISPRS Annals of Photogrammetry, Remote Sensing & Spatial Information Sciences*, IV-5, 2018, 247-254. DOI: <https://doi.org/10.5194/isprs-annals-IV-4-247-2018>
  4. **Yan, J.\***, Grasso, N., Zlatanova, S., Braggaa, R.C., Marx, D.B. Challenges in Flying Quadrotor Unmanned Aerial Vehicle for 3D Indoor Reconstruction. *International Archives of the Photogrammetry, Remote Sensing & Spatial Information Sciences*, 2017, 42:423-430. DOI: <https://doi.org/10.5194/isprs-archives-XLII-2-W7-423-2017>
- Other published papers:
    1. Li, W.\* , Zlatanova, S., Diakit , A.A., Aleksandrov, M., **Yan, J.** Towards Integrating Heterogeneous Data: A Spatial DBMS Solution from a CRC-LCL Project in Australia. *ISPRS Int. J. Geo-Inf.*, 2020, 9, 63. DOI: <https://doi.org/10.3390/ijgi9020063>
    2. Li, W.\* , Zlatanova, S., **Yan, J.**, Diakit , A.A., Aleksandrov, M. A Geo-Database Solution for the Management and Analysis of Building Model with Multi-Source Data Fusion. *International Archives of the Photogrammetry, Remote Sensing & Spatial Information Sciences*, XLII-4/W20, 2019, 55–63. DOI: <https://doi.org/10.5194/isprs-archives-XLII-4-W20-55-2019>
    3. Aleksandrov, M.\* , Diakit , A.A., **Yan, J.**, Li, W., Zlatanova, S. Systems Architecture for Management of BIM, 3D GIS and Sensors Data. *ISPRS Annals of Photogrammetry, Remote Sensing & Spatial Information Sciences*, IV-4/W9, 2019, 3-10. DOI: <https://doi.org/10.5194/isprs-annals-IV-4-W9-3-2019>
    4. Alattas, A.\* , van Oosterom, P., Zlatanova, S., Diakit , A.A., **Yan, J.** Developing a database for the LADM-IndoorGML model. 6th International FIG 3D Cadastre Workshop 2-4 October 2018, Delft, The Netherlands, 2018, 261-278. URL: <http://resolver.tudelft.nl/uuid:31a20fb8-dabc-4f19-82c8-432f410a3ece>
    5. Wang, Y.\* , Zlatanova, S., **Yan, J.**, Huang, Z., Cheng, Y. Exploring the relationship between spatial morphology characteristics of landscape open space unit and public aesthetic preference by using point cloud data. *Environment and Planning B: Urban Analytics and City Science*, 0(0), 2020, 1-19. DOI: <https://doi.org/10.1177/2399808320949885>

---

# CONTENTS

---

<b>Abstract</b>	<b>ix</b>
<b>Acknowledgements</b>	<b>xi</b>
<b>1 Introduction</b>	<b>1</b>
1.1 Motivation . . . . .	1
1.2 Research Questions and Scope . . . . .	7
1.3 Main Contributions . . . . .	9
1.4 Outline of The Thesis . . . . .	11
1.5 Personal Pronouns . . . . .	12
1.6 Overview of Related Papers to the Chapters . . . . .	13
<b>2 Background</b>	<b>15</b>
2.1 Seamless Navigation . . . . .	15
2.2 The Poincaré Duality Theory . . . . .	18
2.3 Navigation Model . . . . .	19
2.4 (3D) Spaces for Navigation . . . . .	24
2.5 Navigation Path . . . . .	36
2.6 Three International Standards Related to Navigation . . . . .	37
2.7 Summary . . . . .	43
<b>3 Concepts and Terminology</b>	<b>45</b>
3.1 Existing Concepts . . . . .	46

3.2	New Introduced Terminology . . . . .	53
3.3	Summary . . . . .	63
<b>4</b>	<b>Generic Space Definition Framework</b>	<b>65</b>
4.1	Space Definitions . . . . .	66
4.2	Illustration of Thresholds and Space Classification . . . . .	71
4.3	Summary . . . . .	77
<b>5</b>	<b>Space-based Navigation Model and New Path Options</b>	<b>79</b>
5.1	Attributes and Spatial Schema . . . . .	80
5.2	Path Options based on Introduced Spaces . . . . .	85
5.3	Summary . . . . .	96
<b>6</b>	<b>Reconstruction Approaches for Different Types of Spaces</b>	<b>97</b>
6.1	Semi-indoor Space Reconstruction . . . . .	98
6.2	Semi-outdoor & Outdoor Reconstruction . . . . .	103
6.3	Building Shells Reconstruction . . . . .	108
6.4	Summary . . . . .	115
<b>7</b>	<b>Implementation &amp; Case Study</b>	<b>117</b>
7.1	Data, Software, and Flowchart for Implementation . . . . .	117
7.2	Mapping UML to Python Classes . . . . .	122
7.3	Space Classification and Reconstruction . . . . .	124
7.4	Space Selection and Navigation Network Derivation . . . . .	126
7.5	Path Planning . . . . .	129
7.6	Comparison of Results . . . . .	135
7.7	Summary . . . . .	136
<b>8</b>	<b>Conclusion and Future Work</b>	<b>139</b>
8.1	Conclusion . . . . .	139
8.2	Discussion . . . . .	145
8.3	Recommendations for Further Research . . . . .	147
	<b>Bibliography</b>	<b>157</b>
<b>A</b>	<b>Curriculum Vitae</b>	<b>175</b>

---

## LIST OF FIGURES

---

1.1	Living environments in our life. . . . .	4
1.2	Examples of semi-bounded environments with upper boundaries. . . . .	6
1.3	Examples of semi-bounded environments without upper boundaries. . . . .	7
1.4	The outline of this thesis. . . . .	11
2.1	Anchor node used for integrating indoor and outdoor navigation network.	17
2.2	Poincaré duality theory used for navigation network derivation (Lee, <a href="#">2004b</a> ).	18
2.3	Based on Poincaré Duality, two room spaces represented by dual nodes are connected by a dual link penetrating a shared face (Zverovich et al., <a href="#">2016</a> ).	19
2.4	A 2D network derived on the basis of Poincaré Duality, MAT and information about doors (Meijers, Zlatanova, and Pfeifer, <a href="#">2005</a> ). (a) Floor plan; (b) The metric network derived from connections between spaces; and (c) The corrected metric network considering the corridor graph and door locations.	20
2.5	The 2D navigation network derived on the basis of room and door spaces (Lorenz, Ohlbach, and Stoffel, <a href="#">2006</a> ). . . . .	20
2.6	Indoor 2D network derivation based on duality theory (Yang and Worboys, <a href="#">2015</a> ). (a) An indoor structure graph; (b) Metric navigation network.	21
2.7	The navigation network created on the basis of Voronoi diagram (Wallgrün, <a href="#">2004</a> ). (a) original plan, (b) network and (c) simplified network. . . . .	21

2.8	A 3D network derived on the basis of Poincaré Duality and information about room spaces connectivity (Boguslawski and Gold, 2009). (a) 3D model of a building interior, (b) Room spaces, (c) Complete graph of connectivity of room spaces, (d) network of connections between room spaces based on passages only. . . . .	22
2.9	A 3D navigation network extracted from BIM models (Teo and Cho, 2016).	23
2.10	Example of 3D space-based model for indoor navigation (Diakit� and Zlatanov�, 2018). . . . .	23
2.11	The navigation network derived from 2D floor plans embedded in 3D space (Thill, Dao, and Zhou, 2011). . . . .	24
2.12	Space classification based on building (Zhou et al., 2012). . . . .	31
2.13	Space definition according to the reception of satellites signal (Wang et al., 2016). . . . .	31
2.14	Space classification based on the type of signal received by the users (Amutha and Nanmaran, 2014). . . . .	32
2.15	Space definition framework based on if a space is (fully) enclosed (Chen and Clarke, 2019). . . . .	32
2.16	An example of BReps, in which a solid is represented by F faces, E edges, and V vertices (Bowyer, 1996). . . . .	35
2.17	All spaces including walls are represented by voxels (Rodenberg, Verbree, and Zlatanov�, 2016; Li et al., 2019). . . . .	36
2.18	Part of IndoorGML navigation module UML diagram (OGC, IndoorGML Lee et al., 2015). . . . .	37
2.19	Example of the indoor space modelling based on Breps in IndoorGML (Lee et al., 2015). . . . .	38
2.20	The hierarchy structure of part of the currently defined elements within the IFC architectural model. The elements that are highlighted in the gray background are processed in path planning (Lin et al., 2013). . . . .	40
2.21	Road areas consist of traffic areas and auxiliary traffic areas (Gr�ger et al., 2012). . . . .	41
2.22	Buildings components in CityGML shell model (Gr�ger et al., 2012). . . .	42
2.23	Representation of a road by 3D spaces in CityGML 3.0 (Kutzner, Chaturvedi, and Kolbe, 2020). . . . .	42
3.1	A pedestrian is modelled as a 3D object. . . . .	46
3.2	The size of the space required by a pedestrian. $l', w', h'$ describe the size of space required by an agent whose size is $l, w, h$ . The buffer and comfortable distances of width are not illustrated as the figures are side views. . . . .	47

3.3	Dimensions and space requirements based on body measurements (unit: <i>mm</i> ). This figure is made based on the figures in Architects' Data (Neufert et al., 1980). . . . .	48
3.4	The building height defined by Center (2002). . . . .	50
3.5	The rule of measuring building height. The <i>A</i> and <i>B</i> are the highest and lowest foundation points respectively, <i>C</i> and <i>E</i> are on the same plane with <i>A</i> , <i>F</i> is the mid-point of foundation, and <i>D</i> is the highest point of the building. . . . .	51
3.6	<i>TerrainIntersectionCurves</i> (TIC) in CityGML. The TIC is shown in bold black curve. . . . .	52
3.7	Example of roof and top (red rectangles). . . . .	54
3.8	Example of wall and side (blue rectangles). . . . .	54
3.9	Example of floor and ground (marked by white arrows). Both act as the bottoms of spaces. . . . .	55
3.10	Illustration of closure computation, in which the slash-filled parts are physical structures. $l_0$ to $l_5$ are the length of the physically closed parts; $L$ and $W$ are the length and width of the top/bottom/side respectively. . . . .	56
3.11	The abstraction of top, side, and bottom, and estimation of their closure. . . . .	57
3.12	Illustration of the Gradient computation. . . . .	59
3.13	Two examples of semi-bounded spaces with tops. . . . .	60
3.14	An example of a semi-bounded environment without tops. (a) yard; (b) physical boundaries; (c) virtual boundaries; (d) semi-bounded space. . . . .	60
3.15	(a) Space radius ( $r_s$ ), space height ( $h_s$ ) and Gradient ( $G$ ). Blue polygons are physical boundaries, while olive green polygons are virtual. (b) The minimum space required by a pedestrian. It is modelled as cylinder with bottom radius $\sqrt{l^2 + w^2}/2$ and height $h'$ . . . . .	61
4.1	The $C^T$ and $C^S$ of different spaces. $C^T$ and $C^S$ are two physical structure parameters. $\alpha$ , $\beta$ , $\gamma$ , $\delta$ , and $\eta$ are five thresholds. (a) sharply classify space into two categories, sI-/I-space, and sO-/O-space, by using $\eta$ of $C^T$ ; (b) classify sI-/I-space into I-space and sI-space, and sO-/O-space into sO-space and O-space, by employing other four thresholds ( $\alpha$ , $\beta$ , $\gamma$ , and $\delta$ ). . . . .	68
4.2	Flowchart of the space definition framework. . . . .	70
4.3	Definitions of the spaces based on the definition framework. . . . .	71
4.4	The structure with four different closure cases, in which the gray parts are enclosed ( $a_e$ ), while white parts are open. Size of the example structure ( $a_t$ ) is $2 * 1(m^2)$ . . . . .	72

4.5	Top view of length of surrounding boundaries of square spaces, where slash-filled parts are concrete walls. (a) no wall; (b) one wall; (c) and (d) two walls; (e) three walls; (f) four walls. . . . .	73
4.6	Space classification based on the example values of five thresholds. . . . .	74
4.7	Some space examples of built scenes. . . . .	76
4.8	Structures of space have weak characteristics. . . . .	77
4.9	Bridges between two buildings. . . . .	77
5.1	UML diagram of the unified 3D space-based navigation model. All the classes come from IndoorGML. The attributes of <i>CellSpace</i> and <i>CellSpace-Boundary</i> , and the data types are developed by this research, see the parts circled by the red dotted line. . . . .	81
5.2	Example of environments and spaces. (a) A built environment case; (b) physical boundaries; (c) virtual boundaries. . . . .	84
5.3	Example of spaces, physical boundaries, virtual boundaries (blue), <i>Top</i> , <i>Side</i> , <i>Bottom</i> , $C^T$ , $C^S$ and $C^B$ . All the physical boundaries are coloured into gray while virtual boundaries are in light blue. . . . .	84
5.4	Illustration of connected spaces and the navigation network between the two spaces. . . . .	85
5.5	Example of NSI-path planning from departure to destination. . . . .	89
5.6	The path selection strategy. The shortest path is computed based on the original weights ( $W'_{s_i s_j}$ ). . . . .	91
5.7	A navigation example, in which $s_C$ , $s_F$ , and $s_G$ are three sI-spaces. The navigation graph in (c) and (d) are undirected graph. (a) All spaces. (b) Nodes extracted from spaces; (c) Navigation graph derived from spaces based on duality theory, in which the red dots are the extra vertices; (d) Navigation graph with distance. . . . .	92
5.8	The three navigation paths from $s_A$ (departure) to $s_H$ (destination). $s_A \rightarrow s_D \rightarrow s_E \rightarrow s_H$ is path 1 (green), $s_A \rightarrow s_F \rightarrow s_G \rightarrow s_H$ is path 2 (black), and $s_A \rightarrow s_F$ is path 3 (blue). . . . .	94
5.9	The changes of $W_p$ with the changing of the $\zeta$ . . . . .	95
6.1	Four different cases of sI-space reconstruction based on projecting. The original polygons are $A_i$ (in white) and $B_i$ (in yellow), and their projections are $A'_i$ (in gray) and $B'_i$ (in light green) respectively. The created sI-spaces are coloured in dark blue. . . . .	100

6.2	Example of trimming spaces. To distinguish sI-spaces that are created based on different tops and bottoms, they are coloured differently. (a) shows the three building components; (b), (c), and (d) are three sI-spaces based on projections; (e) is the space trimmed by the other two spaces; (f) the final three reconstructed sI-spaces. . . . .	102
6.3	Illustration of sI-space reconstruction. . . . .	103
6.4	The process of sO-space and O-space reconstruction. . . . .	104
6.5	The footprints of indoor (red) and semi-indoor (blue) spaces formed by built structures. (a) a building with eaves; (b) a building with eaves and its lowest floor is above ground; (c) a building with a hanging part. . . . .	105
6.6	Built objects and their non-overlap footprints. (a) Built objects; (b) Corresponding 2D footprints. . . . .	107
6.7	Example of footprints classification based on overlaps (unit: <i>m</i> ). . . . .	107
6.8	Example of reconstructed sO-spaces and O-spaces (height = 5). (a) Classified footprints; (b) Reconstructed sO-spaces and O-spaces. . . . .	108
6.9	The process of building shells reconstruction based on building footprints, building heights and DTM. . . . .	109
6.10	The outward-facing normal of boundaries of a 3D building shells. . . . .	110
6.11	Building footprints for illustration. . . . .	112
6.12	The projected footprints on the terrain. . . . .	112
6.13	The building shells and the terrain that are reconstructed based on PVT method. . . . .	113
6.14	The building shells and the terrain that are reconstructed based on PPT method. . . . .	114
6.15	The other data sources for building shells reconstruction. . . . .	115
7.1	Footprints of spaces on the selected area of UNSW campus. The dot-filled footprint is the building that has BIM model. . . . .	118
7.2	Footprints of road and green areas in the selected area of UNSW campus. . . . .	119
7.3	The I-spaces and BIM model in PostgreSQL. . . . .	120
7.4	The terrain of the precinct. . . . .	121
7.5	Flowchart of the implementation. . . . .	121
7.6	Physical boundaries used for space classification. . . . .	125
7.7	Classified road and green area footprints. The darker white polygons are building footprints. . . . .	125
7.8	Reconstructed sI-spaces, sO-spaces, and O-spaces. The darker white polygons are building footprints. . . . .	126
7.9	The duality used in this implementation. The red dots are extra vertices extracted from shared virtual boundaries. . . . .	127

7.10	All the spaces in the selected area on the UNSW campus. The darker white polygons are building footprints. . . . .	128
7.11	Derived unified navigation network in the test area. Black lines are edges and red dots are nodes. . . . .	128
7.12	From O-space to sO-space (Road16 $\rightsquigarrow$ Village green). . . . .	130
7.13	From O-space to sI-space (Road19 $\rightsquigarrow$ sI-space47). . . . .	131
7.14	From sO-space to I-space (Road80 $\rightsquigarrow$ Room 4036). . . . .	132
7.15	Navigation paths of A $\rightsquigarrow$ B. Differences between shortest path and MTC-path are marked by black ellipses, which shows where the sI-spaces are involved. . . . .	134
7.16	Navigation paths of C $\rightsquigarrow$ D. The part marked by black ellipse shows where the sI-spaces are involved in MTC-path. . . . .	135
8.1	Example of the space modelling in landscape. Adapted from the figures in (Zlatanova et al., 2020). . . . .	148
8.2	Example of outdoor borders. . . . .	149
8.3	Example of space accessibility issues. . . . .	154

---

## LIST OF TABLES

---

1.1 My publications and the related chapters of this thesis. . . . .	14
4.1 Characteristics of living environments (spaces), in which “✓” denotes a space has the structure while “×” denotes has not. . . . .	66
4.2 Estimated $C^T$ and $C^S$ of the example structures. . . . .	75
5.1 Original information of the navigation graph. . . . .	93
5.2 Modified weights ( $W''_{s_i s_j}$ ) based on Equation 5.3. . . . .	93
5.3 Three different navigation paths. . . . .	95
7.1 Example of <i>CellSpace</i> table in the computer memory. . . . .	123
7.2 Example of <i>CellSpaceBoundary</i> table in the computer memory. . . . .	124
7.3 Comparisons of three navigation systems. × means no while ✓ means yes. . . . .	135



---

## LIST OF ABBREVIATIONS

---

<b>BIM</b>	Building Information Modelling
<b>CAD</b>	Computer-aided Design
<b>CDT</b>	Constrained Delaunay Triangulation
<b>CityGML</b>	City Geography Markup Language
<b>CRS</b>	Coordinate Reference System
<b>DBMS</b>	Database Management System
<b>DEM</b>	Digital Elevation Model
<b>DHM</b>	Digital Height Model
<b>DGM</b>	Digital Ground Model
<b>DSM</b>	Digital Surface Model
<b>DTM</b>	Digital Terrain Model
<b>FME</b>	Feature Manipulation Engine
<b>GIS</b>	Geographic Information Systems
<b>GML</b>	Geography Markup Language
<b>GNSS</b>	Global Navigation Satellite System
<b>GPS</b>	Global Positioning System
<b>IFC</b>	Industry Foundation Classes
<b>INS</b>	Inertial Navigation System
<b>IPS</b>	Indoor Positioning System
<b>I-space</b>	Indoor Space
<b>LADM</b>	Land Administration Domain Model
<b>LoD</b>	Level of Detail
<b>MAT</b>	Medial Axis Transform

<b>MTC-path</b>	Most-top-covered Path
<b>NEDF</b>	National Elevation Data Framework
<b>NRG</b>	Node-Relation Graph
<b>NSI-path</b>	The path to the Nearest sI-space from departure
<b>OGC</b>	Open Geospatial Consortium
<b>OSM</b>	Open Street Map
<b>O-space</b>	Outdoor Space
<b>POI</b>	Points of Interest
<b>PPT</b>	Projecting Footprint Polyline onto Terrain
<b>PVT</b>	Projecting Vertices of Footprint onto Terrain
<b>QGIS</b>	Quantum GIS
<b>RFID</b>	Radio Frequency Identification
<b>sI-space</b>	Semi-indoor Space
<b>sO-space</b>	Semi-outdoor Space
<b>TIC</b>	Terrain Intersection Curve
<b>TIN</b>	Triangulated Irregular Network
<b>UAV</b>	Unmanned Aerial Vehicle
<b>UML</b>	Unified Modelling Language
<b>XML</b>	Extensible Markup Language

---

## LIST OF SYMBOLS

---

Symbol	Name
$A_i, B_i, C_i, \dots$	Building components
$z_A, z_B, z_C, \dots$	the average of the z coordinate of the building components
<b>C</b>	Closure
$C^T, C^S, C^B$	topClosure, sideClosure, and bottomClosure of a 3D space
<b>G</b>	Gradient
$G^T, G^S, G^B$	Gradient of a top, side, and bottom
$\alpha, \beta, \gamma, \delta, \eta$	Coefficients for closure
$l, w, h$	Size of an agent itself
$l_{buf}, w_{buf}$	The buffer distance of length and width required by a moving agent
$l_{com}, w_{com}$	The comfortable distance of length and width required by a moving agent
$h_{buf}$	The buffer height required by a moving agent
$l', w', h'$	Size of the space required by an agent
$a_e$	The area of the enclosed part for the top/bottom of a space
$a_t$	The total area of the top/bottom of a space
$l_e$	The length of physically enclosed part of the side of a space
$l_t$	The total length of the side of a space
$s_i$	A 3D space
$r_s$	The radius of the maximum inscribed circle of the bottom projection of a space
$h_s$	Height of a 3D space
$d_{s_i s_j}$	Distance between space $s_i$ and $s_j$
$W'_{s_i s_j}$	Original weight on the edge between $s_i$ and $s_j$

$d_{c_{s_i s_j}}$	Covered distance between space $s_i$ and $s_j$
$d_{uc_{s_i s_j}}$	Uncovered distance between space $s_i$ and $s_j$
$\lambda_{s_i s_j}$	Uncovered ratio of the edge between space $s_i$ and $s_j$
$W''_{s_i s_j}$	Modified weight of the edge between space $s_i$ and $s_j$
$W_P$	Total weight of a path
$P_l$	The length of a path
$P_{l_c}$	Covered length of a path
$P_{l_{uc}}$	Uncovered length of a path
$P_{c_r}$	Path coverage ratio

*Dedicated to everyone who has helped me along the PhD journey*



# CHAPTER 1

---

## INTRODUCTION

---

This chapter presents an introduction to this research. First of all, the motivation of this research is presented by summarising the shortcomings of current seamless indoor-outdoor navigation, and the complexity of the living environments where navigation happens. Then, the main research question and the scope of this research are presented. After outlining the structure of the whole thesis, a short introduction to all of the coming chapters are introduced. The penultimate section of this chapter states the rules of the personal pronouns used in this thesis. At the end of this chapter, a table lists the author's own publications and relates them to these chapters of this thesis.

### **1.1 Motivation**

#### **1.1.1 Seamless Navigation**

Navigation (also called path-finding or way-finding) is a fundamental activity for human beings. It is described as the method of determining the direction of a user from a familiar goal across unfamiliar terrain (May et al., [2003](#)), or the process of orientation to reach a specific distant destination from the origin (Krūminaitė and Zlatanova, [2014](#)).

Outdoor navigation is widely used in our daily life and diverse travel modes are considered, such as walking (Karimi, Jiang, and Zhu, 2013), driving (Millonig and Schechtner, 2007b), transiting (Zar and Sein, 2016), and cycling (Howard and Burns, 2001).

With agents (e.g., pedestrians) moving seamlessly between one kind of environment to another (e.g., between buildings and surrounding areas), navigation guidance tools/systems should extend from merely outdoor or indoor guidance, to provide support in the combined indoor-outdoor context (Nagel et al., 2010; Vanclooster, Weghe, and De Maeyer, 2016). That is, it is necessary to have seamless (universal/continuous) navigation, because different types of living environments (indoor, outdoor, semi-indoor/outdoor) are not isolated; agents experience all different environments as seamlessly connected and they can seamlessly travel between them for activities (e.g., work, shopping, leisure, dining, sport). Seamless navigation here is a term that describes universal navigation service, where human operations or interventions are not required when transitions happen, or the agents would not be aware of how the device works for the seamless services (Peltola and Moore, 2017).

A successful seamless navigation should cover both indoor and outdoor environments (Yang and Worboys, 2011a) and consider how agents experience specific parts of the living environment when offering navigation services (Vanclooster, Weghe, and De Maeyer, 2016). However, no system or research can really offer satisfactory indoor and outdoor seamless navigation, although some attempts are conducted. The shortcomings of current (seamless) navigation systems can be summarised as follows:

- Outdoor navigation networks are quite generalised. Current navigation networks assume that different agents will by default move to the correct areas, which is not inappropriate. In the real world, different agents (pedestrians, bicycles, cars, wheeled users) have specific areas/spaces for their movements, except the shared areas. For example, a road may consist of sidewalks and traffic lanes, in which the former is restricted to pedestrians/wheeled users access only, while the latter is dedicated to vehicles. There are usually several meters between them (Ballester,

Pérez, and Stuiver, 2011). Therefore, the navigation networks for pedestrian navigation use should be derived based on the shape and direction of sidewalks/pedestrian crossings (Karimi, Jiang, and Zhu, 2013; Klochkova et al., 2017), rather than the street centre-line. Otherwise, pedestrians might be risky in security (Andreev et al., 2015; Balata, Berka, and Mikovec, 2018; Bodgan and Coors, 2009; Cambra, Gonçalves, and Moura, 2019).

- Current indoor and outdoor navigation networks are dedicated to specific applications and it is hard to exchange and maintain the integrated navigation network. Generally, the indoor navigation networks are extracted based on 3D (free) spaces, while the main source of navigation network in outdoor space is road/street-based networks (Millonig and Schechtner, 2007a). This kind of practice has attracted a lot of criticism, especially in pedestrian navigation (Vanclooster, Weghe, and De Maeyer, 2016; Bodgan and Coors, 2009). Moreover, a node in an indoor navigation network can be a room (Teo and Cho, 2016) or functional areas (Krūminaitė and Zlatanova, 2014; Diakité and Zlatanova, 2018), while a node in outdoor navigation network is mostly related to an intersection of a road/path. Thus, due to the different resolutions, pedestrians have to accept that access to certain spaces will not be provided, e.g., they cannot find a path to a street elevator or a bench in a garden.
- Some public spaces (e.g., square) and semi-bounded spaces (e.g., porch) (Kray et al., 2013) are not included in navigation maps. Navigation results of current outdoor navigation clearly show that pedestrians are navigated to have undesirable detour around a square, while in reality they can cross directly (Andreev et al., 2015; Graser, 2016; Hannah, Spasić, and Corcoran, 2018; Balata, Berka, and Mikovec, 2018). Furthermore, people cannot find a path to the semi-bounded spaces, although they may prefer to use these spaces for some purposes, e.g. growing plants (Kim, Kim, and Leigh, 2011), learning activities (Nasir, Salim, and Yaman, 2014), adapting to thermal environments (Lin, 2009), and sheltering from the sun and wind (He and Hoyano, 2010; Spagnolo and De Dear, 2003).

- Vertical constraints during the navigation are not considered. Agents are three-dimensional objects with length, width, and height, which means that agents have requirements on the vertical dimension of space. However, current navigation networks are derived based on 2D-connectivity and the path planning assumes agents are 0D points. Thence, although some spaces act as vertical constraints and have decisive effects on the possibility of the agents going through, this kind of condition is not reflected on the navigation map. For instance, clearance for tunnels, bridges, and entrances are some common vertical constraints in the outdoor navigation for vehicles.

### 1.1.2 Living Environments



(a) Entirely bounded (indoor)



(b) Unbounded (outdoor)

FIGURE 1.1: Living environments in our life.

With the expanding of cities worldwide, we can find that the buildings are expanding in size, height, and depth, which makes contemporary living environments more and more complex. Generally, environments entirely physically bounded by building components (e.g., walls, floors, roofs) are named as indoor (Afyouni, Ray, and Claramunt, 2010; Yang and Worboys, 2011a; Yang and Worboys, 2011b; Zlatanova, Liu, and Sithole, 2013; Zlatanova et al., 2014) (Figure 1.1(a)). In contrast, the unbounded, connected and unoccupied environments are commonly perceived as outdoor (Figure 1.1(b)). Objects on the ground can provide some indications of boundaries of outdoor environments, but many

of them would remain unbounded in the vertical direction, such as streets, pavements, squares, rivers.

Beyond that, there are many semi-bounded living environments that are difficult to be classified as indoor or outdoor sharply. They have characteristics of both indoor and outdoor, but cannot be seen clearly as either of them. These semi-bounded environments are referred to with different names in the literature, such as, semi-indoor, semi-outdoor/semi-open/semi-enclosed, and connection/transition zones/buffer areas/transitional spaces.

- Semi-indoor space (Kim, Kim, and Leigh, 2011; Turrin et al., 2009; Chengappa et al., 2007; Liu et al., 2013; Kim, Park, and Kim, 2008; Monteiro and Alucci, 2007). A space covered with canopies that is related to a building, and can combine indoor and outdoor climate conditions. For instance, balcony (installed with external windows), courtyard, open air kitchen with 3 walls, open space equipped with overhead shed/arcades.
- Semi-outdoor/semi-open/semi-enclosed space (Du, Bokel, and Dobbelsteen, 2014; Hwang and Lin, 2007; Lin et al., 2008; Indraganti, 2010; Pagliarini and Rainieri, 2011b; He and Hoyano, 2010; Kim, Kato, and Murakami, 2001; Philokyprou et al., 2017). A space that is not enclosed entirely, but has some settings including human-made structures that moderate the effects of the outdoor conditions, such as space with eave, courtyard, sheltered balconies, outdoor space partly enclosed by a semi-transparent pitched roof.
- Connection/transition zones/buffer areas/transitional spaces (Li, 1994; Slingsby and Raper, 2008; Winter, 2012; Kray et al., 2013). Spaces that are located between indoor and outdoor but neither indoor nor outdoor. For example, Tunnel-like underpass, tunnels, enclosed footbridges, partially roofed courtyards.

In the literature, the most important structural feature of a semi-bounded environment is the upper boundary (e.g., roof, shelter). Therefore, we can temporarily distinguish the semi-bounded environments based on if they have upper boundaries.

There are a lot of semi-bounded environments with upper boundaries formed by built structures in our living environments. Examples of such cases are overpasses, shelters for bus stops, gas stations, porches, courtyards and so on (Figure 1.2). Figure 1.2(a) and Figure 1.2(b) are two semi-bounded environments with upper boundaries, but the former has surrounding boundaries, and the latter has not. A variety of structures can act as the source of upper boundaries, e.g., indoor environment (Figure 1.2(c)), bridge (Figure 1.2(d)), or shelter (Figure 1.2(e)). Furthermore, the function of upper boundaries can be different; some of them can help agents escape from rain or strong sun (Figure 1.2(a), 1.2(b), 1.2(c), 1.2(d), and 1.2(e)), but some cannot (Figure 1.2(f)).



(a) Passageway



(b) Bus Stand



(c) Passageway



(d) Overpass



(e) Shelter



(f) Wood pergola

FIGURE 1.2: Examples of semi-bounded environments with upper boundaries.

We also can easily find many semi-bounded cases without upper boundaries (Figure 1.3). This kind of environment is without the upper boundary but bounded or enclosed on the surrounding direction(s). On the point of upper boundaries, this kind of environment is making it similar to outdoor. A variety of structures can act as the source of surrounding boundaries, e.g., fence (Figure 1.3(a), 1.3(b), and 1.3(c)), building (Figure

1.3(d)), walls (Figure 1.3(e)), or combination of walls and fence (Figure 1.3(f)). Surrounding boundaries can indicate boundaries of a space, which is useful for space modelling.



FIGURE 1.3: Examples of semi-bounded environments without upper boundaries.

## 1.2 Research Questions and Scope

As shown in the previous section, the need for seamless navigation is increasing to have seamless navigation services in both indoor and outdoor. Yet, current seamless navigation applications face several shortcomings. On one hand, the complexity of seamless navigation requires understanding the implications of living environments and their relation to the surrounding, especially the semi-bounded cases. On the other hand, agents in navigation have different locomotion models (i.e., walk, drive or fly) and can vary in size and height.

Thence, it is essential to investigate new theories, models and approaches to support seamless navigation in all kinds of environments. Thus, the main research question that

I seek to answer in this thesis is raised as:

*What a (3D) spatial model can include all types of living environments for supporting seamless navigation path planning?*

The research question is subdivided into three sub-topics with six sub-questions:

### 1. *Environments*

- Q1: Which environments (spaces) should be considered in seamless navigation activities?
- Q2: Is it possible to classify and define all the complex environments as 3D spaces for seamless navigation?

### 2. *Spaces representation*

- Q3: Can we introduce unified names and terminology to define all kinds of spaces?
- Q4: What kind of terminology should be introduced to quantitatively define all kinds of spaces?

### 3. *Unified Navigation Model and Path Options*

- Q5: Is it possible to develop a 3D unified spatial model for seamless navigation?
- Q6: Is it possible to develop new path options by considering the semantics of spaces?

From technical perspective, several components should be available to perform a successful navigation (Worboys, 2011; Zlatanova et al., 2014): (3D) localisation of start point and destination, a (3D) model that represents the spaces (environments) and space subdivision, (3D) algorithms for path computation (on a topological model or a grid), guidance (Points of Interest - POI, landmarks), visualisation of the path and finally tracking/correction (if the path is not followed). This research is going to focus on the second component. Therefore, the following topics are out of scope:

- Positioning and localization-related topics, for example, GNSS, sensors, positioning theories, methods, accuracy, and algorithms, etc. Although seamless indoor and outdoor navigation approaches based on the system integration (e.g., integration of GPS and indoor navigation system) are mentioned, they are limited to theoretical investigations.
- 3D localisation of departure and destination, guidance based on POIs or landmarks, and tracking/correction (if the path is not followed) are not included in this research. However, the computation and visualization of navigation paths are performed in implementation and case study, in which 3D locations of the start point and destination are specified manually.
- This research solely specifies a pedestrian as the agent for navigation tests, but does not conduct research on the pedestrian itself, for instance, operational (walking), tactical (short term path choice) and strategical (route choice, activity chaining) behaviours. Instead, it will take some existing research outputs of the pedestrian as inputs or references. For instance, pedestrians like to maintain around  $10\text{cm}$  from walls and obstacles during walking Bosina et al. (2016); the average speed of a pedestrian is  $1.5\text{ m/s}$  (Ishaque and Noland, 2008). These results will be employed in the implementation and case study without any further investigations.
- Approaches for 3D detailed indoor and outdoor models construction are not included in this research, such as indoor 3D models with furniture or outdoor models with facilities. Besides the algorithm for newly defined spaces, approaches for 3D detailed models are built manually to prove the developed concepts.

### 1.3 Main Contributions

This thesis presents solutions for conducting seamless navigation in all kinds of living environments based on a 3D-space based navigation model. In particular, this research brings in four contributions to seamless indoor-outdoor navigation:

- A generic space definition framework is developed, which introduces systematic and robust definitions for all environments that agents may move in. On the basis of this framework, living environments are classified and defined as indoor, semi-indoor, semi-outdoor and outdoor spaces. This framework can support seamless navigation path planning in all types of living environments. It is possible for 3D spatial navigation models to rely on it to use the same network extraction approaches across the built environments, thereby building seamless navigation solutions.
- A unified 3D space-based navigation model is developed by extending IndoorGML. This model enriches the *CellSpace* and *CellSpaceBoundary* classes, which enables navigation to include all types of spaces (indoor, semi-indoor, semi-outdoor, and outdoor) into navigation map. More importantly, these different types of spaces can share the same operations, such as management, and navigation network extraction approaches. This model brings in solutions to the shortcomings existing in current seamless navigation. In particular, this model makes the semi-bounded spaces that are missing in current navigation maps become available in navigation, such as using them as departures, destinations, or transitions.
- Two navigation path types based on semi-indoor spaces are developed to meet the user's pursuit of the protection from the top direction during their navigation. The two navigation path options are the most-top-covered path (MTC-path) and the path to the nearest semi-indoor (NSI-path). The MTC-path aims at maximizing the coverage ratio (covered by roof/shelter) while constraining the travel distance while The NSI-path is designed to help pedestrians to find a closest roofed/sheltered place from their departures, which is a compromise option when neither the traditional shortest path nor MTC-path is not recommended. Furthermore, to help agents to make path choices between the traditional shortest path and the two types of the navigation path, a path selection strategy is presented.

- 3D space reconstruction approaches of all types of spaces are developed. In particular, a projection-based method is put forward for semi-indoor space reconstruction. An approach of enclosing semi-outdoor and outdoor spaces as 3D volumes is introduced, in which the topological consistency between 3D space and terrain is addressed. Reconstructed 3D spaces make all types of spaces to mimic the indoor environments to derive a network based on their connectivities. Quantitative indicators for qualified navigable spaces selection are developed, which helps to provide more navigation path options, such as MTC-path, NSI-path (Section 5.2). Furthermore, on the basis of 3D spaces, vertical constraints can be considered in seamless navigation path planning.

## 1.4 Outline of The Thesis

The outline of the thesis is illustrated in Figure 1.4.

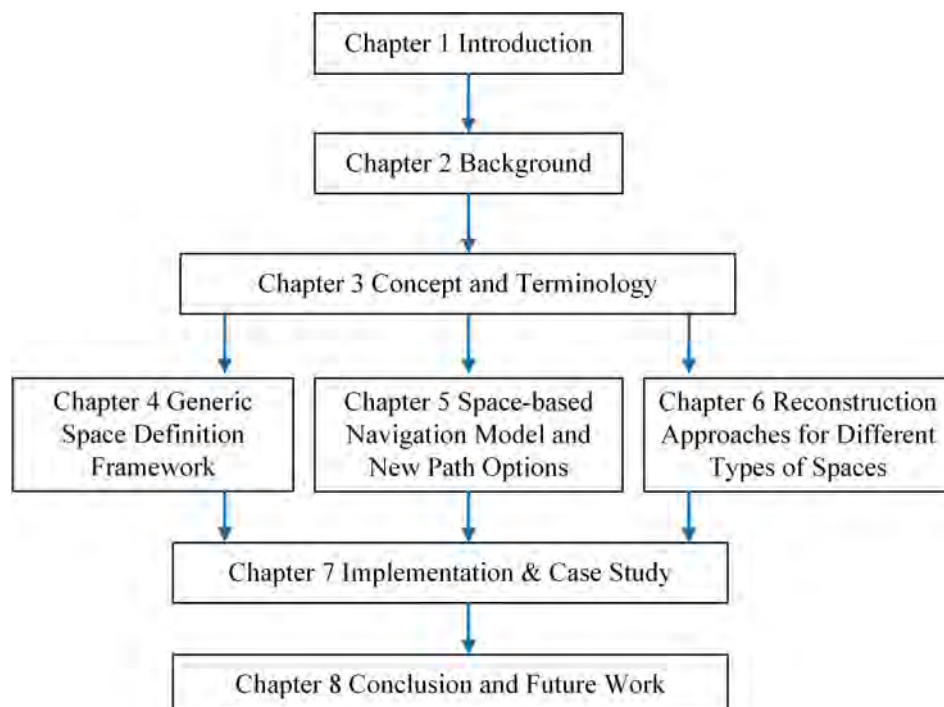


FIGURE 1.4: The outline of this thesis.

Chapter 2 presents background of this research. After elaborating current attempts on the seamless navigation, it introduces the Poincaré Duality theory, navigation model, and 3D spaces for navigation. Then, it summaries the existing navigation paths and three international standards related to navigation.

Chapter 3 introduces concepts and terminology that are used in this thesis, which includes the existing terms and newly introduced ones by this research.

Chapter 4 provides a generic space definition framework to support seamless indoor-outdoor navigation systems, in which the details of the descriptive and quantitative definitions of all types of spaces are presented.

Chapter 5 presents a unified 3D space-based navigation model, including classes and attributes of the model. Further, two new path types based on the introduced spaces and a path selection strategy are presented.

Chapter 6 introduces approaches of reconstructing semi-indoor, semi-outdoor and outdoor spaces, and building shells into 3D volumes.

Chapter 7 implements the developed theories, approaches and models, which includes data preparation, space classification and reconstruction, navigation network derivation, and path planning. Finally, the uncertainties and limitations of the whole work are discussed.

Chapter 8 concludes the whole research by reflecting on the research questions and sub-questions one by one. Then, the aspects we will concentrate on further for elaboration and testing of the current work are presented as future work.

## **1.5 Personal Pronouns**

This thesis is based on my first/corresponding author publications in which I am the leading and the main contributor but not the sole author. Hence, I use ‘we’ as a courtesy to my co-authors when I refer to results and experiments initially published in the papers. In contrast, I use ‘I’ in parts exclusive to this thesis.

If a number is used to measure my contributions in the papers where I am the first author/corresponding author, the number can be 95% and above. For instance, we published the paper titled "*Top-Bounded Spaces Formed by the Built Environment for Navigation Systems*", in which I did conceptualization, investigation, writing – original draft, and visualization independently. My colleague, Dr. Mitko Aleksandrov, helped me with the methodology and data curation, and my supervisors gave me supervisions and helped with the writing – review & editing.

## **1.6 Overview of Related Papers to the Chapters**

My publications that relate to chapters of this thesis are listed in Table 1.1, in which four published international journal papers, two published international refereed conference papers, and two under review papers are included.

These publications are not listed as references for this thesis, because almost all of the main contents of each publication are adapted as a part of the thesis. For instance, the main content of the paper paper 5 is adapted as Chapter 4 Generic Space Definition Framework. Paper 4, 6, 7 and 8 are adapted as Sections of Chapter 6.

TABLE 1.1: My publications and the related chapters of this thesis.

No.	Publication (sequenced by publication date)	Related Chapters
1	<b>Yan, J.*</b> , Zlatanova, S., Diakit�, A.A. A Unified 3D Space-based Model for Seamless Navigation in Indoor and Outdoor. <i>Environment and Planning B: Urban Analytics and City Science</i> . 2020 (Under review)	2 (Section 2.1), 5 (Section 5.1), 7 (Section 7.3, 7.4, 7.5)
2	<b>Yan, J.*</b> , Zlatanova, S., Diakit�, A.A. Two New Pedestrian Navigation Path Options based on Semi-indoor Space. <i>ISPRS Annals of Photogrammetry, Remote Sensing &amp; Spatial Information Sciences</i> , VI-4/W1-2020, 175–182.	5 (Section 5.2), 7 (Section 7.5)
3	Zlatanova, S., <b>Yan, J.*</b> , Wang, Y., Diakit�, A., Isikdag, U., Sit-hole, G., Barton, J. Spaces in Spatial Science and Urban Applications – State of the Art Review. <i>ISPRS Int. J. Geo-Inf.</i> 2020, 9, 58.	2 (Section 2.4, 2.6)
4	<b>Yan, J.*</b> , Diakit�, A.A., Zlatanova, S., Aleksandrov, M. Finding Boundaries of Outdoor for 3D Space-based Navigation. <i>Transactions in GIS</i> . 2020, 24(2), 371–389.	6 (Section 6.2), 7 (Section 7.1, 7.3)
5	<b>Yan, J.*</b> , Diakit�, A.A., Zlatanova, S. A Generic Space Definition Framework to Support Seamless Indoor/outdoor Navigation Systems. <i>Transactions in GIS</i> . 2019, 23(6), 1273-1295.	3 (Section 3.2), 4 (Section 4.1, 4.2)
6	<b>Yan, J.*</b> , Diakit�, A.A., Zlatanova, S., Aleksandrov, M. Top-Bounded Spaces Formed by the Built Environment for Navigation Systems. <i>ISPRS Int. J. Geo-Inf.</i> 2019, 8, 224.	3 (Section 3.2), 6 (Section 6.1)
7	<b>Yan, J.*</b> , Zlatanova, S., Aleksandrov, M., Diakit�, A.A., Pettit, C. Integration of 3D objects and Terrain for 3D Modelling Supporting the Digital Twin. <i>ISPRS Annals of Photogrammetry, Remote Sensing &amp; Spatial Information Sciences</i> , IV-4/W8, 2019, 147-154.	3 (Section 3.1), 6 (Section 6.3)
8	<b>Yan, J.</b> , Diakit�, A.A.*, Zlatanova, S. An Extraction Approach of the Top-Bounded Space Formed by Buildings for Pedestrian Navigation. <i>ISPRS Annals of Photogrammetry, Remote Sensing &amp; Spatial Information Sciences</i> , IV-5, 2018, 247-254.	3 (Section 3.2), 6 (Section 6.3)

# CHAPTER 2

---

## BACKGROUND

---

This chapter presents an overview of the seamless navigation and the work related to this PhD research. They are current progresses of seamless navigation, the key theoretical background of navigation model derivation - the Poincaré duality, navigation models, 3D spaces for navigation, navigation paths, as well as three international standards related to navigation. This chapter is partly based on my papers 1 and 3 (see Section 1.6).

### **2.1 Seamless Navigation**

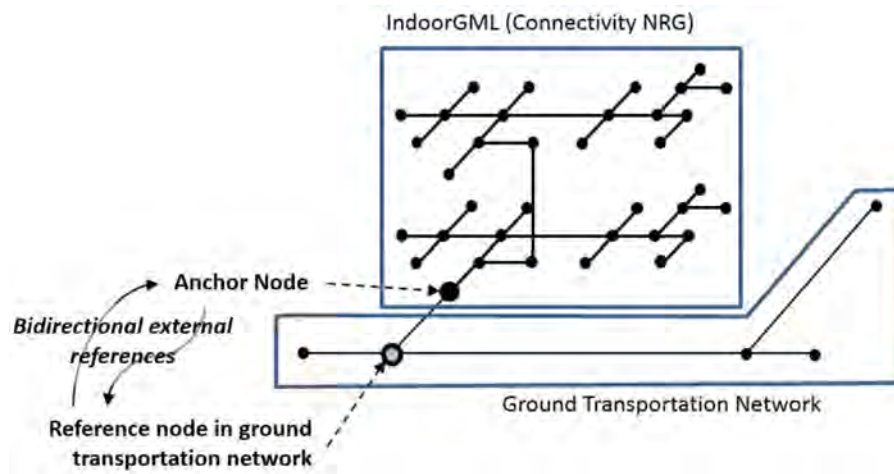
In the past decades, seamless navigation has attracted a lot of attention and a tremendous amount of approaches have been reported in the literature or made available as commercial applications in our daily life (Kim, Kim, and Lee, [2019](#)) for different travel modes (e.g., driving, walking or flying). This section summarises the existing two major

approaches/attempts on the seamless navigation in indoor and outdoor. Furthermore, the navigation path types in current navigation systems/research are investigated.

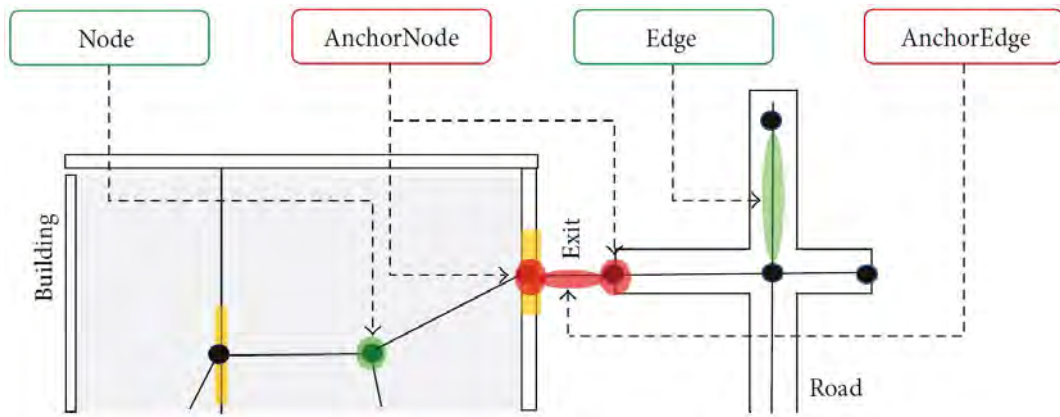
A number of great attempts have been conducted to develop integrated indoor and outdoor navigation that provide seamless navigation path and guidance. Most current well-known efforts to combine indoor with outdoor navigation are focused on localization (tracking) techniques; in particular the transition of positioning systems from indoor to outdoor environments or vice versa (Vanclooster and De Maeyer, 2012). Typically, outdoor localisation is based on GNSS, while indoors exhibits much larger variety, such as Indoor Positioning System (IPS) (Torres-Sospedra et al., 2015), Inertial Navigation System (INS) (Cheng et al., 2014), QR codes (Nikander et al., 2013; Shelke et al., 2016), active Radio Frequency Identification (RFID) tag (Kouroggi et al., 2006). However, the integrated indoor and outdoor localization systems are important for seamless localization and tracking, but they do not have direct effects on navigation path planning approaches. Therefore, this research will not focus on this approach.

Another approach of seamless navigation commonly used in research is to integrate indoor and outdoor navigation networks. That is, link indoor navigation networks to outdoor road/street-based networks as new spatial models by specific structures, such as anchor nodes (Lee et al., 2015; Park, Ahn, and Lee, 2018; Kim, Kim, and Lee, 2019) and entrance node (Kim and Wilson, 2015; Teo and Cho, 2016; Wang and Niu, 2018). This method is an attempt to fundamentally address the issue of seamless navigation paths computations, although it still falls short in achieving seamless navigation.

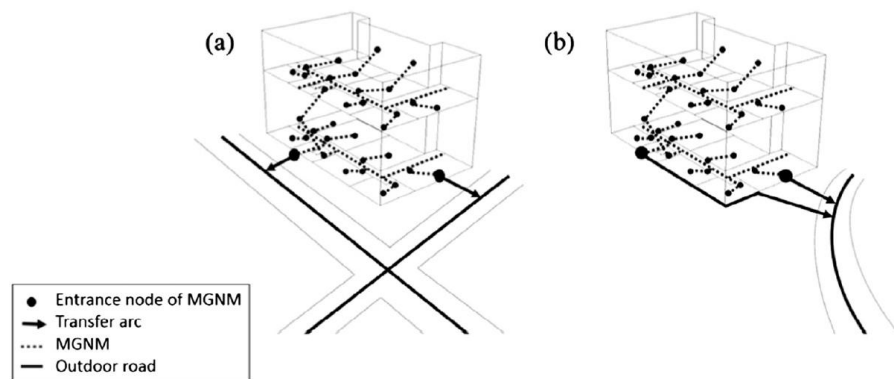
This review mainly focuses on the direction of indoor and outdoor navigation network integration. IndoorGML (this standard will be introduced in Section 2.6.1) and subsequent indoor/ outdoor seamless navigation research based on IndoorGML leverage anchor node to link the indoor navigation network with outdoor navigation network (Figure 2.1(a) and 2.1(b)). In addition, entrance node is another analogous structure for integration (Figure 2.1(c)).



(a) Anchor node in OGC IndoorGML (Lee et al., 2015)



(b) Spatial data fusion based on anchor node (Park, Ahn, and Lee, 2018)



(c) Entrance node used for linking indoor to outdoor (Teo and Cho, 2016)

FIGURE 2.1: Anchor node used for integrating indoor and outdoor navigation network.

## 2.2 The Poincaré Duality Theory

The Poincaré duality (Munkres, 1984) provides a theoretical background for mapping (3D) space to Node-Relation Graph (NRG) (Lee, 2004a) representing topological relationships, i.e., it is the theoretical background of simplifying the complex spatial relationships between (3D) objects by a combinatorial topological network model. As seen in Figure 2.2, a  $k$ -dimensional object in  $N$ -dimensional primal space is mapped to a  $(N-k)$ -dimensional object in dual space. 3D solid objects in primal space are mapped to vertices (0D) in dual space. The common 2D face shared by two solid objects is transformed into an edge (1D) linking two vertices in dual space. Thus, edges of the dual graph represent adjacency and connectivity relationships.

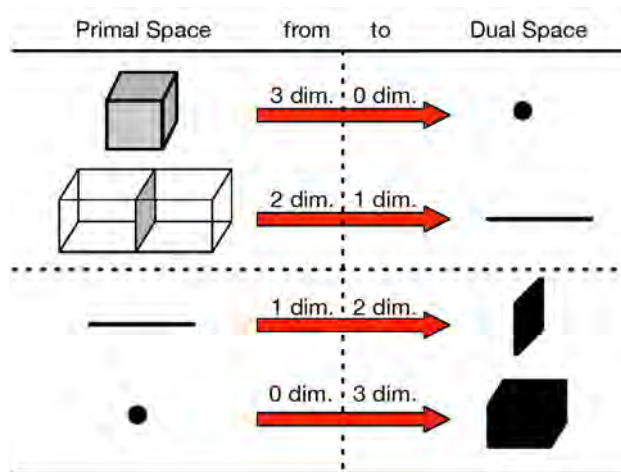


FIGURE 2.2: Poincaré duality theory used for navigation network derivation (Lee, 2004b).

The Poincaré Duality has been utilised as the theoretical basis for indoor (3D) space-based navigation network derivation, such as IndoorGML (Lee et al., 2015). Based on this theory, (3D) spaces (e.g., rooms within a building) are abstracted as nodes, and their connectivity (accessibility) spatial relationships are represented as edges, which may correspond to doors, windows, or hatches between rooms in primal space. For instance, two (room) spaces are represented as 3D volumes in the primal structure with an associated dual node unambiguously representing this space. Adjacent spaces are connected by dual edges bounded by dual nodes (Figure 2.3).

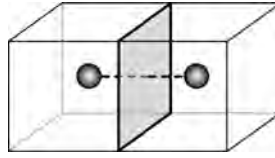


FIGURE 2.3: Based on Poincaré Duality, two room spaces represented by dual nodes are connected by a dual link penetrating a shared face (Zverovich et al., 2016).

## 2.3 Navigation Model

A navigation model is a precondition of navigation path planning (Vanclouster, Weghe, and De Maeyer, 2016). There are two kinds of navigation models, grid-based navigation model (raster) and network-based navigation model (vector) (Liu, 2017), but this research focuses on the network-based navigation model, because it enables lower data processing time which is essential in large scenes both indoor and outdoor space (Krūminaitė, 2014). The network-based navigation model is composed of nodes and edges, in which nodes indicate the locations/places (e.g., landmarks or decision points) and edges between them are their spatial interrelationships. Moving from one node to the other is allowed only when there is an edge between them. Usually cost of edges indicates distance or travel time between nodes (Mortari et al., 2014) and nodes can contain semantic information about the location, such as name, type, description. Furthermore, this network has less detailed routing assuming human intelligence will compensate for inaccuracies (Zlatanova et al., 2014).

Most outdoor navigation models (networks) rely on the available road/street network for vehicles (Millonig and Schechtner, 2007a; Vanclouster, Weghe, and De Maeyer, 2016). In contrast, there is a variety of approaches for indoor navigation network derivation, which are based on the geometric, semantic and topological information of indoor (2D/3D) models (e.g., floor plan, BIM model). Approaches for indoor navigation derivation can be summarised into two types: 2D approaches and 3D approaches.

**Approaches for 2D navigation network derivation.** 2D indoor navigation models represent the indoor spaces and spatial relationships in a simplified way (i.e., 2D NRG),

They carry sufficient information for supporting indoor navigation path planning. Meijers, Zlatanova, and Pfeifer (2005) derives 2D network from 2D floor plans on the basis of Poincaré Duality, Media Axis Transform (MAT) and information about doors (Figure 2.4).

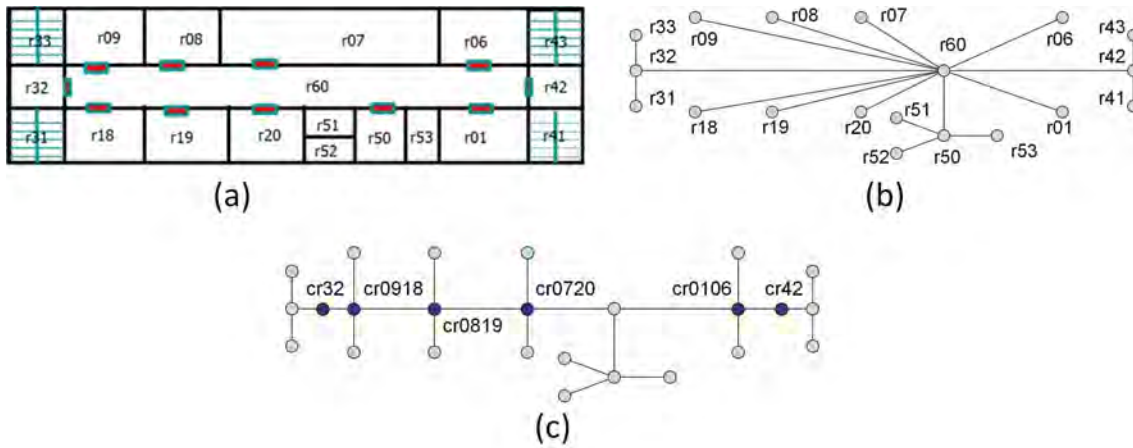


FIGURE 2.4: A 2D network derived on the basis of Poincaré Duality, MAT and information about doors (Meijers, Zlatanova, and Pfeifer, 2005). (a) Floor plan; (b) The metric network derived from connections between spaces; and (c) The corrected metric network considering the corridor graph and door locations.

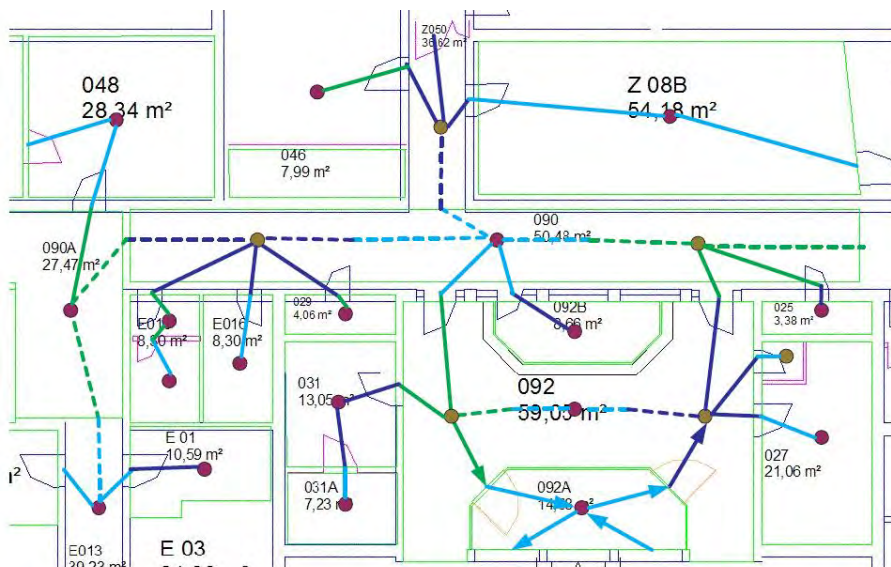


FIGURE 2.5: The 2D navigation network derived on the basis of room and door spaces (Lorenz, Ohlbach, and Stoffel, 2006).

Because this approach may bring in insufficiently detailed paths in the larger areas,

Lorenz, Ohlbach, and Stoffel (2006) modifies this approach by adding doors in the navigation network, i.e., both rooms and doors are considered as spaces and then abstracted as nodes (Figure 2.5). Yang and Worboys (2015) derives a 2D navigation network with the similar modification, but more detailed semantics are assigned to the navigation nodes (Figure 2.6).

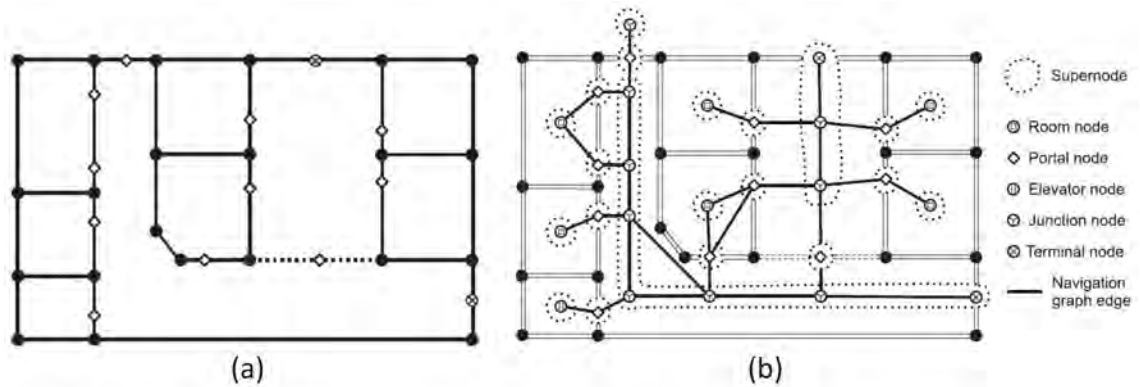


FIGURE 2.6: Indoor 2D network derivation based on duality theory (Yang and Worboys, 2015). (a) An indoor structure graph; (b) Metric navigation network.

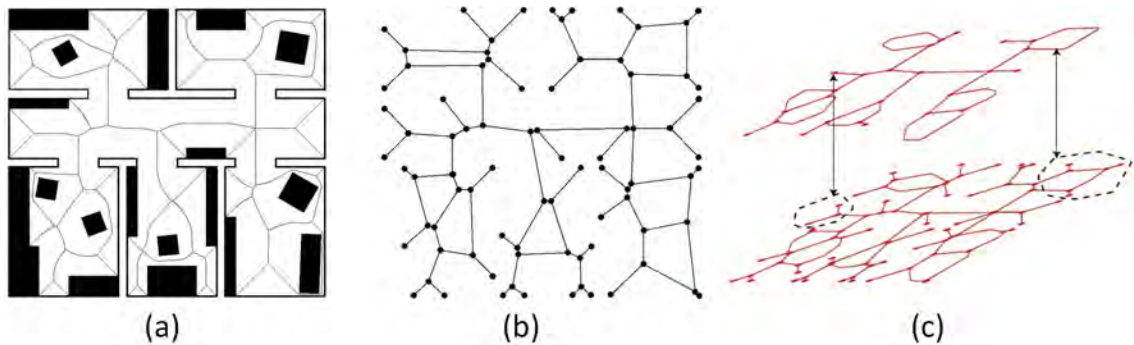


FIGURE 2.7: The navigation network created on the basis of Voronoi diagram (Wallgrün, 2004). (a) original plan, (b) network and (c) simplified network.

The above approaches based on duality and MAT have an assumption that the indoor spaces are empty (i.e. there is no furniture). Thus, Wallgrün (2004) develops an approach of navigation network derivation based on the generalized Voronoi diagram (Figure 2.7). The navigation networks generated by this approach take the obstacles into

consideration, but they have (pure) geometry and the semantics of nodes (such as room, door) are missing.

**Approaches for 3D navigation network derivation** 3D navigation models represent the 3D spaces and spatial relationships with 3D NRG. Deriving 3D navigation models based on 3D spaces has been well-studied in indoor navigation research, such as IndoorGML (Lee et al., 2015), multilayered space-event model (Becker, Nagel, and Kolbe, 2009), 3D object-based navigation (Boguslawski and Gold, 2009), indoor navigation (Zlatanova, Liu, and Sithole, 2013; Diakit  and Zlatanova, 2018), indoor and outdoor combined route planning (Teo and Cho, 2016), route computation for emergency response (Zverovich et al., 2016).

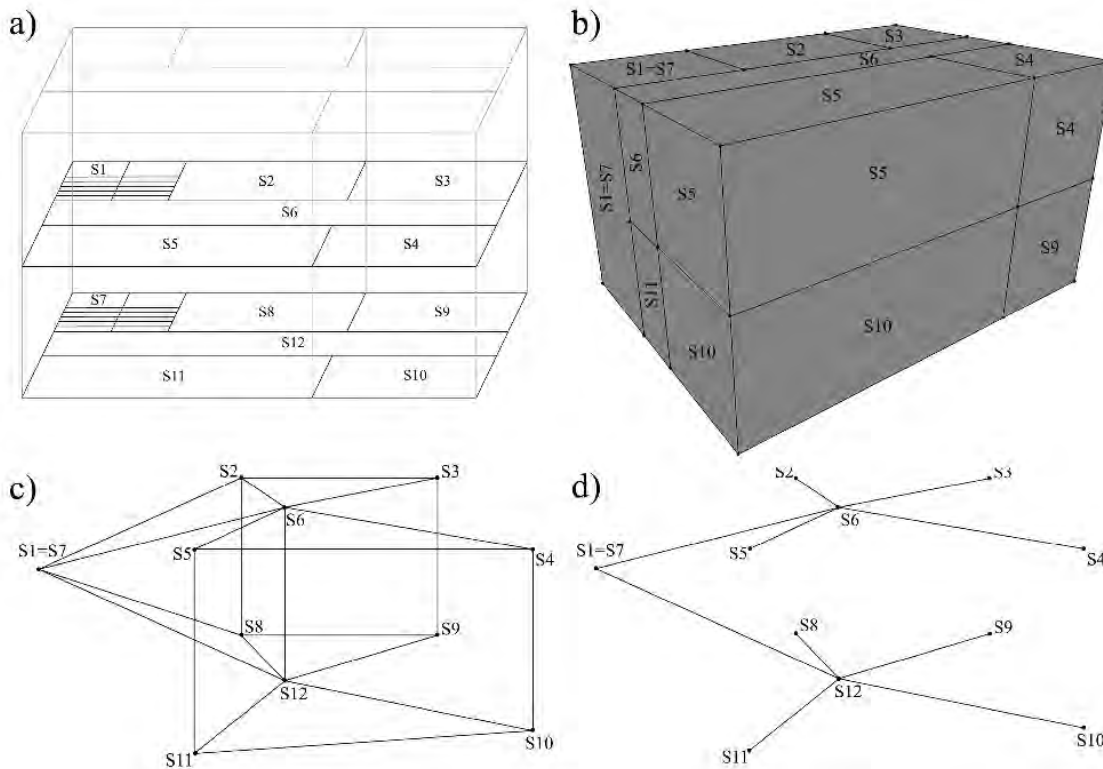


FIGURE 2.8: A 3D network derived on the basis of Poincar  Duality and information about room spaces connectivity (Boguslawski and Gold, 2009). (a) 3D model of a building interior, (b) Room spaces, (c) Complete graph of connectivity of room spaces, (d) network of connections between room spaces based on passages only.

Boguslawski and Gold (2009) presents an approach to derive 3D navigation network based on the geometric, semantic and topological information of 3D models (Figure 2.8).

This approach abstracts each separate room, corridor or stair cage as a node based on the Poincaré duality. Then the network is derived by removing weak connections from complete graph, in which the weak connections means the no passage links (such as S4-S10, S5-S11).

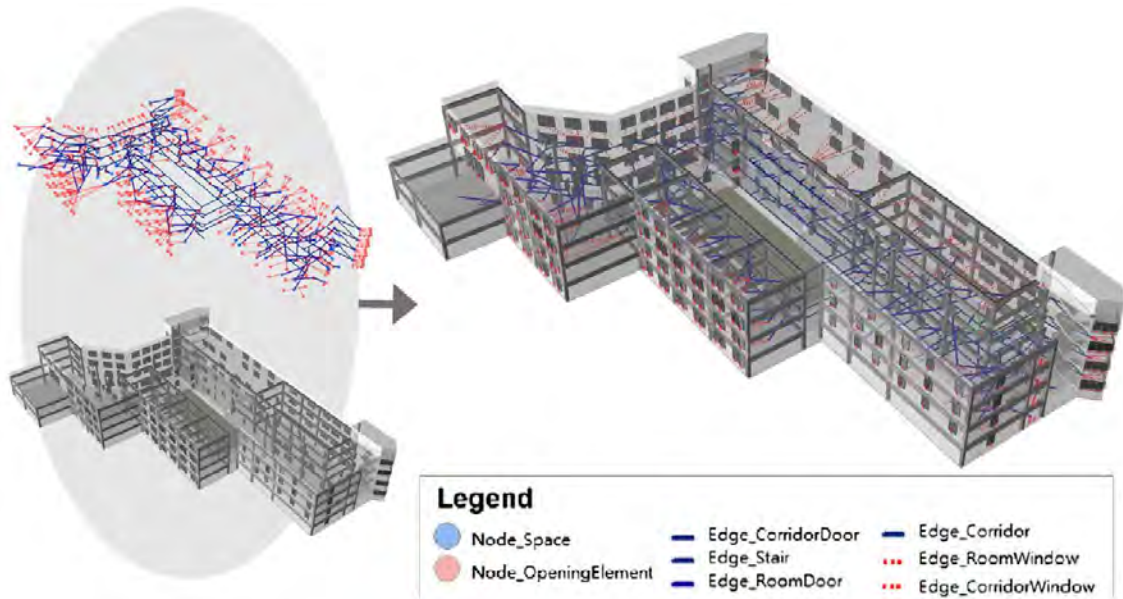


FIGURE 2.9: A 3D navigation network extracted from BIM models (Teo and Cho, 2016).

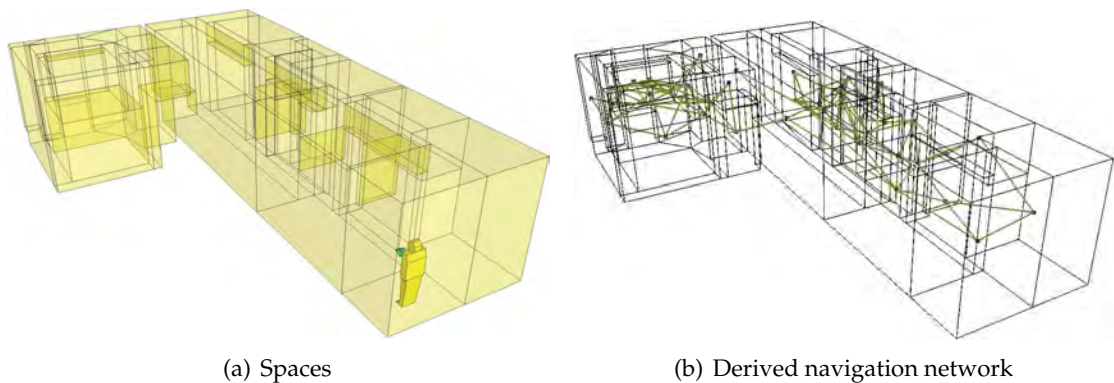


FIGURE 2.10: Example of 3D space-based model for indoor navigation (Diakit  and Zlatanov , 2018).

A similar research on deriving networks is based on BIM models (Teo and Cho, 2016), see Figure 2.9. Because this approach generates very rough networks, Diakit  and Zlatanov  (2018) proposed a method to extract indoor navigation network considering

indoor furniture and the navigable spaces (Figure 2.10). Such a navigation network can support very detailed indoor navigation path planning.

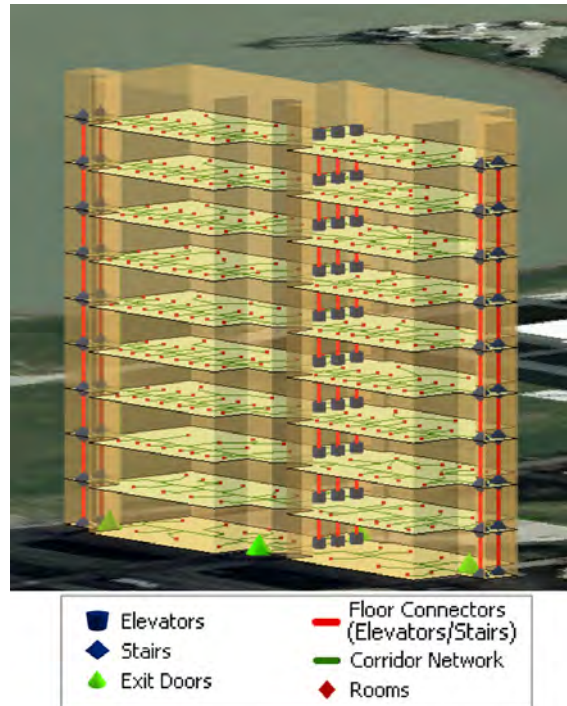


FIGURE 2.11: The navigation network derived from 2D floor plans embedded in 3D space (Thill, Dao, and Zhou, 2011).

A quite special approach to 3D space is embedding 2D navigation networks into 3D spaces and linking them as 3D navigation networks, which is usually for regular buildings. For instance, Thill, Dao, and Zhou (2011) generates a network by stacking up 2D navigation networks on each floor, in which the 2D navigation networks are linked by adding connections between the points where the elevator and staircase are (Figure 2.11). This method is actually not a 3D approach (Zlatanova et al., 2014).

## 2.4 (3D) Spaces for Navigation

Navigation takes place in our living environments, which are abstract. To employ them in seamless navigation, they need to be represented by concrete concepts, such as "space". This section reviews the classifications, definitions and representations of the living environments.

### 2.4.1 The Notion of Space

In spatial science and urban applications, "space" is presented as a notion referencing our living environments. That is, space is used as a general term to help people to understand particular characteristics of the indoor/outdoor environments. This approach is preserved when space is modelled by different disciplines in digital counterparts of the real world. Space is an important notion in the human lexicon aiming to indicate physical or imaginary parts of living environments. WordNet (Princeton University, 2010), one of the largest lexical English databases provides nine meanings of the noun "space", three of which are very relevant to this research (Miller, 1995). Space is "the unlimited expanse in which everything is located", "an empty area, usually bounded in some way between things" and "an area reserved for some particular purpose". These three expressions clearly indicate the diversity in perceiving and describing space: empty or containing things, unlimited or bounded, physical or imaginary.

Most of the English dictionaries provide a more philosophical definition to reflect the fundamental importance of space to the understanding of the physical universe. Dictionaries and lexical databases, such as Oxford Dictionary (Lexico.com, 2019), Merriam-Webster (Merriam-Webster, Incorporated, 2019), Cambridge Dictionary (Cambridge University Press 2019, 2019), Collins Dictionary (Collins, 2019), consider space as "continuous", "boundless" and "empty". But space can also be perceived as a portion of the space, e.g., space in a room. The definitions are not that explicit in specifying whether the spaces are empty or imaginary. The notion of limitless space is expressed by referring to its metrics in a three-dimensional reference frame. The distinction between indoor and outdoor is introduced in a very intuitive way: the space inside of a structure (interior of a house, building, etc.) is indoor space, while the space outside the structure is outdoor space.

In daily life, humans more often refer to portions of space such as areas or locations rather than universal unlimited space. An everyday expression such as "the space is packed with people", "there is no space in this room", "the kitchen space is spacious" suggest that the people tend to think of spaces as singletons (unique and self-contained)

enclosed by physical or imaginary boundaries. The singletons are assigned a broad spectrum of properties, and these properties can range from personal to communal. Ashihara (1981) argues that distinguish between bounded space and unbounded nature space is necessary, in which bounded space is considered to be positive space since it is created to fulfill human (who use this space) intentions and functions while the unbounded nature space is negative. Thence, researchers and developers discretize space into portions to be able to introduce useful properties, represent relations and visualise them (Zlatanova et al., 2014). Examples of such properties are weather conditions (temperature, humidity, wind), accessibility (accessible, partially accessible, non-accessible), or legal rights (right to cross, ownership).

In this thesis, the notion of *Space* will still be used to represent the living environments, but it refers to a bounded portion of space. That is, spaces are the 3D hollow parts bounded by physical or imaginary (non-existing) elements (Isikdag, Zlatanova, and Underwood, 2013). Space is used as the term to model the living environments, and the portion of space is referred to as space unit, space cell or as just space.

## 2.4.2 Space Classification & Definition

### Indoor & Outdoor

Spaces in navigation have been classified as being located either indoors or outdoors. No strict definition for outdoor is found in the literature, except that people regard objects in the open air as outdoor (assuming unbounded from above), such as streets, pavements, squares, rivers. In contrast, research dealing with indoor environments is more explicit with partitioning spaces into cells and attempts to provide formal definitions. For instance, IndoorGML (Lee et al., 2015) defined the space as to be bounded by architectural components, which is similar to the definition that indoor space is a building environment (such as a house, or a commercial shopping centre), where people usually behave in (Afyouni, Ray, and Claramunt, 2010). Zlatanova, Liu, and Sithole (2013) and Zlatanova et al. (2014) defined the indoor space as a place bounded by physical boundaries (e.g., walls, floor, doors) and intended to support human activities. Indoor space is

often referred to as to a physically enclosed space. Underground enclosures, which offer platforms for human activities, are also referred to as indoor space (Yang and Worboys, 2011b). Winter (2012) presented an indoor space definition with the analogy to the human body. The body is a container bordered by the skin. Similarly, the wall, floor, roof, fence can be seen as the "skin". According to these definitions, semi-enclosed spaces such as a veranda or an inner court would be outdoor spaces. Indoor space in (Yang and Worboys, 2011a) refers to a built environment rather than natural. According to these authors, underground cavities (caves, natural passages) would be classified as outdoor. Rüetschi and Timpf (2004) and Rüetschi (2007) investigated wayfinding in the public transportation infrastructure based on traffic networks, in which the authors suggested to classify the environments for navigation into two types: network space and scene space. Network space consists of the public transport network. Scene space consists of the environment at the nodes of the public transport system, through which travellers enter and leave the system and in which they change means of transport. That is, outdoor spaces covered by navigation networks are network space while the spaces between indoor and outdoor are the scene space.

### **Semi-bounded Spaces**

Only a few papers discuss semi-enclosed spaces that cannot be clearly attributed to indoor or outdoor. Examples are covered footbridges, sheds, balconies or partially roofed courtyards. Winter (2012) defined these spaces as transition zones by giving examples and further proposed that ubiquitous navigation must be able to deal with the contrasting properties and conceptualizations of outdoor and indoor environments, and with the spaces in between. Kray et al. (2013) defined these spaces as transitional spaces. There can be also extended environments, potentially vaguely bounded, where a crisp distinction between indoors and outdoors is difficult. More examples are tunnels, enclosed footbridges, or partially roofed courtyards.

As mentioned in Section 1.1.2, the key point of distinguish a semi-bounded space

is the upper boundary, which makes semi-bounded spaces are mostly mentioned in research related to building micro-climates, because the upper boundaries can have a significant influence on the climate of the space. Many papers have discussed architectural designs to improve residential and building micro-climates and reduce cooling and heating energy requirements (Kim, Kim, and Leigh, 2011; He and Hoyano, 2010; Du, Bokel, and Dobbelsteen, 2014; Cao et al., 2017). Typically, three main spaces are identified: semi-indoor, semi-outdoor, and connection/transition/buffer and an attempt is made to provide definitions.

Turrin et al. (2009) defined the covered space as a semi-indoor space, which is partially surrounded by indoor spaces. Van Timmeren and Turrin (2009) presented that a semi-indoor space can be created by using a special roof (Vela Roof) as cover to passively avoid uncomfortable (coldest and overheated) conditions, thereby reducing the energy demand significantly. Moreover, they defined space that is not entirely enclosed by walls, windows, doors, etc. as outdoor. The semi-indoor space defined in the research (Hooff and Blocken, 2009) is a semi-indoor stadium, which has a roof that can be used to close the indoor volume to a relatively large extent. Thus, spectators and equipment are protected from wind, rain, and snow. This space still has direct openings to the outside. In contrast, Bouyer et al. (2007) took the stadium as a semi-outdoor space in the assessment research of thermal comfort. In the research of condensation in residential buildings (Kim, Kim, and Leigh, 2011), semi-indoor spaces are created by installing external windows to balconies in Korean apartment units, which are used as environmental buffer spaces to improve comfort and reduce cooling and heating costs. In the research of the impact of improved cook-stoves on indoor air quality in the Bundelkhand region in India, Chengappa et al. (2007) mentioned the kitchen with 3 walls is semi-indoor compared with outdoor (open-air) kitchen with a makeshift thatched roof for summer. Liu et al. (2013) showed the open space equipped with overhead sheds is semi-indoor spaces, which can provide the citizens with sheltered space for public activities. In their research, they argued that illuminating such a huge semi-indoor space only by artificial lighting is against the energy-saving principle. Thus, they added lighting

ducts to enable natural light to travel through the plate of the collector shed and reach the hall on the ground floor. In South Korea, traditional markets have been enclosed as semi-indoor by installing arcades along street edges to improve their physical environment (Kim, Park, and Kim, 2008), e.g., to alleviate inconveniences caused by inclement weather. Monteiro and Alucci (2007) considered semi-indoor and semi-outdoor spaces are two transitional spaces for thermal comfort. In their examples, a semi-outdoor space is covered by a fabric membrane while semi-indoor space is a studio of 8m high where its roof has 33% of zenital apertures for natural lightning.

In contrast, Pagliarini and Rainieri (2011a) took the space, which is partially open towards the outdoor environment as a semi-outdoor space. They even reinforced the concept that outdoor space partly enclosed by a semi-transparent pitched roof (e.g., glass roof) is a semi-outdoor space in a later research (Pagliarini and Rainieri, 2011b). Spagnolo and De Dear (2003) defined the semi-outdoor as locations that, “while still being exposed to the outdoor environment in most respects, include human-made structures that moderate the effects of the outdoor conditions.” Examples include roofs acting as radiation shields or walls acting as vertical windbreaks. Hwang and Lin (2007) defined the semi-outdoors as exterior spaces that are sheltered and attached to the building. The authors also mentioned that an outdoor environment indicates a space without any covering to provide shelter and an indoor space refers to a naturally ventilated room. The microclimate of the semi-outdoor (partially enclosed space) usually has a lower effect of wind and is less hot than the outdoor (Pagliarini and Rainieri, 2011b). Semi-outdoor spaces in (Turrin et al., 2012) are areas covered by large roofs, leaving a direct connection with the outdoor environment. Museums and cultural centre gardens, university campuses, shopping and leisure areas, hotels and resorts, are a few examples of building environments where covered semi-outdoor spaces are commonly integrated. In (Goshayeshi et al., 2013), semi-outdoor spaces are defined as the spaces which are partly open in the direction of the outdoor. Three categories are introduced: inside the buildings such as entry atrium; covered spaces; shaded spaces, situated in an outdoor environment entirely. Covered streets are regarded in this category. Furthermore, semi-enclosed space (He and

Hoyano, 2010; Kim, Kato, and Murakami, 2001), or semi-open space (Philokyprou et al., 2017) are used to name the space that is not enclosed entirely, and has some settings including human-made structures that moderate the effects of the outdoor conditions.

Some research offered the definitions only by examples. For instance, the bus shelter is a semi-outdoor in (Lin, Matzarakis, and Huang, 2006), because it can offer shelter in the form of a roof. The semi-outdoor space in (Yang, Wong, and Jusuf, 2013) refers to the internal architectural space with maximum exposure to the lobbies, corridors, atrium, courtyards, passages, and verandas. In the research of building microclimate and summer thermal comfort in free-running buildings with diverse spaces, Du, Bokel, and Dobbelsteen (2014) named the space between indoor and outdoor as semi-outdoor space with the example of the space combination of eaves section and courtyard. Similarly, Hwang and Lin (2007) and Lin et al. (2008) defined semi-outdoor as exterior spaces that are sheltered and attached to the building. Balconies are regarded as shaded semi-outdoor spaces to provide the much needed thermal relief to the occupants of flats during the hot seasons (Indraganti, 2010). Ortiz et al. (2015) defined indoor and semi-indoor spaces as GPS-denied environments.

#### **Four Examples of Space Classification and Definition Framework**

In past research, a few space classification and definition framework based on certain rules are introduced, such as spaces are defined and classified based on the buildings, the sensor (e.g., GNSS) reception perspective, or the types of the signal received by the users, or if a space is fully enclosed.

A typical example is the space classifications provided by (Zhou et al., 2012). The authors used lightweight sensing services to analyse indoor/outdoor environments with respect to positioning options for mobile applications. They partitioned and classified space into indoor, semi-outdoor and outdoor (Figure 2.12). The outside of a building is defined as outdoor, while the inside is indoor. Close to or semi-open building space is considered as semi-outdoor.

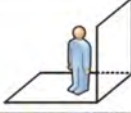
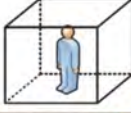
Environment	Outdoor	Semi-outdoor	Indoor
Definition	Outside a building	Near a building	Inside a building
Example			
Scene			

FIGURE 2.12: Space classification based on building (Zhou et al., 2012).

Wang et al. (2016) also provided a space classification according to the reception of the GPS signal as follows: open outdoors, semi-outdoors, light indoors, and deep indoors. As shown in Figure 2.13, areas which have an open sky condition (i.e. unbounded from above) and provide enough satellites for positioning are open outdoors. Areas such as urban canyon or wooded area, are classified as semi-outdoors. Light indoor is similar to semi-outdoor but inside the building. These are areas around windows, which still have some satellite availability. Deep indoors refer to places without any satellite coverage.

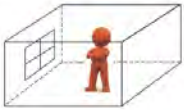
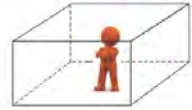
Environment	Open Outdoors	Semi-Outdoors	Light Indoors	Deep Indoors
Definition	Outside a building	Near a building	In a room with windows	In a room without windows
Example				

FIGURE 2.13: Space definition according to the reception of satellites signal (Wang et al., 2016).

Amutha and Nanmaran (2014) developed a visual aid to the visually impaired person, in which they classified the navigation environments into three types, indoor, outdoor, and semi-indoor. The criterion for this space partitioning is the type of signal received by the users. Specifically, outdoor is the space which only can receive GPS signal, indoor is where ZigBee signal (communication protocol) is dominant, and semi-indoor is

the portion of space where both signals can be detected (Figure 2.14).

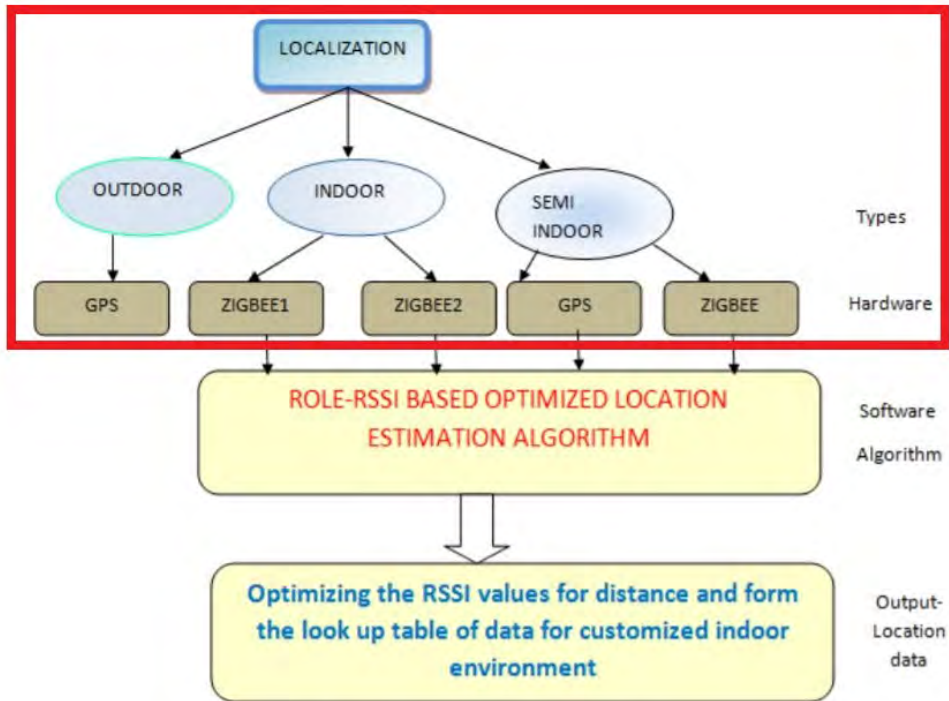


FIGURE 2.14: Space classification based on the type of signal received by the users (Amutha and Nanmaran, 2014).

Based on if a space is (fully) enclosed, Chen and Clarke (2019) suggested classifying and defining spaces into indoor, quasi-indoors, quasi-outdoors, and outdoor (Figure 2.15), but no strict definition is provided. For example, a courtyard surrounded by buildings is quasi-indoors, because the yard is an inseparable part of the surrounding building and should be included as part of the building’s indoor map to ensure continuity in navigation.

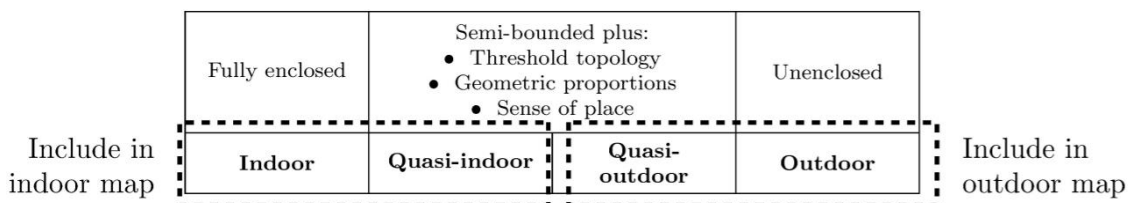


FIGURE 2.15: Space definition framework based on if a space is (fully) enclosed (Chen and Clarke, 2019).

### 2.4.3 3D Space Reconstruction

Space is commonly perceived as having three-dimensions and many of the above-mentioned disciplines progressively attempt to advance the digital space representations to 3D. To be able to manage, analyse and visualise the space, geometric representations are required. Research in indoor navigation is a typical example, although the number of true 3D applications is still limited.

Spaces in indoor navigation are generally modelled as 3D volumes. Many researchers have used 3D geometric representations for space-based indoor navigation model such as IndoorGML (Lee et al., 2015) (Section 2.6.1), multilayered space-event model (Becker, Nagel, and Kolbe, 2009), and 3D object based navigation (Boguslawski and Gold, 2009). Outdoor spaces are generally represented as 2D surfaces as they are naturally unbounded in the Z direction. Only few research papers considered outdoor spaces as 3D and applied 3D geometric approaches. Among the proposed approaches, the most notable one is the Space Syntax (Hillier and Hanson, 1984). It converts outdoor into discrete configurations based on viewshed, axial space and convex space, which are then represented subspaces as maps and graphs that describe the relative connectivity and integration of those spaces. Beirão, Chaszar, et al. (2014) and Beirão, Chaszar, and Čavić (2015) reports a model to subdivide continuous urban spaces into convex and solid voids (3D volumes) for analysis and classification based on physical measures, in which outdoor is roughly classified as urban void and the subdivision procedure is conducted based on convex polygon. Sileryte, Cavic, and Beirão (2017) proposes a versatile data model for analysing urban architectural void, in which space compartmentalization is conducted based on Gestalt theory and its model can be rendered both as a 2D and 3D representation. Jiang and Liu (2010) represented spaces with the axial lines based on the concepts of isovists and medial axes in 2D.

Over the past few decades, the reconstruction of the 3D models has developed very rapidly. For instance, reconstructing 3D spaces from airborne laser scanning data (Haala and Brenner, 1997; Verma, Kumar, and Hsu, 2006), 2D GIS data (Shiode, 2000; Ledoux and Meijers, 2009), aerial photographs and terrestrial laser scans (Fruh and Zakhor, 2001), or

Unmanned Aerial Vehicle (UAV) images (Xie et al., 2012; Yan et al., 2017), etc. Other than that, with the developments of terrestrial laser scans, the approaches for reconstructing indoor details (e.g., floor, ceiling and walls) are considered, such as (Budroni and Boehm, 2010; Previtali et al., 2014; Macher, Landes, and Grussenmeyer, 2017; Nikoohemat et al., 2020). New ways for reconstructing 3D spaces of buildings and cities are being increasingly adopted, supported by international standards such as the IFC or CityGML (these two standards will be introduced in Section 2.6). The current versions of these standards include representations of spaces as 3D objects, but still, this is limited to the indoor environment.

In short, the existing approaches for 3D space reconstruction either mainly focus on building shells or on the interior of buildings only. More importantly, they cannot be used to reconstruct the semi-bounded spaces that are partially or entirely open.

#### 2.4.4 Representation of 3D Space

Spaces are commonly abstracted and represented using Boundary Representation (BRep) (Raghothama and Shapiro, 1998), Constructive Solid Geometry (CSG) (Rossignac, 1987) or Spatial Occupancy Enumeration (Ramakrishnan et al., 1992). While appropriate for realistic visualisation, BRep can fall short in performing spatial operations such as volume validation and computation. Therefore, for many applications Spatial Occupancy Enumeration (e.g., Voxels (Yuan and Schneider, 2010; Nourian et al., 2016; Gorte, Aleksandrov, and Zlatanova, 2019; Aleksandrov et al., 2019)) can be seen as alternative (Li et al., 2018; Gorte, Zlatanova, and Fadli, 2019). There is no strict pattern in which geometric representation is employed in different disciplines. In many cases, the geometry used depends on the geometric expressions of the modelling software, such as GIS (Geographic Information Systems), CAD (Computer-aided Design).

#### **BReps**

A boundary representation (BRep) is a geometric and topological description of the boundary of an object. The object boundary is segmented into a finite number of bounded

subsets, called faces. A face is represented in a BRep by its bounding edges and vertices (e.g., Figure 2.16). Thus, a 3D BRep consists of three primitive topological entities: faces (2-dimensional entities), edges (1-dimensional entities) and vertices (0-dimensional entities) (Powers, Gray, and Green, 1996).

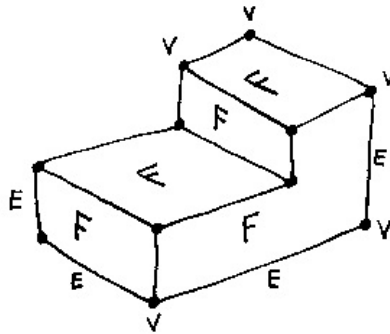


FIGURE 2.16: An example of BReps, in which a solid is represented by F faces, E edges, and V vertices (Bowyer, 1996).

Spaces in indoor navigation are generally modelled as 3D volumes by BReps, such as multilayered space-event model (Becker, Nagel, and Kolbe, 2009), and 3D object based navigation (Boguslawski and Gold, 2009).

### Voxels

Another idea of 3D space representation is using voxels (one kind of Spatial Occupancy Enumeration) (Figure 2.17). Space is modelled by a set of cells with the same size marked as obstacle or non-obstacle.

Based on this representation, navigation paths can be computed by checking the availability of cell movements to their neighbours. This model supports navigation in the 3D space by filling out the indoor space with the obstacle and non-obstacle cubes. The obstacle cubes are further classified into insurmountable and surmountable ones to facilitate 3D navigation. However, the performance of this approach depends on the size of a voxel. If the voxels are too coarse, important information or space might be lost, while fine voxels can increase the time for processing and need more memory to be stored, which could be problematic for outdoor navigation.

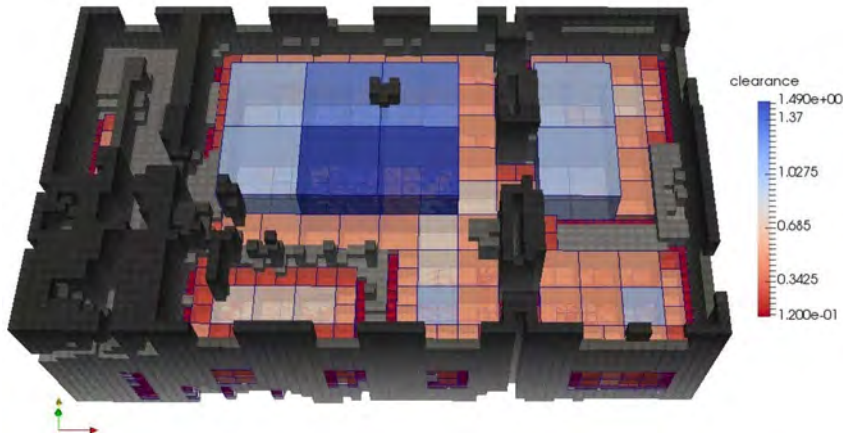


FIGURE 2.17: All spaces including walls are represented by voxels (Rodenberg, Verbree, and Zlatanova, 2016; Li et al., 2019).

## 2.5 Navigation Path

Current navigation systems primarily take the travel distance (shortest) or time (fastest) as the main criteria for optimal path planning (Kimmel, Amir, and Bruckstein, 1995; Dudas, Ghafourian, and Karimi, 2009; Ghafourian and Karimi, 2009), although diverse travel modes are considered, such as walking (Karimi, Jiang, and Zhu, 2013), driving (Millonig and Schechtner, 2007b), transit (Zar and Sein, 2016), and cycling (Howard and Burns, 2001). There are various algorithms can be used for computing the shortest path, such as the Dijkstra algorithm (Dijkstra, 1959), A\* (Zeng and Church, 2009), and Ant colony (Kolavali and Bhatnagar, 2008).

A lot of research have been reported on personalized/agent-tailored navigation paths for different agents, such as simplest (minimum/fewest turns) path (Duckham and Kulik, 2003; Vanclooster et al., 2019), least/most-space-visited, least-obstruction (Liu and Zlatanova, 2013), safe path (Andreev et al., 2015; Balata, Berka, and Mikovec, 2018; Cambra, Gonçalves, and Moura, 2019; Wang and Zlatanova, 2019), health-optimal routing (e.g., specific level of calories burn) (Sharker, Karimi, and Zgibor, 2012), and minimum traffic related air pollution exposure (Alam, Perugu, and McNabola, 2018).



on 3D spaces and network/graph. This standard is the most well-known standard for indoor navigation based on 3D space-based navigation model.

The navigation module of this standard provides semantic information for indoor space to support indoor navigation applications. As seen in Figure 2.18, there are two classes in the navigation module, *CellSpace* and *CellSpaceBoundary*. A *CellSpace* is a semantic class corresponding to one space object in the Euclidean primal space of one layer. A *CellSpaceBoundary* is used to semantically describe the boundaries of each space object. Space features are further classified into two groups: *NavigableSpace* and *NavigableSpaceBoundary*. *NavigableSpace* represents all indoor spaces (e.g. rooms, corridors, windows, stairs) that can be used by a navigation application. *NavigableBoundary* represents all features that connect the navigation spaces (e.g. door).

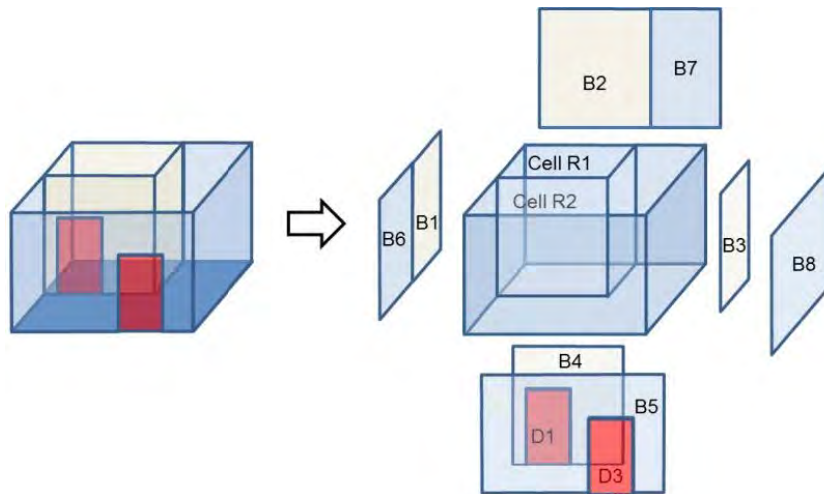


FIGURE 2.19: Example of the indoor space modelling based on Breps in IndoorGML (Lee et al., 2015).

IndoorGML defined the space as a space cell that is bounded by architectural components, which is similar to the common understanding that indoor space is inside buildings (such as a house, or a commercial shopping centre), where people usually behave in. Figure 2.19 illustrates an indoor scene with two rooms and two doors. Then all the building components(walls, doors) and indoor spaces themselves are represented, in which *B1* to *B8* are walls, *D1* and *D2* are doors, while *CellR1* and *CellR2* are two indoor spaces.

IndoorGML covers geometric and semantic properties relevant for indoor navigation in an indoor space. These spaces may differ from the spaces described by other standards such as CityGML and IFC. In this respect, IndoorGML is a complementary standard to CityGML and IFC to support location based services for indoor navigation. It should be noted that although some modifications have been proposed for the IndoorGML navigation model (e.g., Alattas et al., 2018c), this research concentrates on the current version 1.0.3 of the standard.

### 2.6.2 Industry Foundation Classes (IFC)

The most well-known international standard that represents spaces as 3D objects is probably the Industry Foundation Classes (IFC) standard, developed by the International Alliance for Interoperability (IAI) (buildingSMART International Ltd., 1996-2019). In this standard, space is an area or a volume that is bounded by physically or imaginary elements. Spaces are intended to describe certain functions of the building. Commonly, a space in the IFC standard is associated with a building/building storey, which indicates that space is interior. However, it can also be associated with a construction site, case in which that space is exterior. The space definition in Building Information Modelling (BIM) serves therefore for a large number of purposes including calculations of energy use, acoustic analysis, navigation, orientation within the building, egress simulations. Property measurement and valuation-related standards define various types of interior areas and volumes (Kara et al., 2018). These different types of area and volume definitions show various different interpretations of interior spaces in the domain of property and facility management.

As a major data exchange standard for BIM, the IFC standard is able to restore both geometric information and rich semantic information of building components to support indoor navigation. Thus, IFC building models have been used for indoor navigation (Isikdag, Zlatanova, and Underwood, 2013; Lin et al., 2013; Boysen et al., 2014; Tang et al., 2015). Lin et al. (2013) achieved the shortest path planning for 3D indoor spaces based on IFC, in which they extracted both geometric and semantic information of building

components defined within the IFC file, including *IfcSpace*, *IfcWall*, *IfcDoor*, etc., see Figure 2.20.

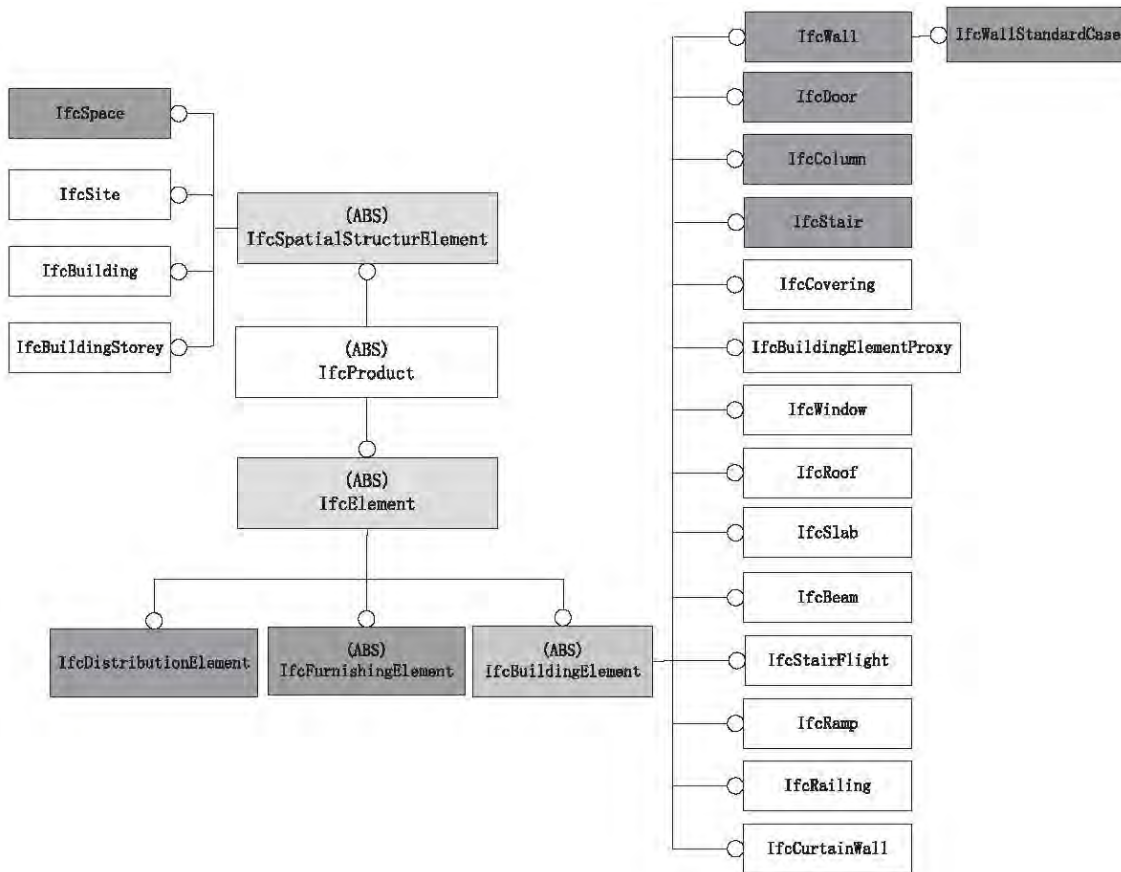


FIGURE 2.20: The hierarchy structure of part of the currently defined elements within the IFC architectural model. The elements that are highlighted in the gray background are processed in path planning (Lin et al., 2013).

### 2.6.3 CityGML

City Geography Markup Language (CityGML) (Gröger et al., 2012) is an OGC standard for an open data model and XML-based format for the storage and exchange of virtual 3D city models. It provides a generic semantic, attributes and relations of a 3D city surface model. This is especially important for cost-effective sustainable maintenance of 3D city models, allowing reuse of data in different application fields. In this standard, a large number of indoor and outdoor physical entities are given digital representations.

Furthermore, One of the targeted application areas of CityGML is vehicle and pedestrian navigation.



FIGURE 2.21: Road areas consist of traffic areas and auxiliary traffic areas (Gröger et al., 2012).

In the current version 2.0 of CityGML, spaces are not explicitly mentioned, but notations as rooms, doors, windows, being represented as volumes indicate that indoor spaces are critical. The road areas consist of traffic areas and auxiliary traffic areas (Figure 2.21). The former includes pedestrian pavements and vehicle lanes, while the latter consists of grass areas and tree areas.

In the CityGML data model, several classes available in that standard make it interesting to work with for the purpose of detecting the semi-bounded spaces with upper boundaries. Building elements like balconies, chimneys, dormers or outer stairs are represented by the *BuildingInstallation* class. The shell based representation provided by the standard gives direct access to interesting components such as *RoofSurface*, *GroundSurface*, *OuterCeilingSurface* and *OuterFloorSurface* (Figure 2.22). Those latter elements are allowed to be encapsulated or referenced by the *boundedBy* property of *BuildingInstallation*, along with *WallSurface* and *ClosureSurface* elements. Other elements of interest, such as *FloorSurface*, *CeilingSurface*, *InteriorWallSurface*, and *ClosureSurface* are more relevant to

the indoor spaces. For this reason, they are allowed to be encapsulated or referenced by the *boundedBy* property of the *Room* class.

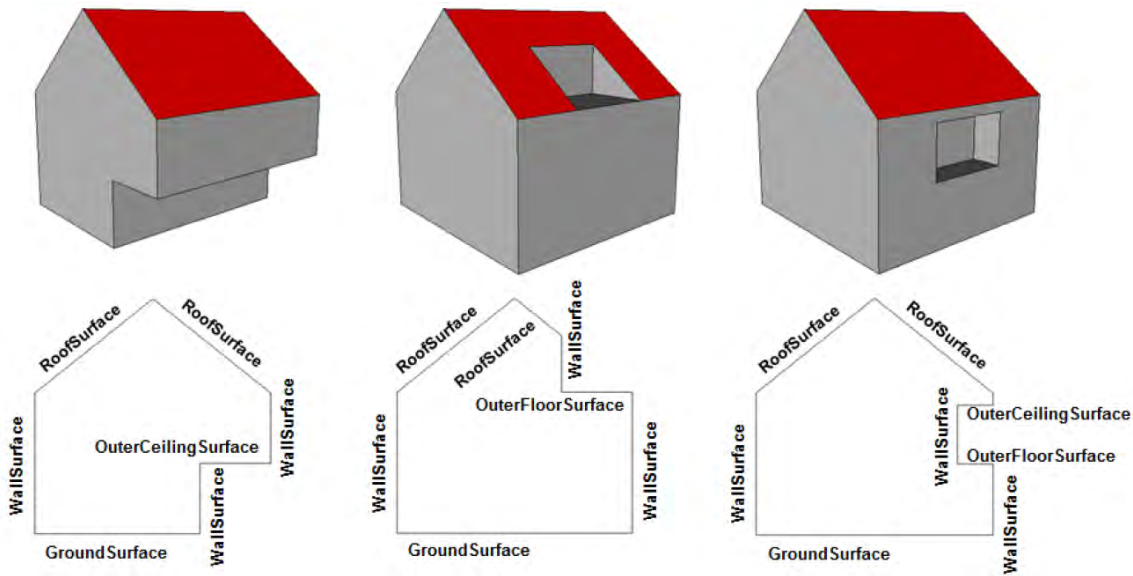


FIGURE 2.22: Buildings components in CityGML shell model (Gröger et al., 2012).

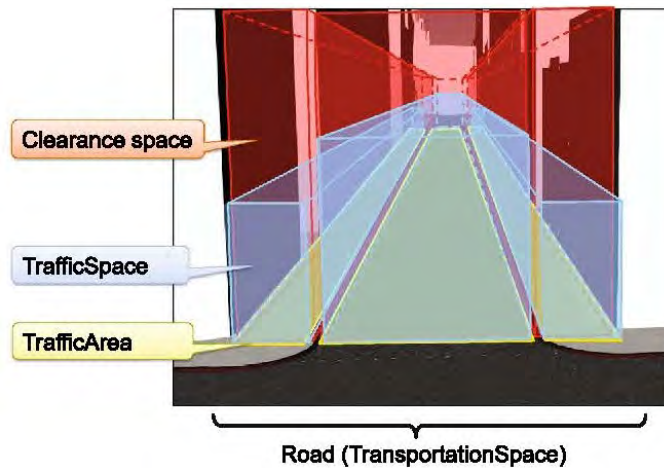


FIGURE 2.23: Representation of a road by 3D spaces in CityGML 3.0 (Kutzner, Chaturvedi, and Kolbe, 2020).

Although some modifications have been proposed for CityGML, this research concentrates on the current version 2.0 of the standard. For instance, the discussions on introducing spaces as a generic class in CityGML 3.0 are on-going (Kutzner, Chaturvedi,

and Kolbe, 2020). A road is represented to have a driving lane and two sidewalks (Figure 2.23). Then, the free spaces above the driving lane and the sidewalks are traffic spaces (in blue); whereas, the ground surfaces (in green) are utilized as the lower boundary of the traffic spaces. Moreover, the height of the traffic spaces and sidewalks spaces are set as 4.5 m and 2.5 m respectively based on the standard heights of roads in Germany. In addition, it also represents the clearance spaces in red.

## 2.7 Summary

The current seamless navigation practice that integrating indoor and outdoor navigation network might be useful in specific situations, but seamless navigation is still not full maturity. The general “unified” navigation model that integrating IndoorGML and outdoor road/street-based navigation network is insufficient for the path planning of seamless indoor-outdoor navigation. We argue that it is beneficial to utilize a unified 3D space-based navigation model for seamless navigation in all living environments. Despite that different types of environments are different in several aspects (e.g., scale and dimension, landmarks, positioning technologies), they are the same from the perspective of navigation.

The main sources of the outdoor navigation networks are still road/street networks, which often lead to incorrect or even restrictive paths (Bodgan and Coors, 2009). This can be explained by the fact that the semi-bounded spaces are failed to be classified, modelled and included in the navigation networks. As a result, the agents are guided to have undesirable detours during their navigation, e.g., although agents can go through a square directly, they are guided to have detours around it. Considering the navigation is the continuous movement of agents from one 3D unoccupied and accessible space to another, and all living environments can be observed as spaces, we argue that if these missing 3D spaces into the navigation network can be added, the shortcomings mentioned above would be avoided.

The environments are commonly classified and defined as indoor and outdoor, and

space is the proper term to represent/abstract environments. The semi-bounded spaces are also considered in current research, especially in the field of building micro-climate and thermal comfort, but they are still not well-defined.

Navigation happens not only in indoor and outdoor but also in semi-bounded environments. Thus, it is necessary to abstract/reconstruct all environments as 3D spaces, although the formal 3D space reconstruction approaches are very limited. Existing approaches are focused either on 3D building shells or on the bare terrain. As a result, terrain and 3D objects are maintained independently and integrated only for specific purposes.

Seamless navigation path types are still insufficient. Although many personalized or agent-tailored navigation paths are developed, almost all these navigation path types are dedicated to either indoor or outdoor, rather than to seamlessly cover both. It can be explained navigation systems are originally customized for indoor or outdoor only, and another aspect is that they lack information about spaces for specific navigation purposes.

All three international standards represent 3D geometry according to the well-known Breps to avoid redundancy. IFC and IndoorGML utilise 3D spaces to represent living environments. IndoorGML shows that the 3D space-based navigation network can support indoor navigation. Thus, although IndoorGML is dedicated to indoor navigation only, it is possible to extend *CellSpace* and *CellSpaceBoundary* in the navigation module to reflect all possible spaces (indoor, outdoor and semi-bounded) and their boundaries to support seamless navigation path planning.

# CHAPTER 3

---

## CONCEPTS AND TERMINOLOGY

---

This chapter introduces the concepts and terminology that are used in this research. Using existing terms is the first choice, but either no existing terms can precisely convey or there are no appropriate existing terms to represent the information this research wants to present. For example, calling the structure that looks like a roof but only used for reinforcement (e.g., Figure 4.8(a)) as a roof is inappropriate. Therefore, several new terms are introduced in the second section.

The first section presents five existing concepts employed in this research, in which agent is elaborated to clarify the recipients of navigation services. Other than that, footprints, building height, terrain, and terrain intersection curve (TIC), which are related to the 3D space reconstructions are included (Chapter 6). In the second section, eleven new terms introduced by this research are presented, which consists of top, side, bottom, topClosure, bottomClosure, sideClosure, gradient, physical boundary, virtual boundary, space radius, and space height. They are introduced as the basic terms of the generic

space definition framework (Chapter 4), attributes for the unified 3D space-based navigation model (Chapter 5), and parametrized indicators of space size to help with selecting spaces for navigation (Section 7.4). This chapter is partly based on my papers 5, 6, 7 and 8 (see Section 1.6).

## 3.1 Existing Concepts

### 3.1.1 Agent

Agents are users that use or engage in navigation activities or use resources offered by spaces. Agents can be broadly categorised as humans and robots. Further based on their locomotion modes, they can be classified into walking (pedestrians), rolling (e.g., trolleys, wheelchairs), flying objects (e.g., drones) or combinations of these. In navigation, agents can vary in size and height and have certain requirements for spaces. Thus, agents should not be regarded as 0D points in the navigation, but 3D objects.

The path planning tests of this research are conducted based on a pedestrian. The definition of a pedestrian is a person travelling on foot, walking or running. Persons who travel on tiny wheels such as roller skates, skateboards, and scooters or on the wheels of self-balancing scooters are not considered as pedestrians because they have lost the flexibility of pedestrians. For instance, pedestrians can walk on stairs, but persons using (tiny) wheeled devices cannot unless they revert to travelling on foot.

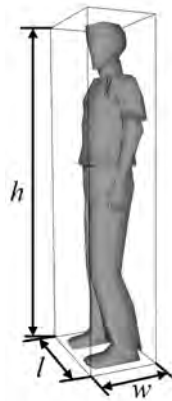


FIGURE 3.1: A pedestrian is modelled as a 3D object.

In this thesis, a pedestrian is abstracted as a cuboid that has a length ( $l$ ), width ( $w$ ), and height ( $h$ ) (Figure 3.1). According to the literature, moving people need extra buffer space around them (Neufert et al., 1980), and they like to maintain a certain distance from walls and obstacles as a comfort distance (Bosina et al., 2016). The two kinds of buffer distances are denoted by  $l_{buf}$  and  $l_{com}$  respectively. As seen in Figure 3.2, the slash-filled parts are physical structures, e.g., roofs and walls. The dashed lines indicate the virtual boundaries of the space. Dot-filled ( $l_{buf}$ ) and grid-filled ( $l_{com}$ ) parts are buffer and comfortable distances respectively. Furthermore, taking the length direction as an example, space can be classified into three cases based on the number of sides, in which (a) has 0 side, (b) has 1 side, and (c) has 2 sides.

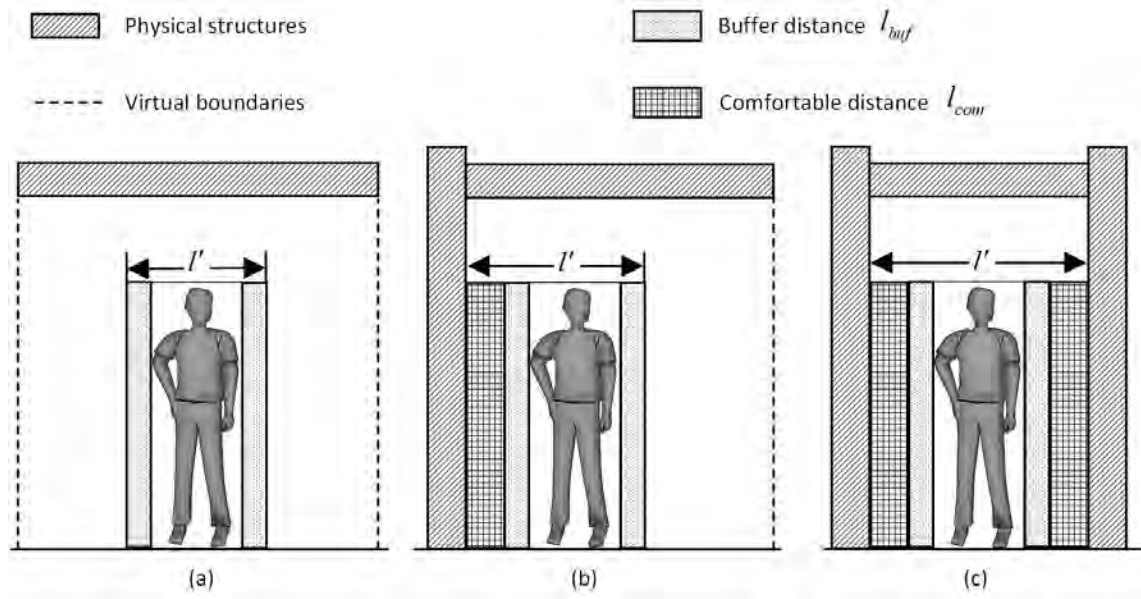


FIGURE 3.2: The size of the space required by a pedestrian.  $l', w', h'$  describe the size of space required by an agent whose size is  $l, w, h$ . The buffer and comfortable distances of width are not illustrated as the figures are side views.

Thus, the minimum size of the space required by a pedestrian becomes  $\{l', w', h'\}$ , which can be computed by Equation 3.1.

$$\begin{cases} l' = l + 2l_{buf} + k_l * l_{com} \\ w' = w + 2w_{buf} + k_w * w_{com} \\ h' = h + h_{buf} \end{cases} \quad (3.1)$$

where  $l, w, h$  = size of a pedestrian

$l_b, w_b$  = buffer distances required by a moving pedestrian

$l_c, w_c$  = comfortable distances required by a pedestrian to side(s) and/or obstacles

$k_l, k_w$  = number of side(s) along the length and width ( $k_{l,w} = \{0, 1, 2\}$ )

$h_{buf}$  = the buffer height required by a moving pedestrian

$l$	$w$	$h$	Description	Examples
625~875	375	> 2000	Stand uprightly	
625~875	750	> 2000	Side by Side With back pack(s)	
800~2125	550~725	> 2000	With suitcase(s) or handbag	
750~2375	375~1125	> 2000	With walking stick or umbrella(s)	

FIGURE 3.3: Dimensions and space requirements based on body measurements (unit:  $mm$ ). This figure is made based on the figures in Architects' Data (Neufert et al., 1980).

On the basis of the size of a pedestrian (Figure 3.3) and the two types of buffer distances for a moving pedestrian, the parameters for a pedestrian are shown in Equation 3.2. The extra buffer space is considered in this research is 10% of the pedestrian size (Neufert et al., 1980). The comfort distance is set as 10cm, because Bosina et al. (2016)

found that pedestrians like to maintain around 10cm from walls and obstacles during walking.

$$\left\{ \begin{array}{l} l, w, h = 625, 375, 1930 \\ l_{buf}, w_{buf} = 62.5, 37.5 \\ l_{com}, w_{com} = 100, 100 \\ h_{buf} = 19.30 \end{array} \right. \quad (3.2)$$

Then, considering that spaces generally are one or two side bounded, i.e.,  $k_{l,w} = \{1, 2\}$ , a pedestrian is modelled as a 3D object with length ( $750mm < l' < 850mm$ ), width ( $450mm < w' < 650mm$ ), and height ( $h' > 1949.3mm$ ) (Equation 3.3).

$$\{l', w', h'\} = \left\{ \begin{array}{ll} 850, 450, 1949.3 & k_l = 1 \ \& \ k_w = 0 \\ 950, 450, 1949.3 & k_l = 2 \ \& \ k_w = 0 \\ 750, 550, 1949.3 & k_w = 1 \ \& \ k_l = 0 \\ 750, 650, 1949.3 & k_w = 2 \ \& \ k_l = 0 \end{array} \right. \quad (3.3)$$

### 3.1.2 Footprints

A footprint is the shape (e.g., 2D polygon) representing projection of something (e.g., building) on a 2D plane (e.g., ground). The building footprint is the area used by the building structure, which is defined by the perimeter of the building plan (Farlex, Inc, 2003-2019). The building footprint is fundamental for a number of urban precinct modelling tools such as the Envision Scenarios Planner (Trubka et al., 2016). Except buildings, city objects, such as streets and green areas, also have footprints (Beil and Kolbe, 2017).

Footprints of city objects can be found in a large number of different data sets, e.g., Open Street Map (OSM) (Fan et al., 2014), or reconstructed from airborne LiDAR data (Zhang, Yan, and Chen, 2006; Hammoudi, Dornaika, and Papanoditis, 2009), or extracted from digital surface models (Brédif et al., 2013).

The footprints in this thesis are 2D polygons that represent projections of city objects, including buildings, shelters, roads, green areas, hand railings, enclosing walls, and fences.

### 3.1.3 Building Height

Building height is a term to describe the vertical height of the building from the ground. The building height is a piece of critical information for 3D building shell model reconstruction based on the extrusion of footprints. Flat roofs or the accurate roofs may bring in different heights for a building, which will result in different building shell 3D models.

There are different ways to define the height of building, only the selection process of the starting point is slightly different. For instance, Center (2002) defined the building height as the average maximum vertical height of a building or structure measured at a minimum of three equidistant points from finished grade to the highest point on the building or structure along each building elevation. Architectural elements such as parapet walls, chimneys, vents, and roof equipment are not considered as part of the height of a building or structure (Figure 3.4).

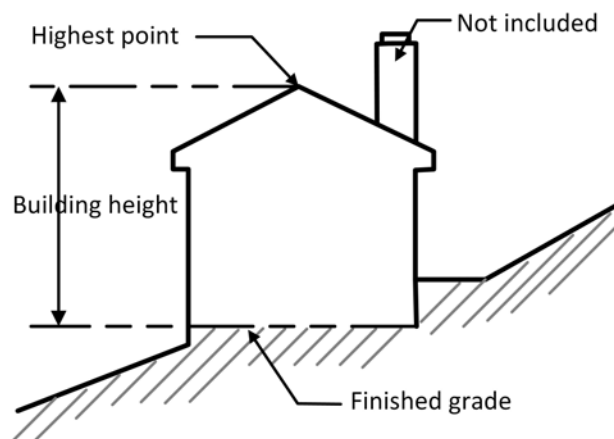


FIGURE 3.4: The building height defined by Center (2002).

Another way of measuring the building height is based on the highest and lowest foundation points, if there is less than 3 metres elevation change between these two

points, the height of the building is the distance from the highest foundation point to the highest point of the building, otherwise, the height becomes the distance between the lowest foundation point and the highest point<sup>1</sup>. For example, if the elevation changes between *A* and *B* for less than 3 metres (Figure 3.5), the height of the building is the distance from the highest foundation point (*A*) to the highest point of the building (*D*), otherwise the height becomes the distance between *B* and *D*.

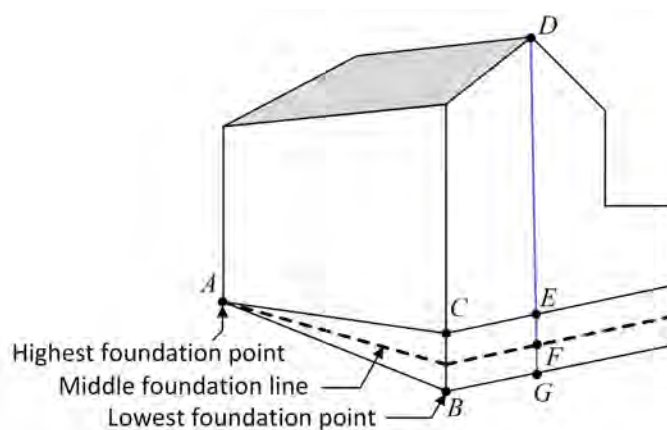


FIGURE 3.5: The rule of measuring building height. The *A* and *B* are the highest and lowest foundation points respectively, *C* and *E* are on the same plane with *A*, *F* is the mid-point of foundation, and *D* is the highest point of the building.

This thesis considers the height of a building is the distance from the mid-point of the foundation to the highest point of the roof, no matter if the elevation change between the highest foundation point and lowest foundation point is more/less than 3 metres. For instance, the height of the building in Figure 3.5 is the distance between *F* and *D*. Therefore, the definition of building height is: the average maximum vertical height of a building or structure measured at a minimum of three equidistant points from mid-point of foundation to the highest point on the building or structure along each building elevation. Architectural elements of a building or structure, such as parapet walls, chimneys, vents, and roof equipment are not considered part of the height of a building or structure.

<sup>1</sup>[http://centralpt.com/upload/375/4785\\_Buidling%20Height%20Definition.pdf](http://centralpt.com/upload/375/4785_Buidling%20Height%20Definition.pdf)

### 3.1.4 Terrain & Terrain Intersection Curve (TIC)

A terrain is referred to as ground or a tract of ground, especially with regard to its natural or topographical features or fitness for some use (Collins, 2019). In the digital domain, the Earth's surface is commonly modelled by means of Digital Terrain Model (DTM) (Brandli, 1996), such as Triangulated Irregular Network (TIN), which is an efficient alternative to the dense grid Digital Elevation Model (DEM) to present terrain surface (Lee, 1991). It represents a surface formed of non-overlapping contiguous triangular facets that are with irregular sizes and shapes, which can describe in an intuitive way the continuous elevation changes of terrain. There are other alternative names, which also may represent different products, such as Digital Height Model (DHMs), Digital Ground Model (DGMs), as well as Digital Terrain Elevation Models (DTEMs). In this research, a terrain is a DTM that represented by Constrained Delaunay triangulation (CDT).



FIGURE 3.6: *TerrainIntersectionCurves* (TIC) in CityGML. The TIC is shown in bold black curve.

*TerrainIntersectionCurve* (TIC) is a curve that indicates where 3D objects are touching the terrain (Figure 3.6), which is introduced by the CityGML to address the topological issue that the 3D objects may float over or sink into the terrain will occur when integrating 3D city objects with the terrain. That is, the terrain is locally fixed to fit the TIC. In this research, the TIC ensures correct positions and topological relationships between

reconstructed 3D spaces and the DTM.

## 3.2 New Introduced Terminology

As seen in IndoorGML (Section 2.6.1), a *CellSpaceBoundary* is used to semantically describe the boundary of each *CellSpace* object. In other words, all of the boundaries share the same name "*CellSpaceBoundary*". On closer inspection, they are different. For the (room) space, walls act as surrounding boundaries, roofs as upper boundaries, and the floors as lower boundaries. To give formal names, several terms are introduced to define and distinguish the boundaries and their attributes. Furthermore, it is also necessary to characterize size and bottom slope of spaces to determine whether they can be used for navigation, that is, those spaces that are too small to accommodate a pedestrian or whose bottom is too steep for pedestrians to stay on its bottom surface need to be excluded. In this section, they are given precise and detailed definitions.

### 3.2.1 Generalized Terms for Building Structures

Roof, wall, and floor/ground are three basic building elements, which play critical roles in defining the structural boundaries for spaces. To allow more complex boundary configurations to be considered, this research employs three generalized notions instead: *Top*, *Side*, and *Bottom* to replace the three building elements. For example, a roof is a top while the opposite is not always true. Similarly, a wall is always a side, but a side is not necessarily a wall.

**Top:** A top is a structure above the ground, with the capability to cover a space under it. It provides a physical or virtual upper boundary to a space. A physical top can stand as (i) protection from weather conditions (e.g., rain, wind, cold, heat) or (ii) a limitation to estimate clearance (e.g., for flying or carrying large items). The areas delineated with red rectangles in Figure 3.7(a) and 3.7(b) illustrate respectively a roof and a top. The top can be a human-made or natural structure/object (e.g., wood, stone, tree).



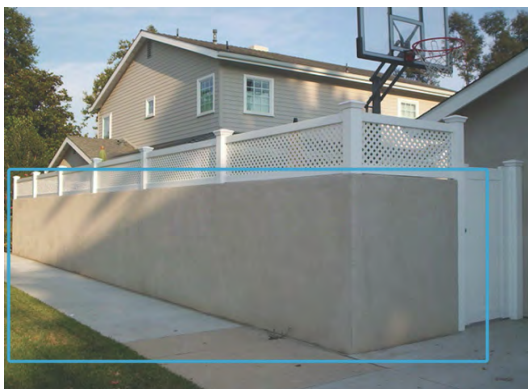
(a) Roof



(b) Top

FIGURE 3.7: Example of roof and top (red rectangles).

**Side:** A side is a structure that encloses a space from lateral directions. It stands as a physical or virtual surrounding boundary of a given space. A physical side can act as (i) protection from weather conditions (e.g., wind) or (ii) a limitation to estimate entering possibilities (e.g., getting around to find a door, or flying above). To a certain extent, a physical side is more like a fence, although it may have similar functions as a wall, such as carrying a load (e.g., load-bearing pillars). A side can be used to delimit or prevent people to enter or exit. The blue rectangles in Figure 3.8(a) and 3.8(b) illustrate respectively a wall and a side. Similarly to a top, a side can be man-made (e.g., wall, fence) or a natural structure/object (e.g., tree, river).



(a) Wall



(b) Side

FIGURE 3.8: Example of wall and side (blue rectangles).

**Bottom:** A bottom is a structure that encloses a space from the lower direction and

offers a platform where pedestrians can stand on it. Similar to the two former structures, a bottom can be an artificial (e.g. floor or slab) or a natural structure/object (e.g., ground). In this work, the ground/floor is assumed to be the default bottom structure and has always been assumed to be present. That is, space starts at the bottom. If there is no bottom, there is no space. The areas marked by white arrows in Figure 3.9(a) and 3.9(b) illustrate respectively a floor and a ground.



FIGURE 3.9: Example of floor and ground (marked by white arrows). Both act as the bottoms of spaces.

### 3.2.2 Closure of Generalized Building Structures

To quantify the level of closure of the three structures, three other notions *topClosure*, *sideClosure*, and *bottomClosure* are introduced, in which the notion of *sideClosure* has been reported in the research (Beirão, Chaszar, and Čavić, 2015). The closures are three coefficients that have only numerical values. Their definitions are the following:

**topClosure** ( $C^T$ ): the topClosure is a coefficient that expresses how much a space is physically bounded from its top. It corresponds to the ratio between the substantial (material) area and the entire area of the top boundary structure.

**bottomClosure** ( $C^B$ ): the bottomClosure is a coefficient that expresses how much a space is physically bounded on its bottom. It is then the ratio between the substantial (material) area and the entire side area of the bottom boundary structure.

**sideClosure ( $C^S$ ):** the sideClosure is a coefficient that expresses how much a space is physically bounded on its sides. It is defined as the ratio between the length of side parts physically enclosed by substantial (material) and the total side(s) length.

The  $C^T$  and  $C^B$  are similar, which can be computed by the Equation 3.4. The  $C^S$  can be computed by Equation 3.5.

$$C^{T/B} = a_e/a_t \quad (3.4)$$

where  $C^{T/B}$  corresponds to either  $C^T$  or  $C^B$ , while  $a_e$  and  $a_t$  are the area of the enclosed part, and the total area of the top/bottom respectively.

$$C^S = l_e/l_t \quad (3.5)$$

where  $C^S$  corresponds to sideClosure, while  $l_e$  and  $l_t$  are the length of physically enclosed part of surrounding boundary and the total length of surrounding boundaries respectively.

Two simplified cases are employed to visually illustrate the computations of the  $C^T$ ,  $C^B$  and  $C^S$  (Figure 3.10). In the two cases, the slash-filled parts are physical structures, while the rests are empty.

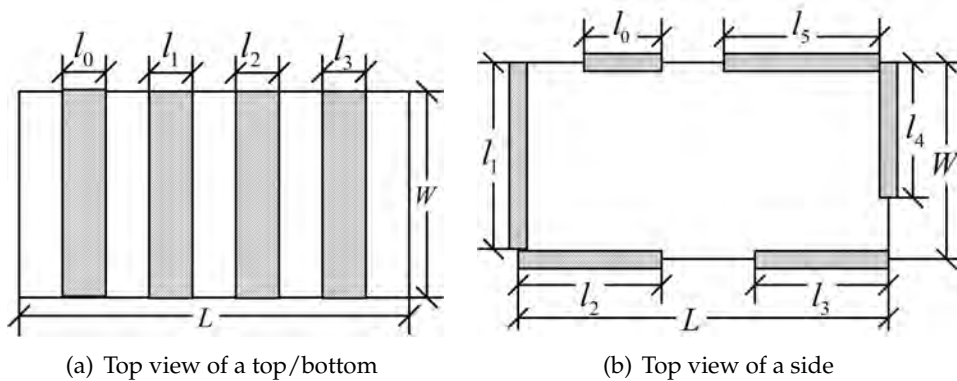


FIGURE 3.10: Illustration of closure computation, in which the slash-filled parts are physical structures.  $l_0$  to  $l_5$  are the length of the physically closed parts;  $L$  and  $W$  are the length and width of the top/bottom/side respectively.

The first case (Figure 3.10(a)) illustrates the closure computation of top/bottom, in which the area of the enclosed part is  $a_e = l_0 * W + l_1 * W + l_2 * W + l_3 * W$  while the total area of the top/bottom is  $a_t = L * W$ , thus, the top/bottom closure of the case can be computed based on Equation 3.4, i.e.,  $C^{T/B} = a_e/a_t = (l_0 * W + l_1 * W + l_2 * W + l_3 * W)/(L * W)$ .

In comparison, the  $C^S$  of the case (Figure 3.10(b)) is  $C^S = l_e/l_t = (l_0 + l_1 + l_2 + l_3 + l_4 + l_5)/(2L + 2W)$ , in which the length of physically enclosed part of surrounding boundary is  $l_e = l_0 + l_1 + l_2 + l_3 + l_4 + l_5$  and the total length of surrounding boundaries is  $l_t = 2L + 2W$ .

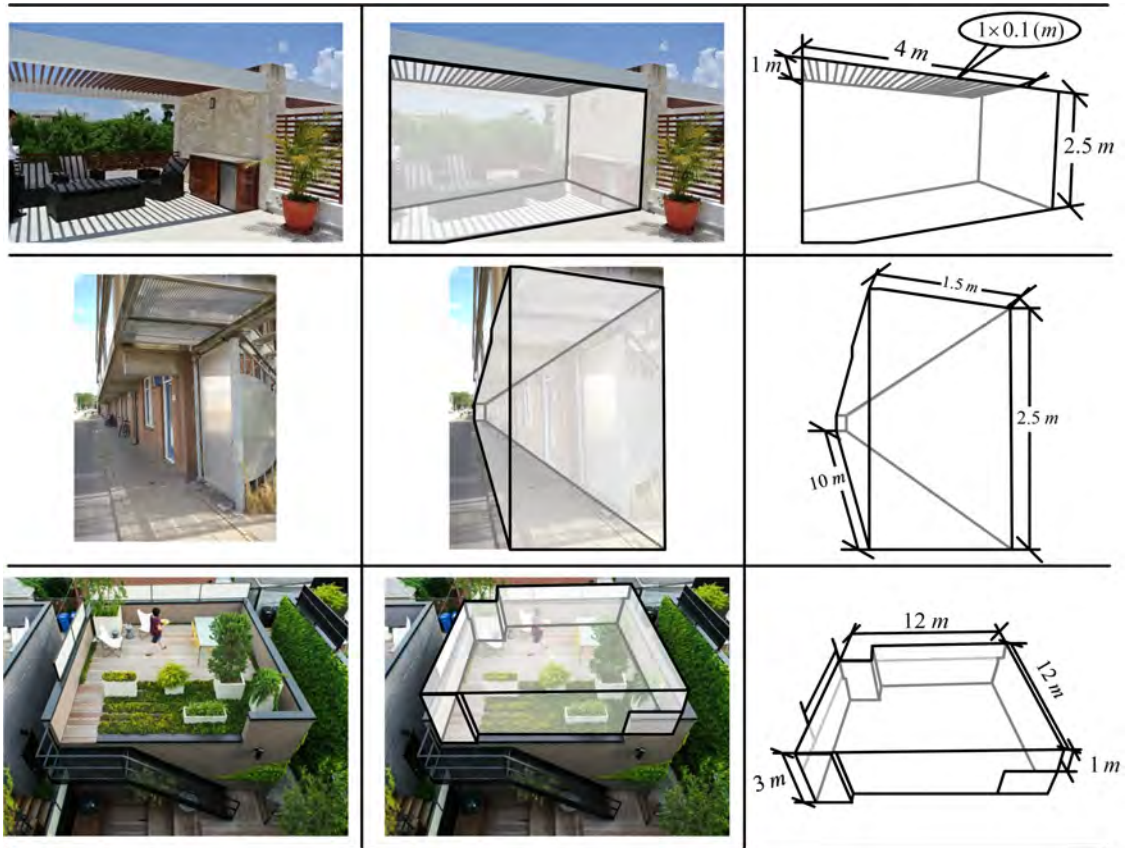


FIGURE 3.11: The abstraction of top, side, and bottom, and estimation of their closure.

Figure 3.11 illustrates how the top, side, and bottom are abstracted and how the  $C^T$ ,  $C^S$  and  $C^B$  are estimated for three real built structures. The spaces are sketched as closed boxes. We estimate the area of each polygon of the box, compute the closure per polygon

and average the closures when more than one polygon is involved.

The first case is a pergola, which has dimensions  $4 * 1 * 2.5 = 10$ . The total area  $a_t$  of the top is  $4 * 1 = 4$  and  $a_e$  is 2.5, because the top has 25 beams (each is  $1 * 0.1$ ). Thus,  $C^T = a_e/a_t = 2.5/4 = 0.625$ . The space has four sides and one bottom, in which two sides are concrete walls (length of each is 1), and another two sides (each is 4) are entirely open. Therefore,  $C^S = l_e/l_t = 2/10 = 0.2$ , where  $l_e = 1 * 2 = 2$  and  $l_t = 1 * 2 + 4 * 2 = 10$ . The bottom of this case is the part of the top projected vertically on the ground, thus,  $C^B = 1$ . The second case is an eave case, thus its  $C^T$  is 1. This space has one totally enclosed side (each is 10) and three open sides ( $10 + 1.5 * 2$ ). Therefore, the average of the four enclosures is computed and  $C^S = 0.43$ . Similar to the first case, the bottom of this case is the part of the top projected vertically on the ground, thus its  $C^B = 1$ . The third case is a roof terrace. The space has dimensions  $(12 * 12 * 3)$ . It has no top, hence its  $C^T = 0$  and  $C^S = 0.93$ . The  $C^B$  of this case is also 1.0, but the bottom of this case is the whole roof.

### 3.2.3 Gradient

Some built structures have slopes (e.g., inclined roofs/pavements to permit rainwater to run off), and these structures also may act as the top, side or bottom of some spaces. In other words, boundaries can be tilted at an angle. The gradient is marked as (**G**). This characteristic of a boundary is introduced to distinguish the side from top and bottom, specifically, if the **G** of a boundary is  $90^\circ$ , it is a side, otherwise, it is a top or bottom. Furthermore, this term can help to consider whether the slope of a bottom is moderate enough to ensure agents can have activities on it.

The **G** of a (polygon) component is referenced to a virtual  $XY$  plane. The normal vectors of a component and virtual  $XY$  plane are  $\vec{A} = (a, b, c)$  and  $\vec{B} = (0, 0, d)$ , respectively (Figure 3.12). Then, the gradient can be calculated by Equation 3.6, where the unit is degrees:

$$\mathbf{G} = \arccos\left(\frac{|c \times d|}{d\sqrt{a^2 + b^2 + c^2}}\right) \times \frac{180}{\pi} \quad (3.6)$$

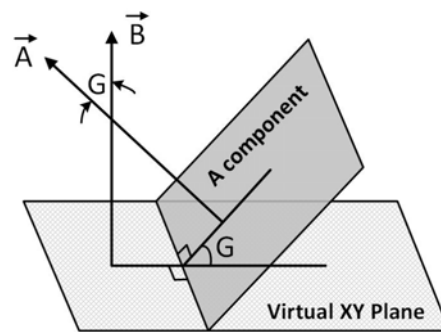


FIGURE 3.12: Illustration of the Gradient computation.

### 3.2.4 Physical/Virtual Boundary

All the top/side/bottom are boundaries for spaces, but it is necessary to distinguish if a boundary is physical or virtual. Because, for navigation, physical and virtual boundaries show different properties in navigation. Generally, the physical boundaries of a space are impassable for agents and virtual boundaries only indicate the borderlines. Their definitions are the following:

**Physical Boundary:** a physical boundary of a space is the boundary formed by a physical structure(s).

**Virtual Boundary:** a virtual boundary of a space is the imaginary boundary that used to allow space enclosure.

The following illustrations intuitively show how the different boundaries are employed to picture semi-bounded spaces.

There are two semi-bounded environments with tops: a bus stand and a gazebo (Figure 3.13). The hollow parts below their roof(s)/shelter(s) are semi-bounded spaces. The bus stand has five physical boundaries on the same plane: a quadrilateral top ( $A$ ), three sides ( $B$ ,  $C$ , and  $E$ ), and a bottom ( $D$ ). To make it as an enclosed 3D volume, two more missing virtual boundaries ( $C1$  and  $F$ ) are needed. Therefore, the boundaries  $A$ ,  $B$ ,  $C$ ,  $D$ , and  $E$  are physical, while  $C1$  and  $F$  are virtual. The gazebo has eight physical boundaries ( $A$  to  $H$ ):  $A$  to  $D$  are four physical tilted triangular tops;  $E$ ,  $F$ , and  $G$  are three physical sides; and  $H$  is the physical bottom. So, in this example, four virtual boundaries

( $E1$ ,  $F1$ ,  $G1$ , and  $I$ ) are needed to make an enclosed space. The two scenes show that the shapes of boundaries are not limited to quadrilaterals and that they can be tilted.

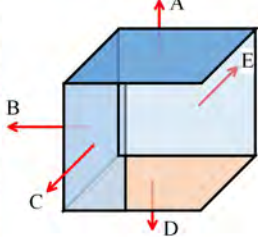
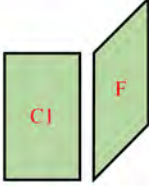
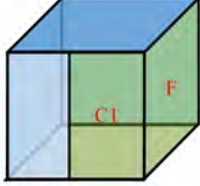
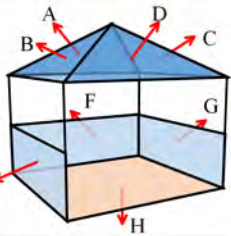
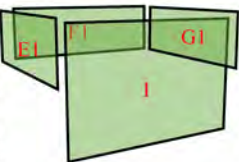
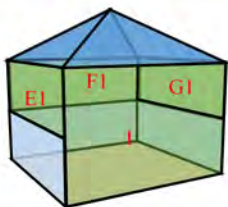
Scene	Physical	Virtual	Space
			
			

FIGURE 3.13: Two examples of semi-bounded spaces with tops.

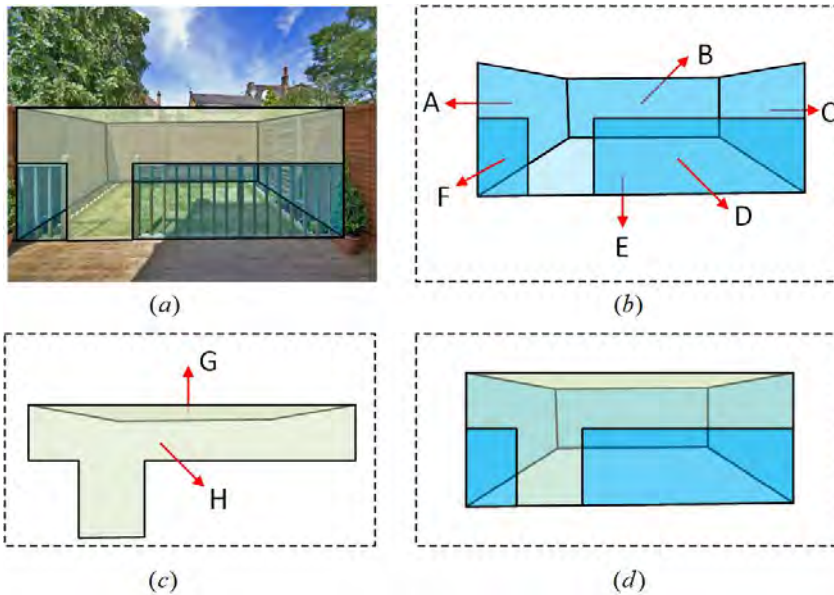


FIGURE 3.14: An example of a semi-bounded environment without tops. (a) yard; (b) physical boundaries; (c) virtual boundaries; (d) semi-bounded space.

Similarly, a yard is utilised to illustrate a semi-bounded environment without tops

and how space is employed to picture it (Figure 3.14(a)). The hollow part within the fences and walls is the semi-bounded space. In Figure 3.14(b),  $A$ ,  $B$ ,  $C$ ,  $D$ , and  $F$  are physical sides, and  $E$  is the bottom;  $G$  and  $H$  in Figure 3.14(c) are needed virtual top and sides when enclosing the space as an enclosed 3D volume. Thus, this semi-bounded environment is successfully pictured as a 3D space by physical and virtual boundaries (Figure 3.14(d)). It should be noted that, theoretically, the height of this semi-bounded space can be arbitrary, but in this illustration, the height is set as that of the highest wall(s).

### 3.2.5 Space Radius and Space Height

As mentioned in Section 3.1.1, the agent of this research is a pedestrian, who is modelled as a 3D object, thereby having certain requirements for spaces. Thus, considering if spaces are large enough to accommodate a pedestrian, the spaces employed for navigation should be selected based on their size.

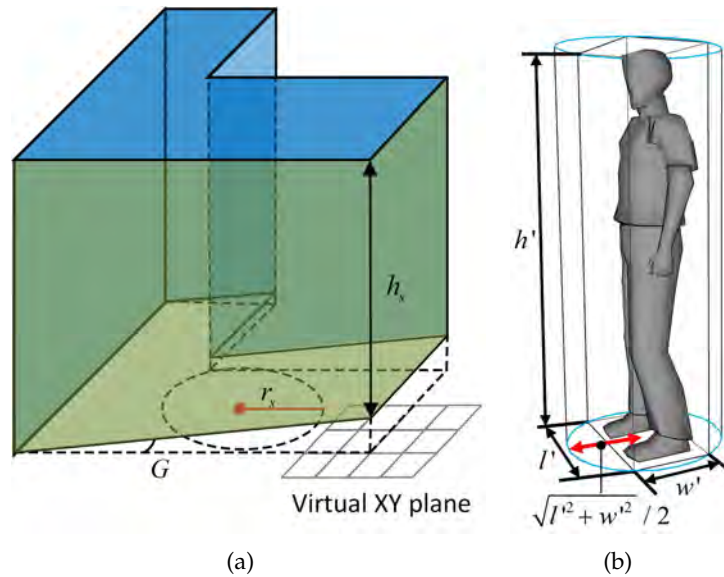


FIGURE 3.15: (a) Space radius ( $r_s$ ), space height ( $h_s$ ) and Gradient ( $G$ ). Blue polygons are physical boundaries, while olive green polygons are virtual. (b) The minimum space required by a pedestrian. It is modelled as cylinder with bottom radius  $\sqrt{l'^2 + w'^2} / 2$  and height  $h'$ .

For the cuboid spaces, their size can be represented as a triple: {length, width and height}. It is convenient for evaluating them by compare these three items with that of

the minimum space required by pedestrian ( $\{l', w', h'\}$ , Equation 3.3) respectively. However, the spaces are not always cuboids, which makes this direct way not always valid. Therefore, Space Radius ( $r_s$ ) and Space Height ( $h_s$ ) are introduced (Figure 3.15(a)). Then, the both cuboid and non-cuboid spaces can be evaluated with the same way.

The definitions of the two terms are the following:

**Space Radius ( $r_s$ ):** it is the radius of the maximum inscribed circle of the bottom projection. The computation process of the projection is projecting the bottom onto a virtual geometric  $XY$  plane along the  $Z$  – *direction*.

**Space Height ( $h_s$ ):** it is regarded as the minimum height based on boundaries that touch the top and bottom at the same time.

To evaluate the non-cuboid spaces, the minimum space required by a pedestrian is further modelled as a cylinder, in which the bottom of the cylinder is the minimum circumscribed circle of the minimum required space (i.e., its bottom radius is  $\sqrt{l'^2 + w'^2}/2$ ), and the height of the cylinder is equal to the height of the minimum required space (i.e., its height is  $h'$ ), see Figure 3.15(b). Then, the evaluation process evolved into two steps: the first step is to compare the  $r_s$  with  $\sqrt{l'^2 + w'^2}/2$ , and the second step is to compare the  $h_s$  with  $h'$ . Only when spaces meet the following two conditions at the same time will be selected (Equation 3.7). Namely, (i) the space radius is larger or equal to the radius of the minimum circumscribed circle of the minimum space required by a pedestrian, and (ii) the space height is larger or equal to the height of the minimum space required by a pedestrian.

$$\begin{cases} r_s \geq \sqrt{l'^2 + w'^2}/2 \\ h_s \geq h' \end{cases} \quad (3.7)$$

where  $r_s$  is the space radius while  $h_s$  is the space height.  $l', w', h'$  are the length, width, and height of the minimum space required by a pedestrian respectively.

### 3.3 Summary

This chapter presents five existing concepts that are used in this research, including agent, footprint, building height, terrain, and terrain intersection curve (TIC). The agent is needed for the space selection and tests of path planning (Chapter 7). Footprint, building height, and terrain are critical information for the reconstruction of the building shells (Section 6.3). The TIC ensures correct positions and topological relationships between reconstructed 3D spaces and the terrain (Chapter 6). It should be noted that, for this research use, we pruned definitions of agent, footprint, building height. In particular, the notion of an agent is specified as a pedestrian with a specific size. Building height is specified based on the mid-point of the foundation and the highest point. The notion of the footprint is extended to include not only the footprints of buildings, but also other city objects, such as shelters, roads, and green areas.

Other than the existing concepts, eleven novel terms are introduced by this research, including Top, Side, Bottom, topClosure, sideClosure, bottomClosure, Gradient, Physical Boundary, Virtual Boundary, Space Radius, and Space Height. The first three generalize notions for building structures are introduced to allow more complex boundary configurations to be considered. The three closures are introduced to quantify the level of closure of the three structures. These six terms are further being used for supporting more refined space definition in the generic space definition framework (Chapter 4) and also be utilized as attributes for the unified 3D space-based navigation model (Chapter 5). The Gradient of a boundary is introduced to distinguish between top, bottom and side. If the Gradient of a boundary is  $90^\circ$ , it is a side, otherwise, it is a top or bottom. Physical Boundary and Virtual Boundary bring in a key difference for a boundary in navigation, i.e., the former acts as obstacles while the latter only indicates the borderlines of a space. The last but not the least two terms are Space Radius and Space Height, which are parametrized indicators of space size to help with evaluating if the space is large enough to accommodate a pedestrian (Section 7.4).



# CHAPTER 4

---

## GENERIC SPACE DEFINITION FRAMEWORK

---

Current research on space classifications and definitions are mainly notion-based or example-based. This chapter introduces a generic space definition framework, which brings in systematic and parametric definitions for all types of spaces where the navigation activities may happen. The definitions can support the development of algorithms to enclose semi-bounded and entirely open spaces. As such, this framework ensures a uniform parametrized space definition that enables the inclusion of all types of spaces into the navigation map for seamless navigation path planning. The generic space definition framework that formally define and classify all the spaces where the navigation activities happen as the union of four types of spaces: indoor (I-space), outdoor (O-space), semi-Indoor (sI-space) and semi-Outdoor (sO-space), as expressed in equation 4.1. It is

necessary to point out that: (i) this classification means the semi-bounded spaces are classified and defined as semi-indoor and semi-outdoor; (ii) any space for navigation must belong to one of the four defined categories; and (iii) all the four types of spaces are completely bounded by boundaries and separated from each other. They may share a point, edge, or face (boundary), but they do not have any overlaps between each other. Their formal definitions are shown in the following sections. This chapter is based on my papers 5 (see Section 1.6).

$$S = I \cup O \cup sI \cup sO \quad (4.1)$$

where  $S$ ,  $I$ ,  $O$ ,  $sI$ , and  $sO$  denote Space, I-space, O-space, sI-space, and sO-space respectively.

## 4.1 Space Definitions

### 4.1.1 Descriptive Definition

The characteristics of different environments (spaces) (Table 4.1) give hints to distinguish them from the structures: Top, Side, Bottom, and entirely bounded. The definitions of Top, Side, Bottom are introduced in Section 3.2.1. On the basis of their characteristics, indoor and outdoor spaces are easily identified, because an indoor space is entirely bounded by top, side, and bottom while an outdoor space has bottom only.

TABLE 4.1: Characteristics of living environments (spaces), in which “✓” denotes a space has the structure while “×” denotes has not.

Environments (Spaces)	Top	Side	Bottom	Entirely bounded
Indoor	✓	✓	✓	✓
Outdoor	×	×	✓	×
Semi-indoor	✓	✓/×	✓	×
Semi-outdoor	×	✓	✓	×

Semi-bounded environments are further categorised as semi-indoor and semi-outdoor, i.e., the semi-bounded environments with upper boundaries are classified and defined as

semi-indoor spaces, while that without upper boundaries as semi-outdoor. The reason why such two names (semi-indoor, semi-outdoor) are employed is the semi-indoor space is more similar to indoor while semi-outdoor is similar to outdoor. In particular, sI-spaces have tops and that have a significant influence on the climate of the space. sO-spaces are open from the upper direction like outdoor spaces. The biggest difference between them is the former is partly or entirely enclosed from surrounding directions, but the latter is entirely unbounded. Thus, during navigation, agents like pedestrians/vehicles can visit an outdoor space from all surrounding directions, while they have to go through specific structures (door/entrance or similar) to visit a semi-outdoor space.

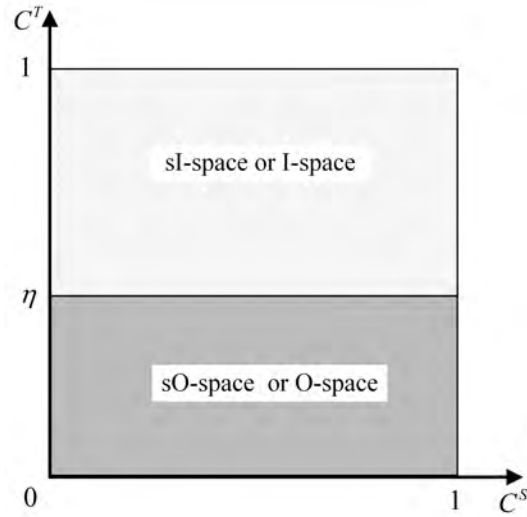
Then, the descriptive definitions of the four categories of spaces are the following:

- Indoor (I-space) is the spaces that physically and entirely enclosed by tops, sides and bottoms.
- Semi-indoor (sI-space) is the spaces that are semi-open to the outdoors, physically enclosed by top(s) in the upper direction, and may have a side(s) but is not physically enclosed completely like indoor. The bottom is assumed to be present by default.
- Semi-outdoor (sO-space) is the spaces that are open to the outdoor from the top direction but enclosed by physical sides from surrounding directions.
- Outdoor (O-space) is the spaces in the outdoor that completely open from the top and surrounding directions.

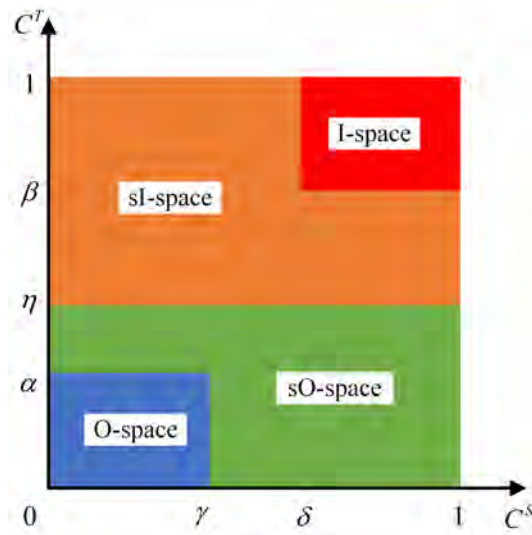
#### 4.1.2 Quantitative Definitions

The descriptive definitions only provide impressions about space classification, which still cannot define spaces precisely and quantitatively. For instance, based on the descriptive definitions, both the spaces, bus stand (Figure 1.2(b)) and wood pergola (Figure 1.2(f)) should be classified as sI-spaces, however, they have a very big difference when focusing on their tops. The top of the former is a shelter that can be used for sun and

rain protection, while that of the latter has only decorative and structural reinforcement function. For navigation use, it is more reasonable to classify the bus stand as an sI-space while the wood pergola as an sO-space or O-space. Therefore, this research further provides the quantitative definitions based on top closure ( $C^T$ ) and side closure ( $C^S$ ).



(a)



(b)

FIGURE 4.1: The  $C^T$  and  $C^S$  of different spaces.  $C^T$  and  $C^S$  are two physical structure parameters.  $\alpha$ ,  $\beta$ ,  $\gamma$ ,  $\delta$ , and  $\eta$  are five thresholds. (a) sharply classify space into two categories, sI-/I-space, and sO-/O-space, by using  $\eta$  of  $C^T$ ; (b) classify sI-/I-space into I-space and sI-space, and sO-/O-space into sO-space and O-space, by employing other four thresholds ( $\alpha$ ,  $\beta$ ,  $\gamma$ , and  $\delta$ ).

This section introduces five thresholds:  $\alpha$ ,  $\beta$ ,  $\gamma$ ,  $\delta$ , and  $\eta$  to provide an estimate of  $C^T$  and  $C^S$  of a space, in which  $\alpha$ ,  $\beta$  and  $\eta$  are dedicated for  $C^T$  while  $\gamma$  and  $\delta$  for  $C^S$ . By controlling these thresholds, the spaces are defined and classified quantitatively. Figure 4.1 offers a visual clue on how these thresholds define the boundaries and consequently the different spaces. On the two axes, the values of  $C^T$  and  $C^S$  are represented, where 0 means no closure and 1 means total closure.

### Thresholds for $C^T$

The three threshold values related to  $C^T$ :  $\alpha$ ,  $\beta$  and  $\eta$

- $\eta$  allows to distinguish between indoor and outdoor spaces. A space with a  $C^T \geq \eta$  is either an I-space or a sI-space. Otherwise, it is an O-space, or a sO-space.
- $\alpha$  is a closure value of the O-spaces. Specifically, a space with a  $C^T \geq \alpha$  cannot be an O-space. It must be a sO-space, I-space, or sI-space.
- $\beta$  is the lower threshold of the I-spaces. Thus, a space with  $C^T < \beta$  cannot be an I-space. It must be a sI-space, sO-space, or O-space.

$\eta$  illustrates how critical the notion of  $C^T$  is in determining whether space is closer to the indoor or the outdoor space, see Figure 4.1(a). Because the notion of indoor is hardly feasible without a minimum of a top bounding element to space, as reflected in the literature. But different constraints apply to the  $C^S$ , see Figure 4.1(b).

### Thresholds for $C^S$

The two threshold values related to  $C^S$ :  $\gamma$  and  $\delta$ .

- $\gamma$  is the upper threshold for the O-spaces with respect to  $C^S$ . A space for which  $C^S \geq \gamma$  cannot be an O-space. It must be sO-space, sI-space or I-space.
- Similarly,  $\delta$  is the lower threshold of the I-spaces such that a space with a  $C^S \leq \delta$  cannot be an I-space. It must be sI-space, sO-space or O-space.

Unlike the  $C^T$ ,  $C^S$  gives the meaning of the boundary between the indoor and the outdoor, but it is less critical in our framework. It provides estimates for the limits of the I-space and O-space but does not affect sO-space and sI-space. For this reason, only two thresholds are introduced and must be combined with the three thresholds of the  $C^T$ . Using the closure coefficients and their ranges, the four space types can be formally defined.

### Quantitative Definitions

A space  $S(C^S, C^T)$  can be defined as being one of the four types of space, as follows (Equation 4.2):

$$S(C^S, C^T) = \begin{cases} O & \text{if } C^S < \gamma \text{ and } C^T < \alpha \\ sO & \text{if } C^S \geq \gamma \text{ and } C^T < \alpha \\ & \text{or } \alpha \leq C^T \leq \eta \\ sI & \text{if } C^S \leq \delta \text{ and } C^T > \eta \\ & \text{or } \eta \leq C^T < \beta \\ I & \text{if } C^S \geq \delta \text{ and } C^T \geq \beta \end{cases} \quad (4.2)$$

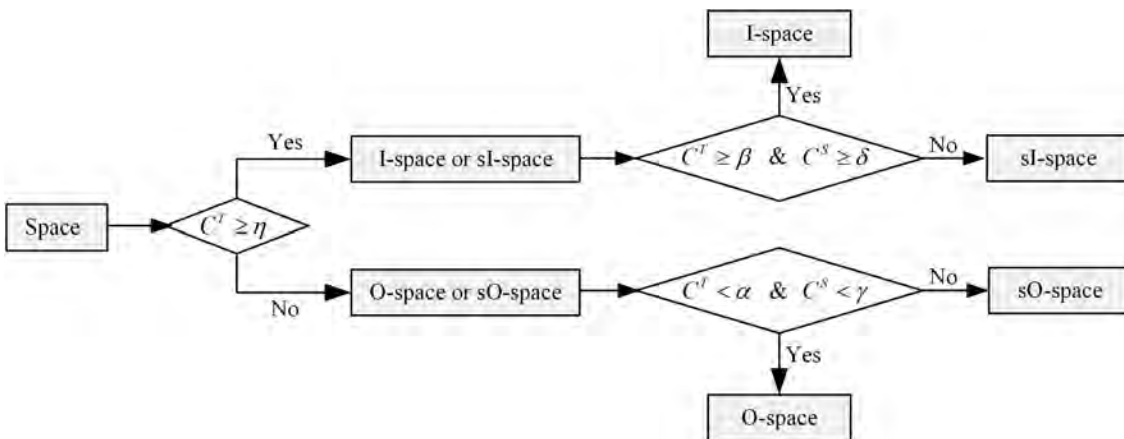


FIGURE 4.2: Flowchart of the space definition framework.

Figure 4.2 illustrates the process of space identification. As mentioned above,  $C^T$  is critical to distinguish between the two indoor and two outdoor spaces. More top closure intuitively leads from outdoor to indoor. Outdoor space is actually never physically bounded but rather bounded by structures of the other subspaces surrounding it (sO-space, sI-space or I-space).

Figure 4.3 shows sketches of possible cases along with real scene examples to illustrate an application of the definition framework on spaces relevant to navigation.

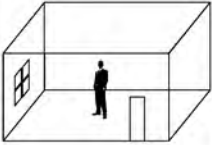
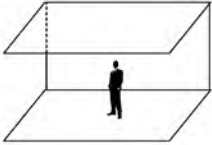
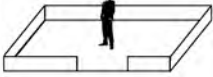
Environment	I-space	sI-space	sO-space	O-space
Definition	$C^T \geq \beta$ & $C^S \geq \delta$	$C^T \geq \eta$ & $C^S \in [0,1]$ except $C^T \geq \beta$ & $C^S \geq \delta$	$C^T < \eta$ & $C^S \in [0,1]$ except $C^T < \alpha$ & $C^S < \gamma$	$C^T < \alpha$ & $C^S < \gamma$
Example				
Scene				
Thresholds	$0 \leq \alpha \leq \eta \leq \beta \leq 1$ & $0 \leq \gamma \leq \delta \leq 1$			

FIGURE 4.3: Definitions of the spaces based on the definition framework.

## 4.2 Illustration of Thresholds and Space Classification

To provide a sense of the types of closure and help in understanding the selected thresholds, this research uses several simplified cases to illustrate the thresholds of  $C^T$  and  $C^S$ .

### 4.2.1 Thresholds of $C^T$

For the visually sensing the thresholds of  $C^T$ , a simple rectangular structure is employed, which provides four example closures, see Figure 4.4.

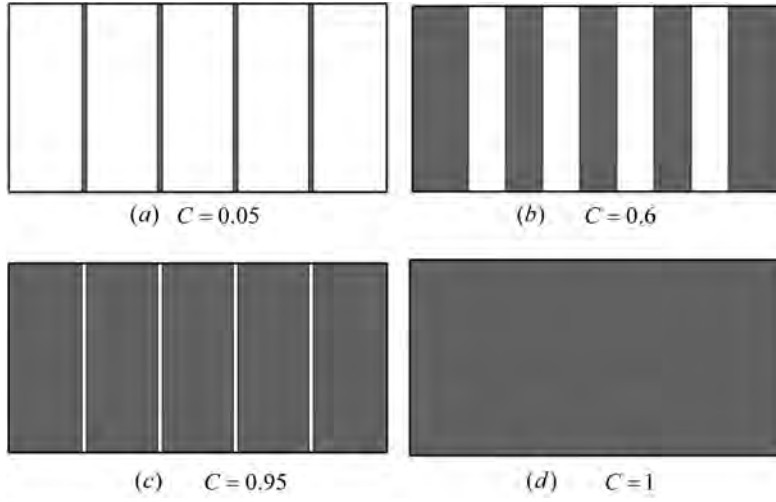


FIGURE 4.4: The structure with four different closure cases, in which the gray parts are enclosed ( $a_e$ ), while white parts are open. Size of the example structure ( $a_t$ ) is  $2 * 1(m^2)$ .

The size of the example structure in Figure 4.4 is  $2 * 1(m)$ , i.e.,  $a_t = 2 m^2$ .  $a_e$  has different values in the four cases. In case (a),  $a_e = 0.1 m^2$  and therefore  $C^T = 0.05$ . Similarly, the closure of the remaining cases can be computed.  $a_e$  (gray parts) of case (b), (c), and (d) are  $1.2 m^2$ ,  $1.9 m^2$ , and  $2 m^2$ , their  $C^T$  are 0.6, 0.95, and 1 respectively. Visually, the first two cases (a) and (b) give the impression of being not well-sealed, while the second two cases (c) and (d) look like better sealed. On the basis of this visual inspection, this research sets the values of the three thresholds ( $\alpha$ ,  $\beta$ , and  $\eta$ ) for  $C^T$  in Figure 4.1 as:  $\alpha = 0.05$ ,  $\beta = 0.95$ , and  $\eta = 0.6$ .

#### 4.2.2 Thresholds of $C^S$

Based on occurrence of physical surrounding boundaries, the sO-spaces and O-spaces can be simplified into six cases (Figure 4.5), in which the case with two surrounding boundaries have two different variations (Figure 4.5(c) and (d)). Base on the Equation 3.5, the  $C^S$  of the six cases can be computed, i.e.,  $C_a^S = 0$ ,  $C_b^S = 0.25$ ,  $C_c^S = C_d^S = 0.5$ ,  $C_e^S = 0.75$ , and  $C_f^S = 1$ .

The space differences can be clearly seen by visual inspection, however, it is still challenging to classify them into sO-space and O-space quantitatively. Hence, for the

presentation purpose, this research sets the threshold of  $C^S$  on the basis of the visiting pattern of sO-space (go through a door/entrance or a similar structure when the agent is a pedestrian or vehicle), i.e.,  $\gamma = 0.75$  and  $\delta = 0.95$ . If a space without upper boundary structure, but its  $C^S \geq 0.75$ , it is a semi-outdoor space, otherwise, it is outdoor. Thus, the six cases in Figure 4.5, (a), (b), (c), and (d) are classified as O-spaces, whereas (e) and (f) are sO-spaces. It should be noted that  $C^S$  of (c) can be more than 0.75 when its length larger than three times of its width. If so, space is also classified as an sO-space. This illustration intuitively shows that "urban canyons" spaces, i.e., small roads/alleys spaces surrounded by high buildings, might end up being sO-spaces or O-spaces.

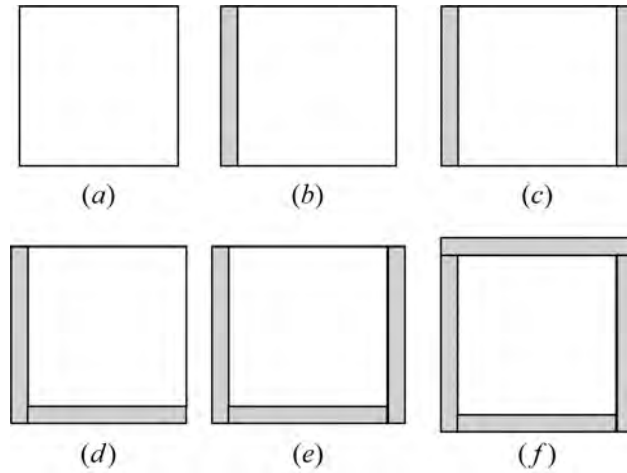


FIGURE 4.5: Top view of length of surrounding boundaries of square spaces, where slash-filled parts are concrete walls. (a) no wall; (b) one wall; (c) and (d) two walls; (e) three walls; (f) four walls.

### 4.2.3 Example of Quantitative Definitions

The five thresholds ( $\alpha = 0.05$ ,  $\beta = 0.95$ ,  $\gamma = 0.75$ ,  $\delta = 0.95$ , and  $\eta = 0.6$ ) imply that if a space has a top ( $C^T \geq 0.6$ ), it is I-space or sI-space. Then, if  $C^T \geq 0.95$  and  $C^S \geq 0.95$ , the space is I-space, otherwise, it is sI-space. If a space has a top with  $C^T < 0.6$ , it could be a sO-space or O-space. Further, if its  $C^T < 0.05$  and  $C^S < 0.75$ , it is an O-space, otherwise it is a sO-space, see Equation 4.3.

$$s(C^S, C^T) = \begin{cases} O & \text{if } C^S < 0.75 \text{ and } C^T < 0.05 \\ sO & \text{if } C^S \geq 0.75 \text{ and } C^T < 0.05 \\ & \text{or } 0.05 \leq C^T \leq 0.6 \\ sI & \text{if } C^S \leq 0.95 \text{ and } C^T > 0.6 \\ & \text{or } 0.6 \leq C^T < 0.95 \\ I & \text{if } C^S \geq 0.95 \text{ and } C^T \geq 0.95 \end{cases} \quad (4.3)$$

The effect of these example thresholds on the boundaries between the different spaces is shown in Figure 4.6. The normalization of the coefficients  $C^T$  and  $C^S$  gives the wrong impression that I-space and O-space are very insignificant and most of the spaces can be classified as sO-space and sI-space. As seen in the examples below, many of the real-world cases have closure close to 1. This means that the orange and green areas in the figure, although showing up as very large, represent a relatively small number of real-world cases.

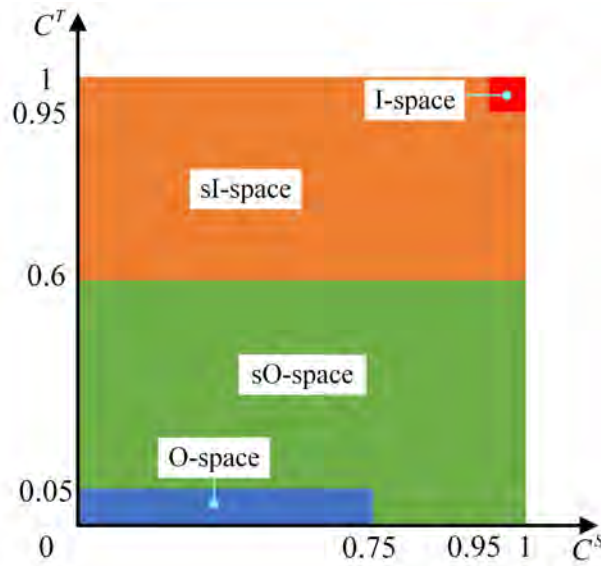


FIGURE 4.6: Space classification based on the example values of five thresholds.

It should be noted that these values are examples and further research is needed to estimate the effect of closure in diverse situations and environmental conditions, and

specify them more accurately.

#### 4.2.4 Classification of Several Real Cases

Using the introduced five thresholds, the three spaces in Figure 3.11 can be classified, in which the pergola and eaves are classified as sI-spaces while the roof terrace as sO-space. Figure 4.7 shows more examples of built scenes with a number of built environments: (a) Room; (b) Open-air; (c) Gas station; (d) The overhanging roof part; (e) Overpass; (f) Porch; (g) Bus stand; (h) Courtyard; (i) Roof terrace with outside stairs; (j) Yard with fence; (k) Road with side fence; (l) Stadium. Following the same approach as explained above, their coefficients  $C^T$  and  $C^S$  are estimated. The results of the computations are given Table 4.2.

TABLE 4.2: Estimated  $C^T$  and  $C^S$  of the example structures.

Figure	Structure	$C^T$	$C^S$	Space Type
Fig 4.7(a)	Room	1.0	1.0	I-space
Fig 4.7(b)	Open air	0.0	0.0	O-space
Fig 4.7(c)	Gas station	1.0	0.0	sI-space
Fig 4.7(d)	Overhanging roof	1.0	0.42	sI-space
Fig 4.7(e)	Overpass	1.0	0.25	sI-space
Fig 4.7(f)	Porch	1.0	0.83	sI-space
Fig 4.7(g)	Bus stand	1.0	0.65	sI-space
Fig 4.7(h)	Courtyard	0.0	0.88	sO-space
Fig 4.7(i)	Roof terrace	0.0	0.8	sO-space
Fig 4.7(j)	Yard	0.0	0.93	sO-space
Fig 4.7(k)	Road with fence	0.05	1.0	sO-space
Fig 4.7(l)	Stadium	0.0	0.8	sO-space

As visible from the examples, many of the cases can easily be classified if their dimensions and closure are known. However, the reality might be not that simple: the dimensions might be not available or the closure not is possible to be estimated. A good example is a stadium. In this research, two spaces are defined: one above the football field and one (or more) under the stadium roof. However, if the entire space (football field and audience space) is considered as one, the stadium space might appear to be sI-space. Other examples are weakly closed spaces for which it is difficult to conclude on



FIGURE 4.7: Some space examples of built scenes.

a closure. Figure 4.8 shows more cases of weakly top-bounded spaces for which the top has only a decorative (Figure 4.8(a)) or structural reinforcement (Figure 4.8(b)) function. The spaces below them are O-spaces, due to the low  $C^T$  that those structures present. In Figure 4.8(c), space corresponds to an sO-space, although the  $C^S$  is made up of vegetation fences and houses.

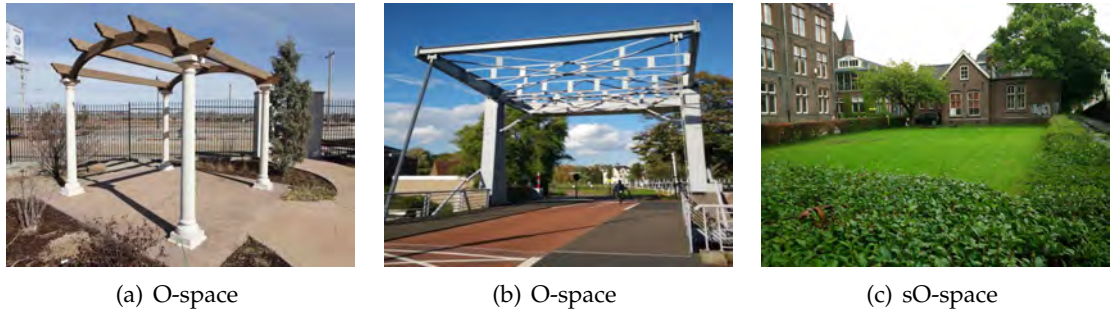


FIGURE 4.8: Structures of space have weak characteristics.

Furthermore, it cannot be concluded that specific structures can always be associated with the same type of space. For example, Figure 4.9 illustrates the case of a bridge between two buildings. While the first one is an I-space (Figure 4.9(a)), the second one is a sI-space (Figure 4.9(b)), and the third one a sO-space (Figure 4.9(c)). The bridge spaces in (a) and (b) have tops and sides, but the  $C^T$  and  $C^S$  of the former are nearly 1, while the  $C^S$  of the latter is at most 0.9. The bridge space in (c) has no top, but its  $C^S$  is more than 0.75. All of the spaces under these bridges correspond to sI-spaces.

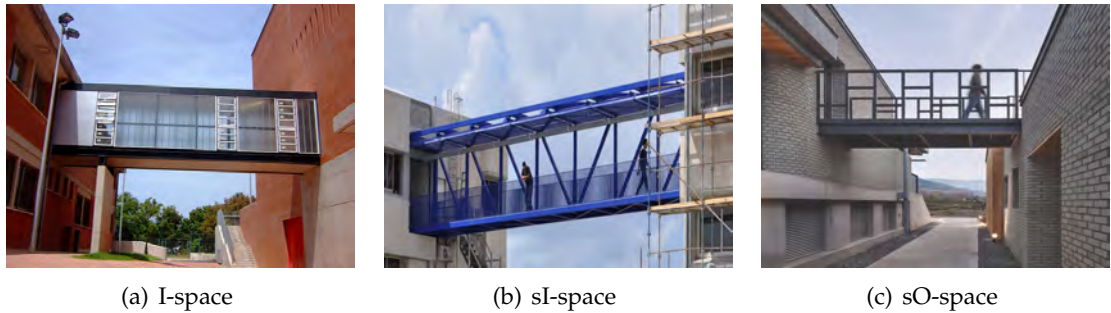


FIGURE 4.9: Bridges between two buildings.

### 4.3 Summary

This chapter presents the generic space definition framework. We have classified and defined the living environments where navigation can happen as four types of spaces: indoor (I-space), outdoor (O-space), semi-indoor (sI-space) and semi-outdoor (sO-space). Following this framework, any space can be classified uniquely into one of the four

categories, which provides a basis for integrated and seamless indoor/outdoor navigation. Based on the developed definitions, sI-spaces and sO-spaces can be used in navigation systems, providing the ability to further tune the paths according to the navigating agents' requirements.

This framework controls classifications and definitions of the I-space, O-space, sI-space and sO-space by thresholds of their topClosure ( $C^T$ ) and sideClosure ( $C^S$ ), which brings flexibility to the space classification and definition. Thus, it is possible for other space-based models to rely on it and further using the same network extraction approaches across the built environment, thereby providing a seamless navigation solution.

## CHAPTER 5

---

# SPACE-BASED NAVIGATION MODEL AND NEW PATH OPTIONS

---

For seamless navigation use, information of spaces and space boundaries are necessary, such as the type of space (indoor, outdoor, semi-indoor, or semi-outdoor), category of a boundary (top, side, or bottom), type of a boundary (physical or virtual), closure of a boundary (topClosure, sideClosure, and bottomClosure). As mentioned in Section 2.6.1, the OGC standard IndoorGML is an open data model and has an XML-based schema, which provides a common framework for representation and exchange of indoor spatial information based on 3D spaces and network/graph. However, in the navigation module of current IndoorGML, a *CellSpace* only represents indoor spaces, i.e., this standard currently only supports for indoor navigation applications. Moreover, *CellSpaceBoundary* merely describes the geometry of space boundaries. To represent, structure and manage the necessary information of seamless navigation in a unified way, this chapter presents

a unified 3D space-based navigation model, which re-uses the theoretical background of the IndoorGML and extends the concept of *CellSpace* and *CellSpaceBoundary*.

Based on one types of the introduced spaces - semi-indoor space, we put forward two new path options: the **Most-Top-Covered** path (MTC-path) and path to the **Nearest sI-space** from departure (NSI-path). The two new path options are developed to meet the user's pursuit of the protection from top direction during their navigation.

In the following sections, the 3D unified space-based model is firstly presented. Then, several parameters for reflecting navigation network and navigation path, MTC-path, NSI-path, as well as a path selection strategy are introduced. This chapter is based on my papers 1 and 2 (see Section 1.6).

## 5.1 Attributes and Spatial Schema

This research extends *CellSpace* and *CellSpaceBoundary* to reflect all possible spaces and their boundaries. The UML diagram of the unified 3D space-based navigation model is shown in Figure 5.1.

In this model, all the classes come from IndoorGML. Thus, the two classes in the navigation module, *CellSpace* and *CellSpaceBoundary* remain the same definitions. But, *CellSpace* is extended to include not only I-space, but also sI-space, sO-space, and O-space (definitions can be seen in Section 4.1). That is, a *CellSpace* is a semantic class corresponding to one (indoor, semi-indoor, semi-outdoor, or outdoor) space object in Euclidean primal space. The *CellSpaceBoundary* is still used to semantically describe the boundary of each space object, but its roles (top, side or bottom) and formation types (physical or virtual) are added.

In short, the 3D space-based navigation model is an extension of the navigation module in current version 1.0.3 of the IndoorGML standard (Section 2.6.1). The modifications consist of two parts: (i) four attributes (*sType*, *topClosure*, *sideClosure*, and *bottomClosure*) are introduced for *CellSpace* and (ii) two attributes (*category* and *bType*) for *CellSpaceBoundary*.

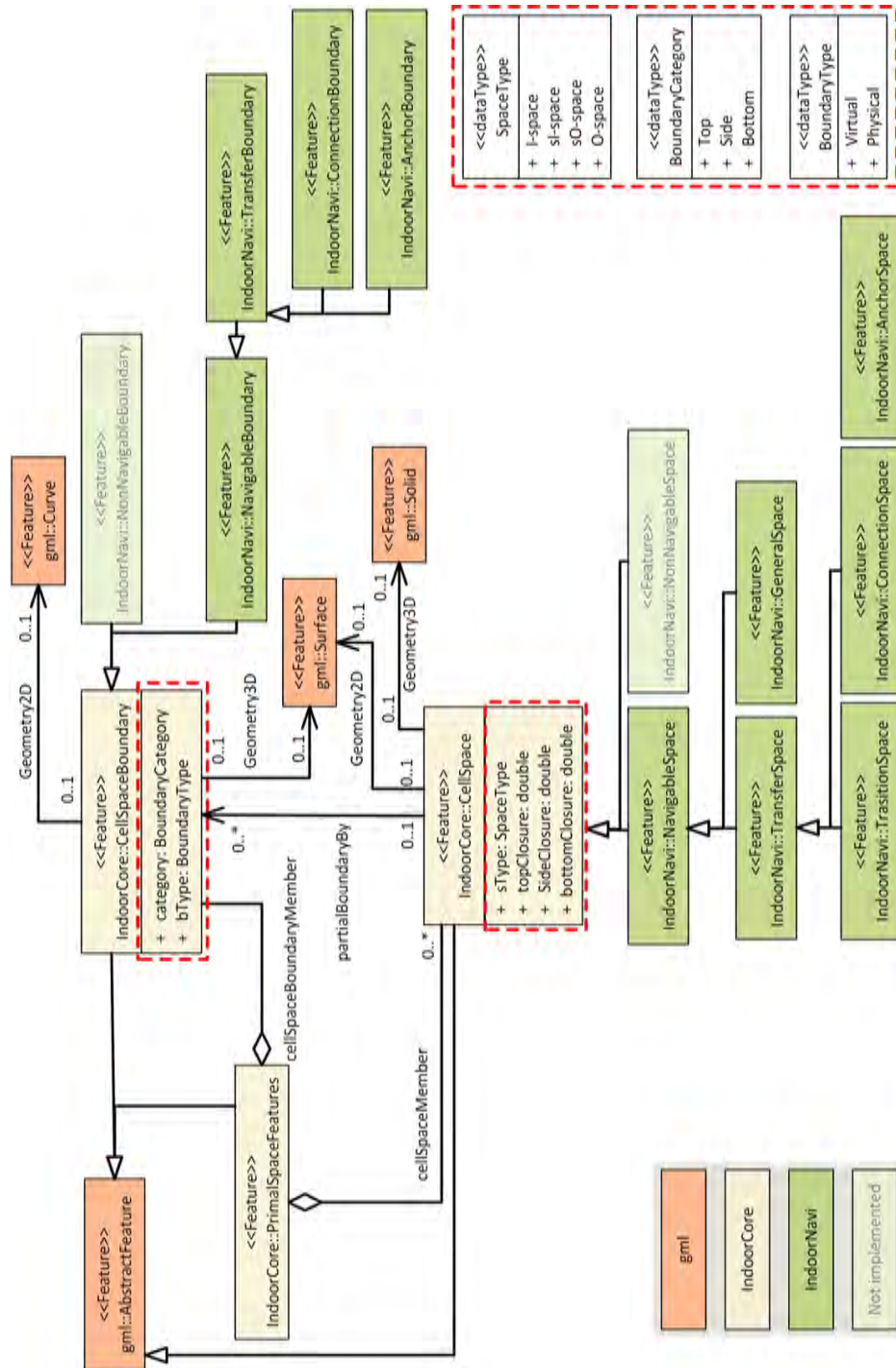


FIGURE 5.1: UML diagram of the unified 3D space-based navigation model. All the classes come from IndoorGML. The attributes of *CellSpace* and *CellSpaceBoundary*, and the data types are developed by this research, see the parts circled by the red dotted line.

### 5.1.1 Attributes for *CellSpace*

Four new attributes are introduced to integrate the information about the space type (*sType*), top closure (*topClosure*), side closure (*sideClosure*), and bottom closure (*bottomClosure*) of a space.

The space type can directly be obtained from the value of *sType* or be determined based on the three closures (*topClosure*, *sideClosure*, and *bottomClosure*) by using the definition framework. The motivation for keeping them at the same time is that some spaces have 3D geometry but without detailed information of boundaries (e.g., I-spaces from BIM models), and some spaces have detailed information of boundaries but have no 3D geometry directly (e.g., sI-spaces, sO-spaces, and O-spaces).

Thus, in the space type determination, the type of the spaces that have 3D geometry only is referred to the value of the *sType* while that of the spaces have detailed information of boundaries are determined based on the closures by using the generic space definition framework. Details of the four attributes for *CellSpace* are the following.

#### **sType**

*sType* indicates the space type of a *CellSpace*. By introducing this attribute, *CellSpace* is extended to represent I-space, sI-space, sO-space, and O-space. That is, this attribute is an enumeration list that includes the four types of spaces.

#### **topClosure, sideClosure, and bottomClosure**

*topClosure*, *sideClosure*, and *bottomClosure* are other three attributes introduced for *CellSpace*. They are used to (i) decide the type of a space (see the Section 4.1.2) and (ii) determine whether agents can fit in the space for specific purposes. The values of the three attributes are decimals between 0 and 1. *topClosure* and *bottomClosure* can be computed by Equation 3.4 and *sideClosure* by Equation 3.5.

### 5.1.2 Attributes for *CellSpaceBoundary*

As mentioned above, *category* and *bType* are two attributes introduced for *CellSpaceBoundary*.

#### **category**

*category* represents the role of a *CellSpaceBoundary*. The *dataType* of this attribute is *BoundaryCategory*, which includes three roles: *Top*, *Side*, and *Bottom*. It means that a *CellSpaceBoundary* acts as *Top*, *Side*, or *Bottom* of a *CellSpace*. Definitions of the three roles can be seen in Section 3.2.1.

#### **bType**

*btype* indicates a *CellSpaceBoundary* is physical or virtual. It is useful to have this attribute, since a physical side can act as protection from weather conditions (e.g., wind) while a virtual one cannot. By referring to this attribute, the *sideClosure* (Defined in Section 3.2.2) is computed. The entrance of a *CellSpace* also can be estimated. In particular, if a *CellSpaceBoundary* is virtual and shared by two *CellSpace*, the agents can be guided through this boundary to visit these two *CellSpace*.

### 5.1.3 Illustration of Using the Model

Figure 5.2 shows an example about how a specific scene is disassembled and structured on the basis of the model. The example scene includes a building with eaves, a garden with a fence, a pavement, and a street (Figure 5.2(a)). In this case, wall(s), fence(s), roof(s), and ground are physical structures, thereby, the boundaries extracted from them are physical (Figure 5.2(b)). The boundaries coloured in light blue in Figure 5.2(c) are the needed virtual boundaries for enclosing the spaces as 3D volumes.

To show more details of the boundaries in the example, all the boundaries of I-space, sI-space, sO-space and O-space are separated and coloured differently. Virtual boundaries are shown in blue and the rest are physical (Figure 5.3). Furthermore, the  $C^T$ ,  $C^S$ ,

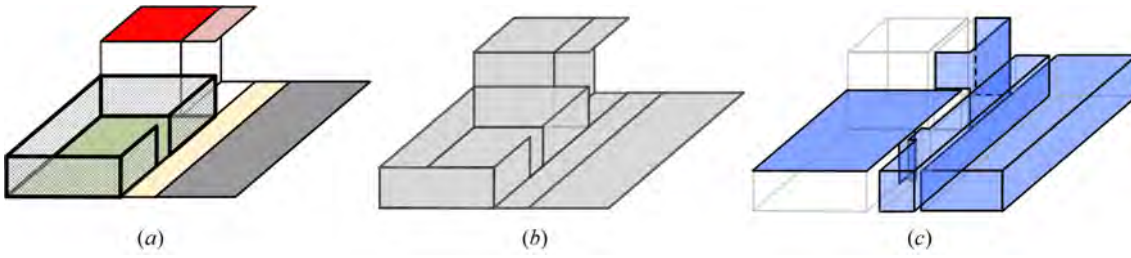


FIGURE 5.2: Example of environments and spaces. (a) A built environment case; (b) physical boundaries; (c) virtual boundaries.

and  $C^B$  of each space are estimated. Then the spaces are determined. For instance, the garden is represented as a seven-tuple:  $\{s3, 'Garden', 'sOSpace', 0, 0.95, 1, [b0, b1, \dots, bx]\}$ , in which  $s3$  is the ID, 'Garden' is the semantic, 'sOSpace' means this space is a sO-space, 0 is  $C^T$ , 0.95 is  $C^S$ , 1 is  $C^B$ , and the  $[b0, b1, \dots, bx]$  is the list of its *CellSpaceBoundary* IDs.

	I-space	sl-space	sO-space	O-space	
Spaces					
Physical boundaries					
Virtual boundaries					
Top	 $C^T = 1$	 $C^T = 1$	 $C^T = 0$	 $C^T = 0$	 $C^T = 0$
Sides	 $C^S = 1$	 $C^S = 0.5$	 $C^S = 0.95$	 $C^S = 0.17$	 $C^S = 0$
Bottom	 $C^B = 1$	 $C^B = 1$	 $C^B = 1$	 $C^B = 1$	 $C^B = 1$

FIGURE 5.3: Example of spaces, physical boundaries, virtual boundaries (blue), Top, Side, Bottom,  $C^T$ ,  $C^S$  and  $C^B$ . All the physical boundaries are coloured into gray while virtual boundaries are in light blue.

## 5.2 Path Options based on Introduced Spaces

### 5.2.1 Parameters

In order to quantitatively reflect the navigation networks and navigation paths, this section introduces several parameters.

#### For Navigation Model

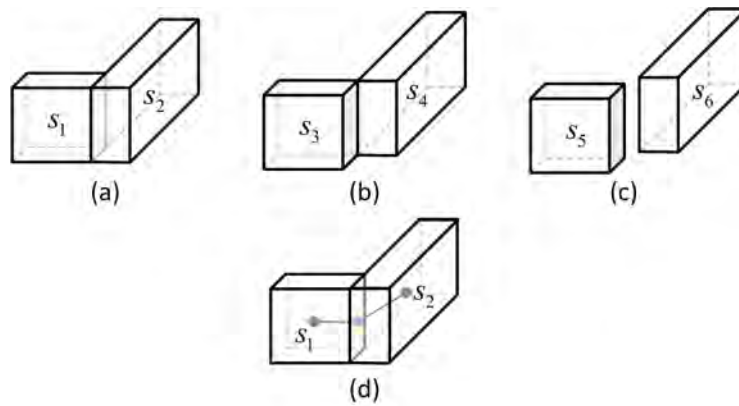


FIGURE 5.4: Illustration of connected spaces and the navigation network between the two spaces.

The parameters for the navigation networks are defined based on two connected spaces (Figure 5.4). Only the two spaces ( $s_1$  and  $s_2$ ) in Figure 5.4(a) are regarded as connected spaces while the spaces ( $s_3$  and  $s_4$ ) in Figure 5.4(b) and ( $s_5$  and  $s_6$ ) in Figure 5.4(c) are unconnected. The Figure 5.4(d) shows the navigation network between  $s_1$  and  $s_2$ , in which the blue dot is the additional vertex on the face two spaces touch to indicate how to traverse the spaces. Five parameters are defined: the distance between the two connected spaces, original weights, covered & uncovered distance, uncovered ratio, and modified weights. The definitions and notations of the parameters are the following:

- The distance between two connected spaces ( $d_{s_i s_j}$ )

On the basis of Poincaré duality, for any two connected spaces ( $s_i$  and  $s_j$ ), edge(s) are added to indicate connection(s), where the costs of edges are distances. Then, the distance between the two spaces ( $d_{s_i s_j}$ ) is the sum of all the costs between them.

For instance, the distance between  $S_1$  and  $S_2$  is the sum of the lengths of the two line segments (Figure 5.4(d)).

- Original weights ( $W'_{s_i s_j}$ )

All the distances are taken into account to compute the weights. Then, the original weights are the standardised distances (Equation 5.1).

$$W'_{s_i s_j} = \frac{d_{s_i s_j} - d_{s_i s_j}(\min)}{d_{s_i s_j}(\max) - d_{s_i s_j}(\min)} \quad (5.1)$$

where  $W'_{s_i s_j}$  is the values that standardised from distances  $d_{s_i s_j}$ ,  $d_{s_i s_j}(\max)$  and  $d_{s_i s_j}(\min)$  are the maximum and minimum in the distance collection respectively.

- Covered ( $d_{c_{s_i s_j}}$ ), & uncovered ( $d_{uc_{s_i s_j}}$ ) distance

The covered distance ( $d_{c_{s_i s_j}}$ ) means the length of the part physically bounded by tops between two connected spaces ( $s_i$  and  $s_j$ ), and the uncovered distance ( $d_{uc_{s_i s_j}}$ ) means the length of the uncovered parts. In this research, the covered parts come from I-spaces or sI-spaces while the uncovered from sO-spaces or O-spaces.

- Uncovered ratio ( $\lambda_{s_i s_j}$ )

The uncovered ratio ( $\lambda_{s_i s_j}$ ) is a variable to express uncovered rate between two spaces. It is the ratio between the uncovered distance ( $d_{uc_{s_i s_j}}$ ) and the distance ( $d_{s_i s_j}$ ) of two spaces ( $s_i$  and  $s_j$ ). Thus, it can be computed by Equation 5.2:

$$\lambda_{s_i s_j} = d_{uc_{s_i s_j}} / d_{s_i s_j}. \quad (5.2)$$

where  $d_{uc_{s_i s_j}}$  is uncovered distance and  $d_{s_i s_j}$  is the distance between the two connected spaces.

- Modified weights ( $W''_{s_i s_j}$ )

The modified weights ( $W''_{s_i s_j}$ ) are computed based on original weights ( $W'_{s_i s_j}$ ) and the uncovered ratio ( $\lambda_{s_i s_j}$ ), in which a coefficient  $\zeta$  is introduced to indicate the importance of the original weights and uncovered ratio (Equation 5.3).

$$W''_{s_i s_j} = \zeta W'_{s_i s_j} + (1 - \zeta) \lambda_{s_i s_j} \quad (5.3)$$

where  $\zeta$  is the coefficient that quantifies the importance of original weights and uncovered ratio, where  $\zeta \in [0, 1]$ ,  $W'_{s_i s_j}$  is the original weight, and  $\lambda_{s_i s_j}$  is the uncovered ratio.

### For Navigation Path

The parameters for the navigation paths are defined based on the planned paths, which are used as quantitative indicators for path comparisons in the later section. The definitions and notations of the parameters are as follows:

- Path length ( $P_l$ )

The  $P_l$  is the distance from departure to destination following the planned path.

$$P_l = \sum d_{s_i s_j} \quad (5.4)$$

- Covered/Uncovered length of a path ( $P_{lc} / P_{luc}$ )

Covered length means the total distance of the path segments formed by I-spaces and sI-spaces in the planned path, while the uncovered distance means the total distance of segments formed by sO-space and/or O-space.

$$P_{lc} = \sum d_{c_{s_i s_j}} \quad (5.5)$$

$$P_{luc} = \sum d_{uc_{s_i s_j}} \quad (5.6)$$

- Top-coverage-ratio of a path ( $P_{cr}$ )

The top-coverage-ratio of a path is an indicator that shows how much a path is physically bounded by tops. It is the ratio between the covered length and path length (Equation 5.7).

$$P_{cr} = P_{lc} / P_l \quad (5.7)$$

- Total weight of a path ( $W_p$ )

The total weight of a path is the summation of the weight of a planned path based on (original/modified) weights. In particular, if a planned path consists of several connected spaces, the  $W_p$  is the sum of weights corresponding to all the spaces (Equation 5.8).

$$W_p = \sum W_{s_i s_j} \quad (5.8)$$

in which the  $W_{s_i s_j}$  is  $W'_{s_i s_j}$  or  $W''_{s_i s_j}$ .

### 5.2.2 MTC-path

The MTC-path is a parameters-based path option and it takes both the travel distance and the top-coverage-ratio of a path ( $P_{cr}$ ) as the criteria. In short, it aims to determine the shortest path within a top-coverage-ratio constraint in the navigation. The path planning of MTC-path consists of three steps:

- Select sI-spaces.

In this step, sI-spaces will be selected based on a threshold of  $C^T$ . This threshold of  $C^T$  is different from that in the generic space definition framework. Here, it is set on basis of navigation purposes. For instance, if a pedestrian plans to use the top for escaping from strong sun, the threshold of  $C^T$  can be set as 0.8 (this value here is only an example). Then, only the sI-spaces with a  $C^T \geq 0.8$  are selected to participate in the navigation network derivation and navigation path planning. In other words, the results of this step are the sI-spaces that have qualified tops.

- Compute the original and modified weights.

Taking the Poincaré duality as the theoretical background, the navigation network is derived based on the selected sI-spaces, sO-spaces, and O-spaces. Then, the original and modified weights are computed based on the Equation 5.1 and Equation 5.3 respectively.

- Plan the MTC-path.

In this last step, the departure and destination are two nodes in the navigation network corresponding to two spaces and they can be located in semi-indoor, semi-outdoor, or outdoor. After assigning the departure and destination, the modified weights ( $W''_{s_i s_j}$ ) are utilized to compute the MTC-path as well as  $P_l, P_{l_c}, P_{l_{uc}}$ .

### 5.2.3 NSI-path

The NSI-path is designed to help pedestrians to find a closest roofed/sheltered place from their departures, which is a compromise option when neither the shortest path nor MTC-path is recommended (see the path selection strategy in Section 5.2.4). The process of planning the NSI-path also starts from selecting sI-spaces based on a threshold of  $C^T$  (the same as that in MTC-path planning). The process of NSI-path planning consists of four steps, which are shown by an illustration (Figure 5.5). In the example, there are eight selected sI-spaces (sI-1 to sI-8) that are marked by black solid square. The details of the process are the following:

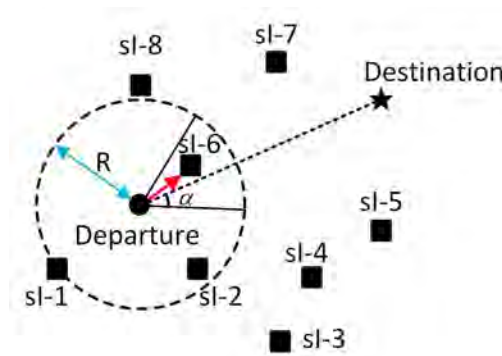


FIGURE 5.5: Example of NSI-path planning from departure to destination.

- Create a straight line by linking the departure and destination.

This step is to create a line segment by using the location of departure as the start and destination as the end. This line is used as a reference for the searching area determination.

- Set time ( $t$ ) and searching angle ( $\theta$ ).

In this step, two parameters are introduced, time ( $t$ ) and searching angle ( $\theta$ ), in which the former indicates the acceptable time for a pedestrian to move to the nearest sI-space, while the latter is an optimization parameter for determining the preferred search range. The  $\theta$  can vary from 0 to 360°.

- Find potential nearest sI-spaces.

With the  $t$  and the speed of a pedestrian ( $v$ ), a search radius ( $s_r$ ) centred on the departure point can be determined, i.e.,  $s_r = vt$ . Then, the searching area becomes a sector by setting a searching angle ( $\theta \in (0, 360^\circ]$ ). The searching process is having all the selected sI-spaces to do intersection operations with this sector. If the intersection is not null, the corresponding sI-space will be kept as a candidate for the nearest sI-spaces. With a given  $\theta$ , if there is no sI-space within the defined sector, the  $\theta$  will be increased.

- Plan the nearest sI-space and NSI-path.

The final step is computing the shortest paths from the departure to each candidate of sI-space based on the Dijkstra algorithm. Then the sI-space corresponding to the path with minimum distance is the nearest sI-space, and this shortest path is the NSI-path. In the demonstration (Figure 5.5), *sI-6* is determined as the nearest sI-space to the departure.

### 5.2.4 A Path Selection Strategy

There are three options for a pedestrian, MTC-path, NSI-path, and the traditional shortest path. More than one paths options can be available and this may create difficulties in selecting a path. It is necessary to have a path selection strategy to help pedestrians to make decisions within the three path options.

Ideally, pedestrians will select the path options with the following order: MTC-path, NSI-path, and the traditional shortest path. However, MTC-path may not always be the best choice. For example, the length of MTC-path may be longer than the shortest path. Thence, this chapter introduces a path selection strategy (Figure 5.6) to help pedestrians to find the balance between distance and top-coverage-ratio and set up rules to estimate in which condition which path is the best option.

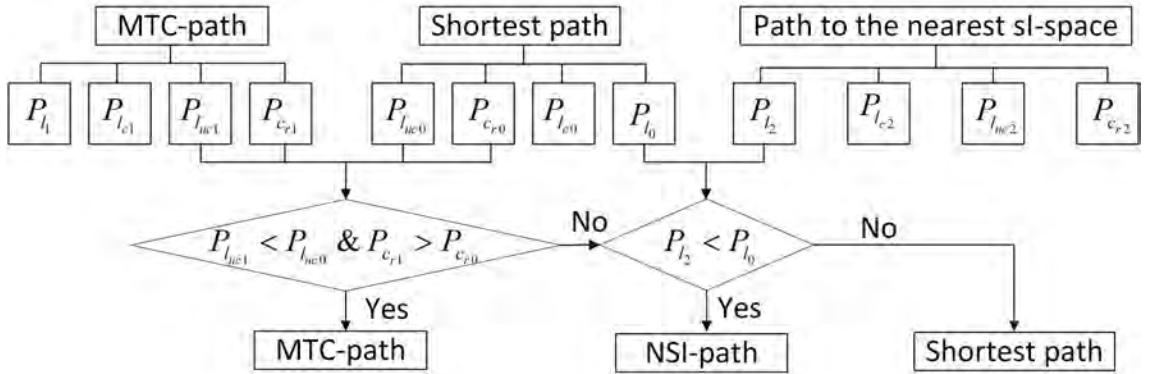


FIGURE 5.6: The path selection strategy. The shortest path is computed based on the original weights ( $W'_{s_i s_j}$ ).

As seen in the path selection strategy, utilizing the traditional shortest path as the reference, two progressive rules are presented: (i) for the MTC-path, if its uncovered distance is shorter than that of shortest path, and at the same time the top-coverage-ratio is larger than that of shortest path (i.e.,  $P_{l_{uc1}} < P_{l_{uc0}} & P_{c_{r1}} > P_{c_{r0}}$ ), it will be recommended to agents preferentially. Otherwise, (ii) the NSI-path will be computed and compared with the traditional shortest path. If the NSI-path is shorter than the shortest path (i.e.,  $P_{l_2} < P_{l_0}$ ), the NSI-path will be suggested for pedestrians. Otherwise, the traditional shortest path is the recommendation.

### 5.2.5 Illustration of the Two Path Options

A navigation example illustrates the two navigation options and the path selection strategy (Figure 5.7). For simplicity, we use abstract cases containing only spaces which connect by sharing virtual boundaries. There are eight spaces ( $s_A$  to  $s_H$ ), in which  $s_C$ ,  $s_F$ , and  $s_G$  are three selected sI-spaces, while the rests are sO-spaces and O-spaces. Spaces are 3D volumes, but in this example, they are demonstrated in 2D polygons for visualization purposes. Figure 5.7(a) and (c) show the navigation network that derived based on Poincaré duality. The costs of edges are distances, which are identified by numbers without the unit (Figure 5.7(d)).

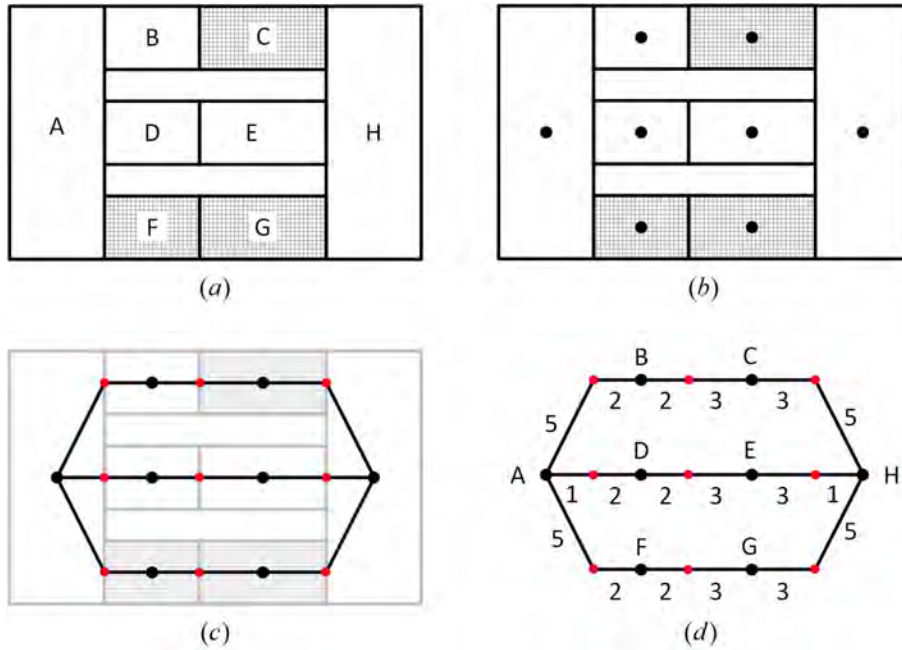


FIGURE 5.7: A navigation example, in which  $s_C$ ,  $s_F$ , and  $s_G$  are three sI-spaces. The navigation graph in (c) and (d) are undirected graph. (a) All spaces. (b) Nodes extracted from spaces; (c) Navigation graph derived from spaces based on duality theory, in which the red dots are the extra vertices; (d) Navigation graph with distance.

With the navigation graph (Figure 5.7(d)) and distances, original weights (Table 5.1) are computed based on Equation 5.2 and 5.1. For instance, the  $W'_{s_A s_F} = (7 - 3) / (8 - 3) = 0.8$ , in which  $d_{s_A s_F} = 7$ ,  $d_{s_i s_j}(\min) = \min\{7, 3, 7, 5, 8, 5, 4, 5, 8\} = 3$  while  $d_{s_i s_j}(\max) = \min\{7, 3, 7, 5, 8, 5, 4, 5, 8\} = 8$ . The uncovered ratio between  $s_A$  and  $s_F$  is  $\lambda_{s_A s_F} = d_{uc_{s_i s_j}} / d_{s_i s_j} =$

TABLE 5.1: Original information of the navigation graph.

$s_i$	$s_j$	$d_{s_i s_j}$	$W'_{s_i s_j}$	$d_{c_{s_i s_j}}$	$d_{uc_{s_i s_j}}$	$\lambda_{s_i s_j}$
$s_A$	$s_B$	7	0.8	0	7	1
$s_A$	$s_D$	3	0	0	3	1
$s_A$	$s_F$	7	0.8	2	5	0.71
$s_B$	$s_C$	5	0.4	3	2	0.4
$s_C$	$s_H$	8	1	3	5	0.625
$s_D$	$s_E$	5	0.4	0	5	1
$s_E$	$s_H$	4	0.2	0	4	1
$s_F$	$s_G$	5	0.4	5	0	0
$s_G$	$s_H$	8	1	3	5	0.625

$5/7 = 0.71$ . Then, modified weights ( $W''_{s_i s_j}$ ) are computed based on Equation 5.3, in which to show the changes in the modified weights, the coefficient  $\zeta$  is set from 1 to 0 with intervals of 0.1 (Table 5.2). For example, when  $\zeta = 0.6$ , the modified weight of the link between space  $s_A$  and  $s_F$  is  $W''_{s_A s_F} = \zeta W'_{s_A s_F} + (1 - \zeta) \lambda_{s_A s_F} = 0.6 * 0.8 + (1 - 0.6) * 0.71 = 0.77$ .

TABLE 5.2: Modified weights ( $W''_{s_i s_j}$ ) based on Equation 5.3.

$s_i$	$s_j$	$W''_{s_i s_j}$										
		$\zeta = 1$	0.9	0.8	0.7	0.6	0.5	0.4	0.3	0.2	0.1	0
$s_A$	$s_B$	0.8	0.82	0.84	0.86	0.88	0.9	0.92	0.94	0.96	0.98	1
$s_A$	$s_D$	0	0.1	0.2	0.3	0.4	0.5	0.6	0.7	0.8	0.9	1
$s_A$	$s_F$	0.8	0.79	0.78	0.77	0.77	0.76	0.75	0.74	0.73	0.72	0.71
$s_B$	$s_C$	0.4	0.4	0.4	0.4	0.4	0.4	0.4	0.4	0.4	0.4	0.4
$s_C$	$s_H$	1	0.96	0.93	0.89	0.85	0.81	0.78	0.74	0.7	0.66	0.63
$s_D$	$s_E$	0.4	0.46	0.52	0.58	0.64	0.7	0.76	0.82	0.88	0.94	1
$s_E$	$s_H$	0.2	0.28	0.36	0.44	0.52	0.6	0.68	0.76	0.84	0.92	1
$s_F$	$s_G$	0.4	0.36	0.32	0.28	0.24	0.2	0.16	0.12	0.08	0.04	0
$s_G$	$s_H$	1	0.96	0.93	0.89	0.85	0.81	0.78	0.74	0.70	0.66	0.63

With the navigation network and weights, three navigation paths from  $s_A$  (departure) to  $s_H$  (destination) are planned (Figure 5.8), in which path 1 ( $s_A \rightarrow s_D \rightarrow s_E \rightarrow s_H$ ) is the traditional shortest path, path 2 ( $s_A \rightarrow s_F \rightarrow s_G \rightarrow s_H$ ) is the MTC-path. The path 3 ( $s_A \rightarrow s_F$ ) is the NSI-path. It should be clarified that in this case, the path 3 is a part of the path 2, because it happens that  $s_F$  is the sI-space closest to the departure  $s_A$ . Nevertheless, if the closest sI-space to  $s_A$  is another space rather than the  $s_F$ , this coincidence will disappear.

The information of the three path options are listed in Table 5.3. To show how the

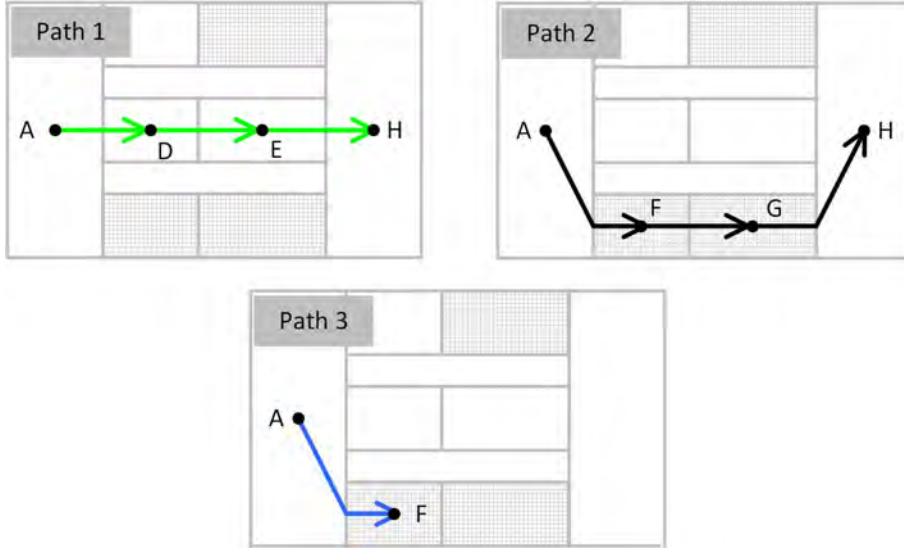


FIGURE 5.8: The three navigation paths from  $s_A$  (departure) to  $s_H$  (destination).  $s_A \rightarrow s_D \rightarrow s_E \rightarrow s_H$  is path 1 (green),  $s_A \rightarrow s_F \rightarrow s_G \rightarrow s_H$  is path 2 (black), and  $s_A \rightarrow s_F$  is path 3 (blue).

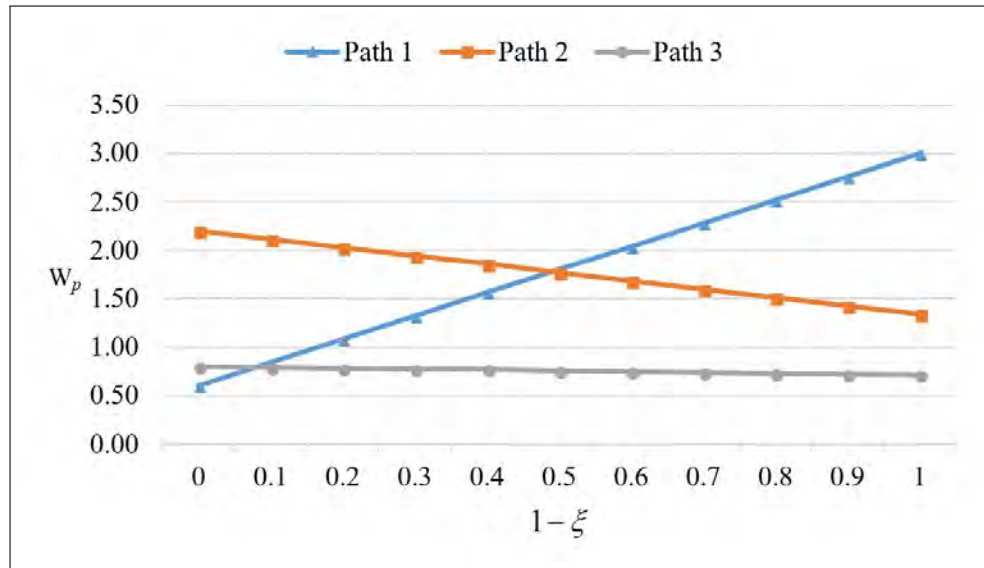
information are computed, we select  $1 - \zeta = 0.3$  (i.e.,  $\zeta = 0.7$ ) as an example. For the path 1,  $W_p = W''_{s_A s_D} + W''_{s_D s_E} + W''_{s_E s_H} = 0.3 + 0.58 + 0.44 = 1.32$ ,  $P_l = d_{s_A s_D} + d_{s_D s_E} + d_{s_E s_H} = 3 + 5 + 4 = 12$ ,  $P_{luc} = d_{uc_{s_A s_D}} + d_{uc_{s_D s_E}} + d_{uc_{s_E s_H}} = 3 + 5 + 4 = 12$ , and  $P_{cr} = (P_l - P_{luc})/P_l = (12 - 12)/12 = 0$ . Similarly, for the path 2,  $W_p = W''_{s_A s_F} + W''_{s_F s_G} + W''_{s_G s_H} = 0.77 + 0.28 + 0.89 = 1.94$ ,  $P_l = d_{s_A s_F} + d_{s_F s_G} + d_{s_G s_H} = 7 + 5 + 8 = 20$ ,  $P_{luc} = d_{uc_{s_A s_F}} + d_{uc_{s_F s_G}} + d_{uc_{s_G s_H}} = 5 + 0 + 5 = 10$ , and  $P_{cr} = (P_l - P_{luc})/P_l = (20 - 10)/20 = 0.5$ . As for the path 3,  $W_p = w''_{s_A s_F} = 0.77$ ,  $P_l = d_{s_A s_F} = 7$ ,  $P_{luc} = d_{uc_{s_A s_F}} = 5$ , and  $P_{cr} = (P_l - P_{luc})/P_l = (7 - 5)/7 = 0.29$ .

It shows that with the changing of the  $\zeta$ , the  $W_p$  of the three navigation paths change (Figure 5.9). Overall, with the decreasing of  $\zeta$  (i.e., the increasing of  $1 - \zeta$ ), the  $W_p$  of path 1 is rising, while that of path 2 and 3 are falling, which reveals that with paying more attention to the top-coverage-ratio of the path, the traditional shortest path becomes less attractive. That is, if  $\zeta$  is less than 0.5, the path 2 is recommended, otherwise, the recommendation becomes the path 3.

Comparing paths 1 and 2, before  $\zeta$  reaching to 0.4, the path 2 is recommended for agents. For instance, if  $\zeta = 0.4$ , The uncovered distance of path 2 ( $P_{luc2} = 12$ ) is shorter than that of path 1 ( $P_{luc1} = 14$ ), although  $W_p$  of path 2 is smaller than that of path 1,

TABLE 5.3: Three different navigation paths.

$1 - \xi$	Path 1				Path 2				Path 3			
	$W_p$	$P_l$	$P_{l_{uc}}$	$P_{c_r}$	$W_p$	$P_l$	$P_{l_{uc}}$	$P_{c_r}$	$W_p$	$P_l$	$P_{l_{uc}}$	$P_{c_r}$
0	0.6	12	12	0	2.2	20	10	0.5	0.8	7	5	0.29
0.1	0.84	12	12	0	2.11	20	10	0.5	0.79	7	5	0.29
0.2	1.08	12	12	0	2.03	20	10	0.5	0.78	7	5	0.29
0.3	1.32	12	12	0	1.94	20	10	0.5	0.77	7	5	0.29
0.4	1.56	12	12	0	1.86	20	10	0.5	0.77	7	5	0.29
0.5	1.8	12	12	0	1.77	20	10	0.5	0.76	7	5	0.29
0.6	2.04	12	12	0	1.68	20	10	0.5	0.75	7	5	0.29
0.7	2.28	12	12	0	1.6	20	10	0.5	0.74	7	5	0.29
0.8	2.52	12	12	0	1.51	20	10	0.5	0.73	7	5	0.29
0.9	2.76	12	12	0	1.43	20	10	0.5	0.72	7	5	0.29
1	3	12	12	0	1.34	20	10	0.5	0.71	7	5	0.29

FIGURE 5.9: The changes of  $W_p$  with the changing of the  $\xi$ .

and the top-coverage-ratio ( $P_{c_{r2}} = 0$ ) is smaller than that of path 1 ( $P_{c_{r1}} = 0.3$ ). For this case, NSI-path is computed. But, path 2 is still be recommended, because the length of NSI-path is longer than that of path 2.

In contrast, comparing the path 2 and path 3, we can find that if  $\xi$  less than to 0.5, the path 2 is recommended, otherwise, the recommendation is the path 3. Because when the  $\xi > 0.5$ , the  $W_p$  of path 3 smaller than that of path 2, the uncovered distance of path 3 is shorter than that of path 2, and the top-coverage-ratio changes larger than that of path 2.

Comparing paths 1 and 3 only, at the beginning (i.e.,  $\xi = 1$ ), the two paths are the same from the  $W_p$  aspect. But, with the decreasing of ( $\xi$ ), path 3 becomes the recommended path considering its  $W_p$  becomes always less than that of path 1. Furthermore, its covered distance is longer than that of path 1 ( $P_{l_{c3}} > P_{l_{c1}}$ ) and top-coverage-ratio is bigger than that of path 1 ( $P_{c_{r3}} > P_{c_{r1}}$ ).

### 5.3 Summary

This chapter presents a unified 3D space-based navigation model that is developed by extending IndoorGML concepts for seamless indoor/outdoor network extraction and path computation. The modifications are relatively small and can be easily adopted by the standard, because the extensions only happened on the attributes of the two classes in the navigation module, *CellSpace* and *CellSpaceBoundary* where the definitions of the classes remain the same. In particular, four new attributes (*sType*, *topClosure*, *sideClosure*, and *bottomClosure*) are introduced for *CellSpace* and two new (*category* and *bType*) for *CellSpaceBoundary*. This model allows us to consider a larger variety of navigation options using the classification of spaces. By assigning certain weights on spaces according to the users' preferences and tasks, it can help to achieve user-dedicated navigation paths. In addition, this model can be used for designing a spatial schema for management in DBMS, which will ensure the path planning can cover a large area, many operations can be completed at a database level, and only needed path will be sent to the end-user application.

Two new path options based on sI-spaces are developed, including MTC-path and NSI-path. The two novel options enrich the traditional shortest distance/time navigation path and opens new directions for developing new path options, thereby can bring in a new navigation experience for pedestrians. From the characteristics of the spaces, sI-spaces and I-spaces are two types of spaces that have tops, but this research considers the sI-spaces only, because the sI-spaces are mostly public (Zhu et al., 2016) while the I-spaces are often regarded as non-public.

## CHAPTER 6

---

# RECONSTRUCTION APPROACHES FOR DIFFERENT TYPES OF SPACES

---

On the basis of 3D spaces and Poincaré duality, navigation networks can be automatically derived. Nevertheless, 3D space models of the four types of spaces are not always available. No existing application can offer 3D space models of semi-indoor, semi-outdoor and outdoor, because the three types of spaces are partially or entirely open. BIM models can be data sources of indoor 3D space models, but the problem is BIM models are not always handy, such as some old built buildings have no such kind of data. This chapter presents the approaches for reconstructing different types of spaces as *CellSpace*, in which the 3D geometry of a *CellSpace* is a volume that are combined of several *CellSpaceBoundary* (surfaces). That is, the 3D *CellSpace* reconstruction is a process of automatically reconstructing *CellSpaceBoundary* and joining them into 3D volumes.

All four types of spaces are reconstructed for the purpose of testing the developed

theories and models in this research. Considering all possible data sources, the reconstructing approach of the different spaces are the following:

- (a) sI-spaces. The approach of sI-spaces reconstruction is creating 3D spaces base on projection operations between components that inspired from CityGML LoD 3 models, such as *RoofSurface*, *GroundSurface*, *OuterCeilingSurface*, and *OuterFloorSurface*.
- (b) sO-spaces and O-spaces. The approach of reconstructing the sO-spaces and O-spaces is enclosing them into 3D enclosed volumes based on their footprints, a contact height, and DTM.
- (c) Building shells. The approach of reconstructing the building shells is extruding their footprints based on building heights and DTM.

This chapter is based on my papers 4, 6, 7 and 8 (see Section 1.6).

## 6.1 Semi-indoor Space Reconstruction

The semi-indoor space reconstruction is a process of enclosing sI-spaces as 3D enclosed volumes by creating missing sides. Taking advanced level of detail models (e.g., minimum CityGML LoD3 or BIM) as the data sources, the reconstruction includes the following steps:

- Identification & ordering of proper building components;
- Determination of top and bottom & space generation;
- Space trimming.

### 6.1.1 Identification & Ordering of Proper Building Components

Built structures, such as balconies, dormers or outer stairs could form sI-spaces. Therefore, the first step is to detect such building components in the input 3D models. The ground is also necessary, especially in cases that have no floors, e.g., a gas station.

For this purpose, we strongly rely on the semantic information provided in the model and we assume advanced level of detail models (e.g., minimum CityGML LoD3 or BIM) are ready and the building components are identified based on their semantics.

Then these identified building components are sorted on the basis of their average value of the  $z$  coordinates. A virtual geometric  $XY$  plane is considered as the reference and its  $z$  coordinates are the minimum among all components. If more than one of the components have the same value of the  $z$ , they are ordered randomly.

The average value of the  $z$  coordinate of each component is computed using equation 6.1:

$$z_A = \frac{1}{n} \sum_{i=1}^n z_i \quad (6.1)$$

where  $z_A$  = the average of the  $z$  coordinate of the component  $A$

$n$  = number of vertices of component  $A$

$z_i$  = the  $z$  coordinate of  $i_{th}$  vertex

### 6.1.2 Determination of Top and Bottom & Space Generation

From higher to lower components (in the direction of the  $Z$  – *direction*), based on projection, overlaps that symbolize the desired space boundaries are detected. If the building components are volumes (e.g., in BIM models), a pre-processing step to this one includes a decomposition of the volumes into relevant upper and lower polygons. The process of space reconstruction between any two polygons includes four steps: (i) project the original two polygons onto the same plane along the  $Z$  – *direction*; (ii) compute the overlaps between their projections by intersection; (iii) find the tops and bottoms by projecting the overlaps back onto the two original polygons along the  $Z$  – *direction*; and (iv) obtain the missing lateral sides that allows forming closed volumes. In the second step, the projections on the same plane lead to one of two possible spatial relationships: either they overlap, or they do not. If their projections overlap, the region of intersection will

be computed. Moreover, if the overlap is not a polygon (a line or point, for example), it is regarded as a case of no overlap.

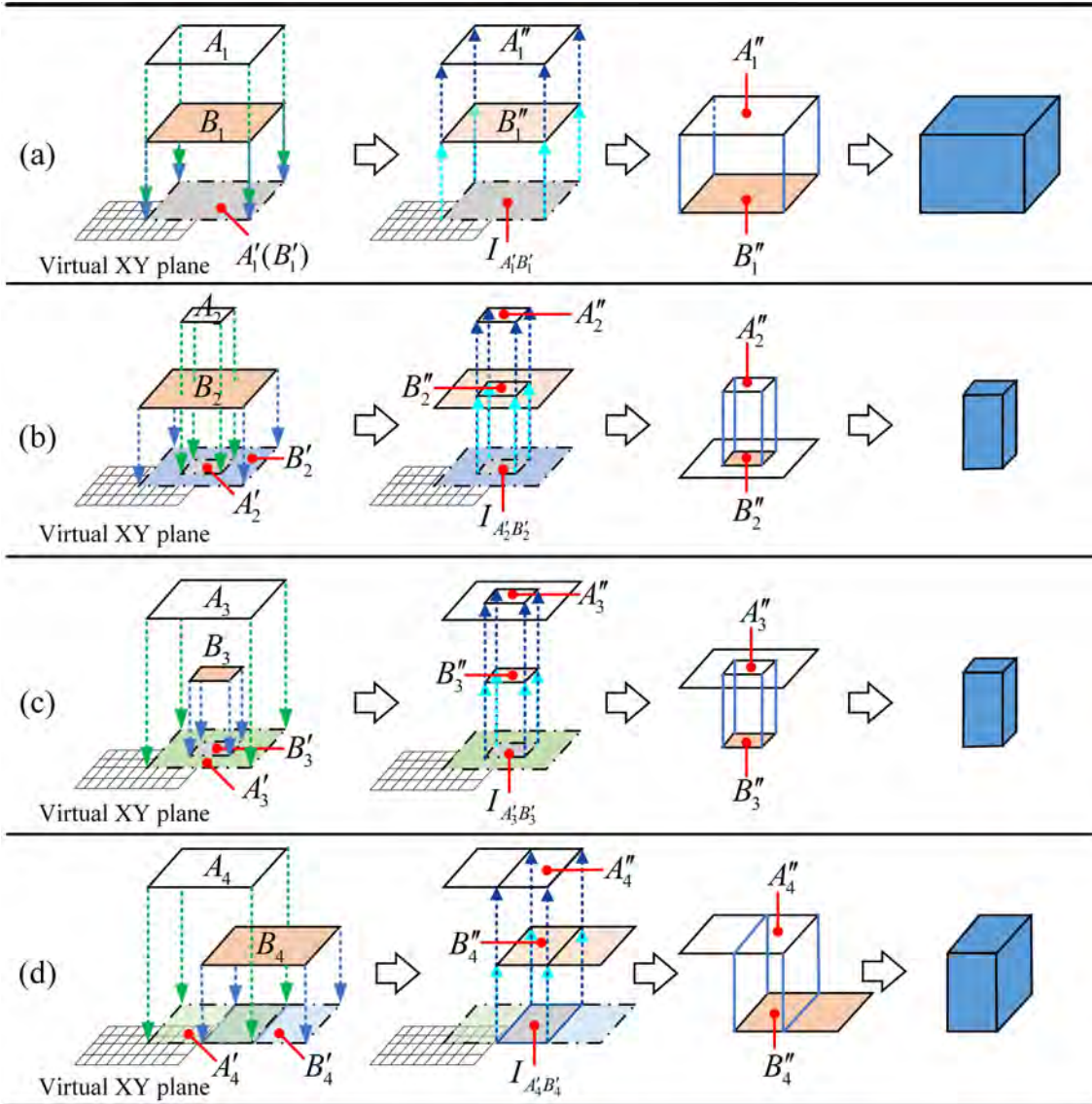


FIGURE 6.1: Four different cases of sI-space reconstruction based on projecting. The original polygons are  $A_i$  (in white) and  $B_i$  (in yellow), and their projections are  $A'_i$  (in gray) and  $B'_i$  (in light green) respectively. The created sI-spaces are coloured in dark blue.

Figure 6.1 illustrates the determination of top(s) and bottom(s). Then, the reconstruction of sI-spaces includes four different cases. The original polygons are  $A_i$  and

$B_i$ . Assuming their projections are  $A'_i$  and  $B'_i$ , respectively, the relationships of their projections are  $A'_1 = B'_1$ ,  $A'_2 \subset B'_2$ ,  $B'_3 \subset A'_3$ , and  $A'_4 \cap B'_4 \neq \emptyset$  (sub-figures in the first column). Then, the overlaps of their projections ( $I_{AB}$ ) are computed by intersection; i.e.,  $I_{A'_1B'_1} = A'_1(B'_1)$ ,  $I_{A'_2B'_2} = A'_2$ ,  $I_{A'_3B'_3} = B'_3$ , and  $I_{A'_4B'_4} = A'_4 \cap B'_4$  (sub-figures in the second column). The third step is to project the overlaps ( $I_{A'_1B'_1}$ ,  $I_{A'_2B'_2}$ ,  $I_{A'_3B'_3}$ , and  $I_{A'_4B'_4}$ ) back to the original polygons along the  $Z$  – direction; then, top(s) and bottom(s) are calculated:  $\{A''_1, B''_1\}$ ,  $\{A''_2, B''_2\}$ ,  $\{A''_3, B''_3\}$ , and  $\{A''_4, B''_4\}$  (sub-figures in the third column).  $A''_i$  and  $B''_i$  are parts of polygons  $A_i$  and  $B_i$ , respectively, acting as top and bottom. Projections of  $A''_i$  and  $B''_i$  are equal to  $A'_i \cap B'_i$ . Because our approach relies entirely on the  $Z$ -direction as the projection direction, the last step is to match the top and bottom directly to obtain the missing lateral polygons (sides) that allow forming closed volumes (sub-figures in the last column). In addition, these operations are applicable to polygons that are not horizontal (inclined cases), but the vertical cases are not, as the projections of vertical components on the  $Z$  – direction are lines rather than polygons.

For the whole procedure of reconstructing all sI-spaces, any two polygons in the ordered component set are chosen to repeat the four steps. Then, all sI-spaces are reconstructed as 3D spaces.

### 6.1.3 Space Trimming

The final step is to trim the reconstructed 3D sI-spaces (volumes) based on their positions, because these spaces may have overlapping parts.

Figure 6.2 illustrates the space reconstruction and trimming among three building components, in which the  $B$  and  $C$  are horizontal, while  $A$  is inclined. Suppose  $A$  is an inclined roof,  $B$  is a floor slab, and  $C$  is the ground. Repeating the four steps described in the last section three times, three sI-spaces are reconstructed, which tops and bottoms are  $\{A''_1, B''_1\}$  (Figure 6.2(b)),  $\{A, C''_1\}$  (Figure 6.2(c)), and  $\{B, C''_2\}$  (Figure 6.2(d)). The space that top and bottom is  $\{A, C''_1\}$  is overlapping with the other two. Thus, it is trimmed by the spaces shown in Figure 6.2(b) and 6.2(d). The trimmed result can be seen in Figure 6.2(e), in which  $A''_2$ , and  $C''_3$  are the top and bottom respectively. Thus, for this example,

the final results of sI-spaces reconstruction are three spaces without overlaps, in which top(s) and side(s) are  $\{A_1'', B_1''\}$ ,  $\{A_2'', C_3''\}$ , and  $\{B, C_2''\}$  (Figure 6.2(f)).

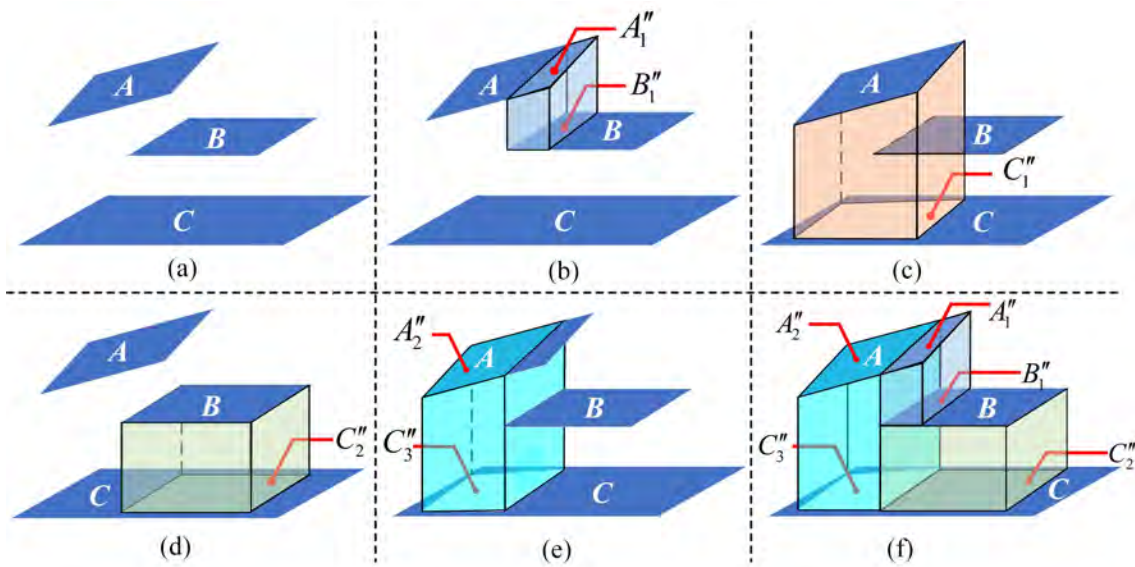


FIGURE 6.2: Example of trimming spaces. To distinguish sI-spaces that are created based on different tops and bottoms, they are coloured differently. (a) shows the three building components; (b), (c), and (d) are three sI-spaces based on projections; (e) is the space trimmed by the other two spaces; (f) the final three reconstructed sI-spaces.

#### 6.1.4 Illustration of Semi-indoor Space Reconstruction

The most of the cases where sI-spaces can be detected will likely appear in CityGML LoD3 (and above) models or BIM models. However, due to the lack of availability of LoD3 or LoD4 data, this research manually created a synthetic LoD3 model for the sake of illustration of the approach. It is a two-story house with inclined roofs, a balcony, a shelter, and a garage (Figure 6.3(a)). First of all, we selected all the *OuterCeilingSurface* and *OuterFloorSurface*. In the meantime, we used a default plane polygon extended from the floor polygon as the *GroundSurface* (Figure 6.3(b)). Secondly, all the sI-spaces are reconstructed (Figure 6.3(c)). After trimming spaces, we finally obtained thirteen sI-spaces (Figure 6.3(d)).

It is worth mentioning that although the illustration is a house, it is already sufficiently complex to be able to represent real-world cases. Thence, with this approach, the sI-spaces of the built structures (e.g., gas station, bus stop) can be reconstructed. Their roofs (covers/shelters) are used as the tops, and the *GroundSurface* as bottom. Another thing should be mentioned is that the CityGML LoD3 models or BIM models are the bottleneck of this approach.

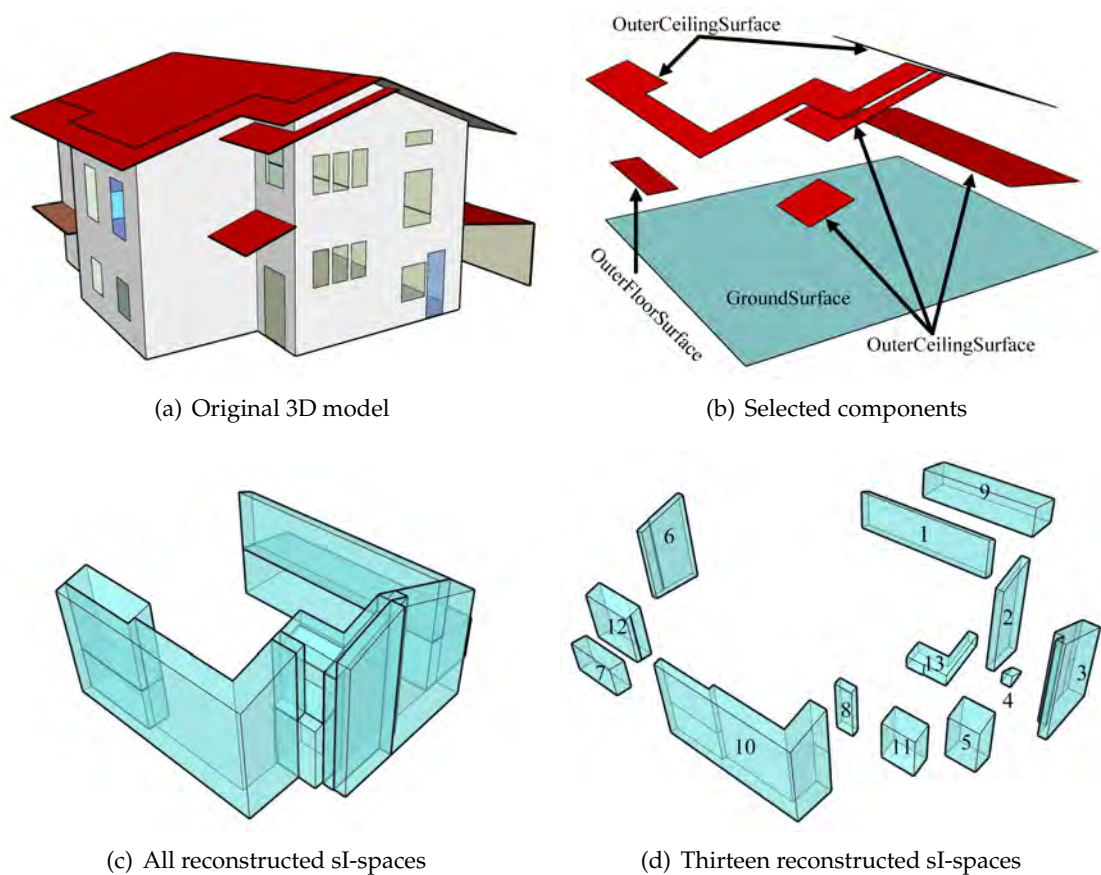


FIGURE 6.3: Illustration of sI-space reconstruction.

## 6.2 Semi-outdoor & Outdoor Reconstruction

This section presents the approach of reconstructing sO-spaces and O-spaces, which is the process to enclose semi-outdoor and outdoor into 3D enclosed volumes and meanwhile keep the topological consistency between the terrain and them. This approach uses

footprints, a contact height, and DTM as inputs and the whole procedure consists of three steps as follows (Figure 6.4):

- Extract object footprints;
- Classify semi-outdoor and outdoor;
- Reconstruct 3D spaces.

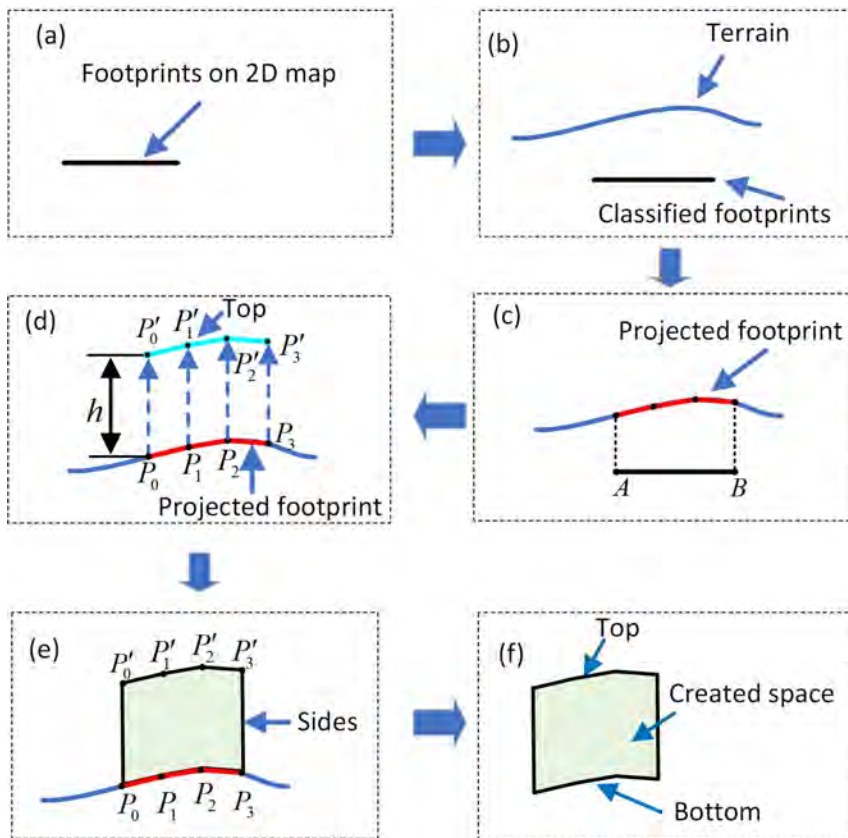


FIGURE 6.4: The process of sO-space and O-space reconstruction.

### 6.2.1 Extract Object Footprints

This research only concentrates on roads and green areas, because they are the main semi-outdoor and outdoor environments where people have activities. Moreover, they are generally open or surrounded by objects like the fence, hand railing, enclosing wall, or building walls. For instance, a playground or yard is separated by a fence from the

street; a disabled passageway is surrounded by hand railings; an alley is formed by buildings on both sides. To put it another way, areas (roads and green) and objects (fence, hand railing, enclosing wall, or building walls) are two indispensable factors in the formation of sO-spaces. Therefore, in this step, footprints of roads, green areas and objects (fences, hand railings, enclosing walls, and building walls) are extracted from a 2D map.

Furthermore, the I-spaces and sI-spaces are generally originating from volumetric objects (buildings). Thereupon, this research only considers extracting footprints of the I-spaces and sI-spaces formed by built structures. Figure 6.5 illustrates three cases of I-spaces and sI-spaces, in which footprints of indoor and semi-indoor space are extracted based on buildings.

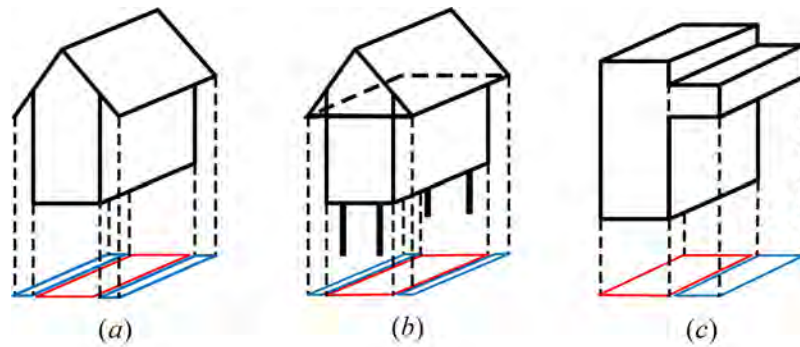


FIGURE 6.5: The footprints of indoor (red) and semi-indoor (blue) spaces formed by built structures. (a) a building with eaves; (b) a building with eaves and its lowest floor is above ground; (c) a building with a hanging part.

### 6.2.2 Classify Semi-outdoor and Outdoor

The procedure of classifying semi-outdoor and outdoor is based on side closure ( $C^S$ ). In particular, for each footprint (polygon) of a road or green area, it will be used to have intersection operations with all the surrounding physical boundaries (curves). If the result of intersection operations is a polyline, rather than a point or nothing, it means this polygon is bounded by the physical boundaries (at least partly). Then, the  $C^S$  of each area (polygon) can be computed by Equation 3.5. After that, all footprints are classified into semi-outdoor and outdoor on the basis of the side closure.

### 6.2.3 Reconstruct 3D spaces

In this step, the original footprints firstly are projected onto the terrain to get the projected footprints. After that, virtual side boundaries are computed by extruding them up along the  $Z$  – *direction* based on the height ( $h$ ) (Figure 6.4(d)). Here, setting the  $h$  is a tricky issue, because there are generally no physical structures that can be used as the references for determining the height of such kind of spaces. In this research, it is set as a contact height - 2 meters, because we consider this height is sufficient for pedestrian navigation (Figure 3.3). To make sure the final 3D spaces are correct volumes, the orientation of each polygon is set to counter-clockwise. In particular, suppose there is a segment of projected footprint, which has four vertices  $P_0(x_0, y_0, z_0)$ ,  $P_1(x_1, y_1, z_1)$ ,  $P_2(x_2, y_2, z_2)$ , and  $P_3(x_3, y_3, z_3)$ . Then, after counter-clockwise sorting, all the vertices will be extruded up to get  $P'_0(x_0, y_0, z_0 + h)$ ,  $P'_1(x_1, y_1, z_1 + h)$ ,  $P'_2(x_2, y_2, z_2 + h)$ , and  $P'_3(x_3, y_3, z_3 + h)$ . Then, these vertices are connected end to end to form a side boundary, which can be represented as a *polygon*( $P_0, P_1, P_2, P_3, P'_3, P'_2, P'_1, P'_0, P_0$ ) (Figure 6.4(e)).

Then, 3D spaces (volumes) are reconstructed by joining top(s), sides and bottom(s). The bottom surface is computed by making polygon surfaces from all vertices of the projected footprint. The reconstruction of top is similar, where the vertices are  $P'_0, P'_1, P'_2$ , and  $P'_3$ . Reconstructed 3D spaces are shown in Figure 6.4(f), where the type of reconstructed space is the same as the corresponding classified footprint, for instance, if a space is reconstructed from a semi-outdoor footprint, the reconstructed space is a sO-space.

### 6.2.4 Illustration of Semi-outdoor and Outdoor Space Reconstruction

In order to simulate a scene that has indoor, semi-indoor, semi-outdoor and outdoor environments at the same time, this illustration is shown based on a synthetic data, which has a building with eaves, a garden with fence, a pavement, and a street (Figure 6.6(a)). The footprints of these objects subdivide the 2D map of this area as several polygons (Figure 6.6(b)). The polygons (footprints), *polygon*(A,B,C,D,E,F,A) is the building, *polygon*(B,C,D,E,K,L,B) is the sI-space, *polygon*(E,F,G,H,I,J,K,E) is the garden,

polygon(L,K,J,I,H,N,M,L) is the pavement, and polygon(M,N,O,P,M) is the street. polyline(J,K,E,F,G,H,I) and polyline(C,B,A,F,E,D) represent physical fence and building walls respectively, which are shown in double black and red lines.

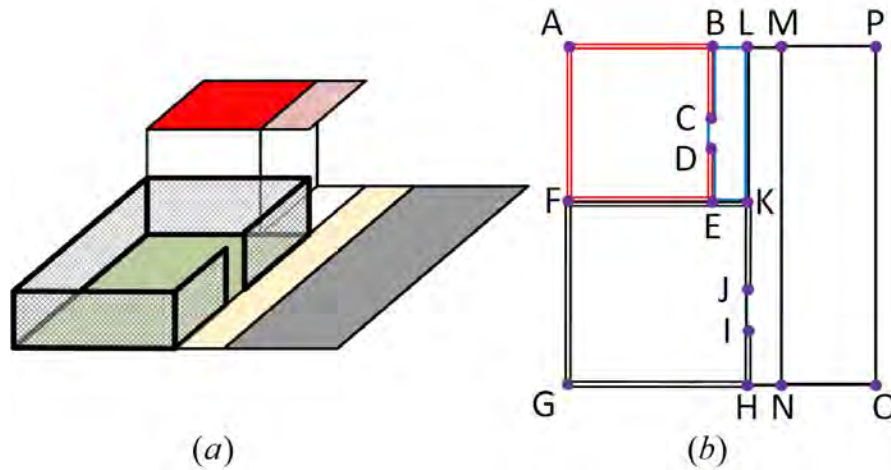


FIGURE 6.6: Built objects and their non-overlap footprints. (a) Built objects; (b) Corresponding 2D footprints.

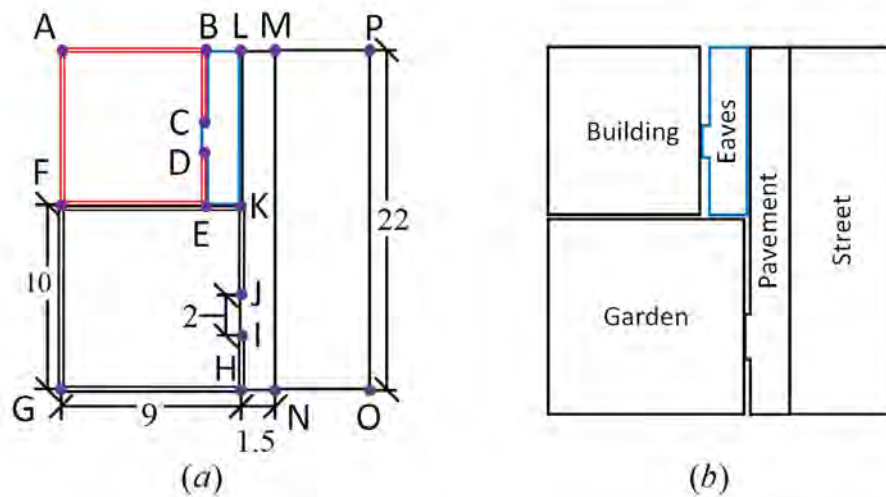


FIGURE 6.7: Example of footprints classification based on overlaps (unit:  $m$ ).

Except for the footprints of indoor (in red) and semi-indoor (in blue), there are four footprints, fence, garden, pavement, and street (Figure 6.7). Using fence and building walls as physical boundaries, the  $C^S$  of the four footprints can be estimated. For the garden, its  $l_{_e} = l_{JK} + l_{KF} + l_{FG} + l_{GH} + l_{HI} = 9 + 10 + 9 + 10 - 2 = 36$ , while  $l_{_t} =$

$l_e + l_{IJ} = 36 + 2 = 38$ . Thus,  $C^S = l_e/l_t = 36/38 = 0.95$ . For the pavement,  $l_e = l_{HK} - l_{IJ} = 10 - 2 = 8$ , and  $l_t = l_{HI} + l_{IJ} + l_{JK} + l_{KL} + l_{LM} + l_{MN} + l_{NH} = 22 + 1.5 + 22 + 1.5 = 47$ , so the  $C^S = l_e/l_t = 8/47 = 0.17$ . There is no physical boundary for the street. Therefore, the  $C^S$  of the garden footprint is 0.95, pavement is 0.17, and the street is 0. Based on the condition that if  $C^S \geq 0.75$ , the garden is classified as sO-space, while the pavement and street are outdoor spaces (Figure 6.7(b)).

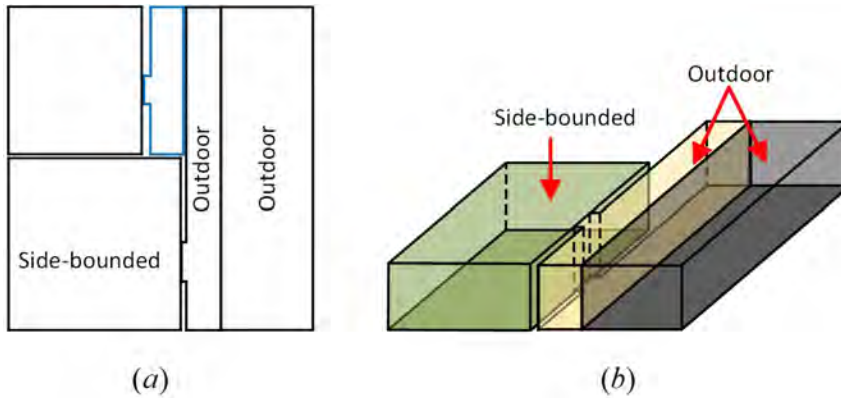


FIGURE 6.8: Example of reconstructed sO-spaces and O-spaces (height = 5). (a) Classified footprints; (b) Reconstructed sO-spaces and O-spaces.

The reconstructed sO-space (garden) and two O-spaces (pavement and street) are illustrated in Figure 6.8. Pedestrians can circulate between the garden space and pavement space, because the two spaces are sharing a virtual boundary surface, so do the pavement and street spaces. But pedestrians cannot directly travel from the garden to street space as the two spaces are isolated from each other.

### 6.3 Building Shells Reconstruction

The inputs for reconstruction of building shells in this research are building footprints, building heights, and DTM. These data are generally available from governmental and open datasets (e.g., OSM). After obtaining building footprints and DTM, the first step is checking if the data have the same coordinate reference system (CRS). If the data are obtained from different sources, they need to be transformed (aligned) in the same

CRS. Then, the building shells reconstruction process consists of four steps as follows (Figure 6.9):

- Compute TIC by projecting footprints onto the terrain;
- Set height and create sides;
- Generate top and bottom to build building shells;
- Rebuild terrain considering TIC as constraints.

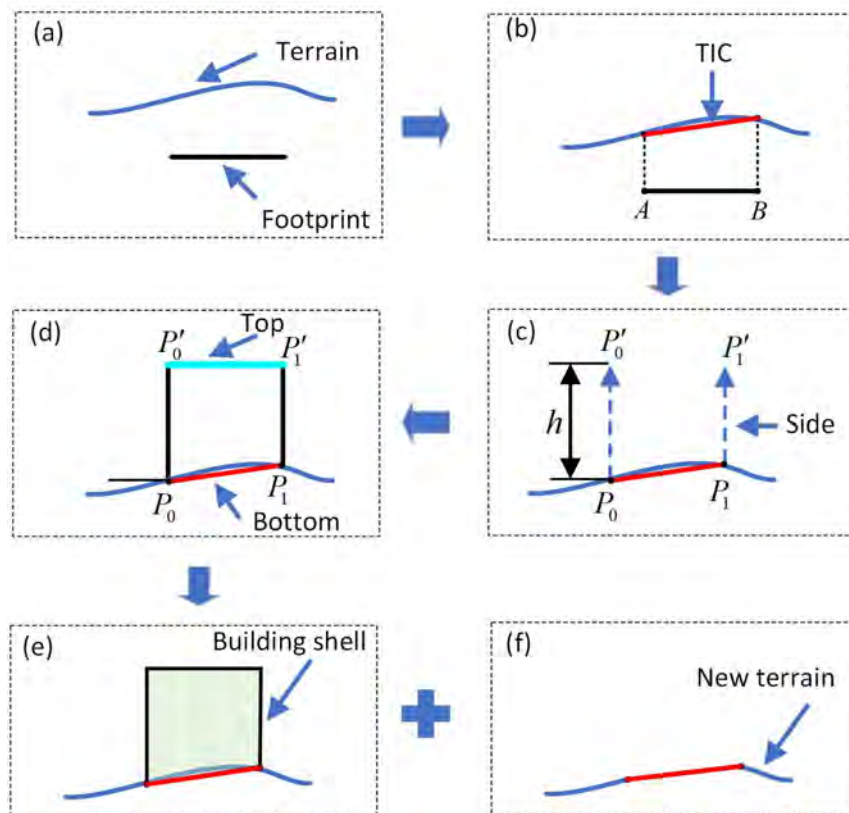


FIGURE 6.9: The process of building shells reconstruction based on building footprints, building heights and DTM.

### 6.3.1 Compute TIC by Projecting Footprints onto the Terrain

The footprints are normally presented as 2D polygons with coplanar vertices. Therefore, the first step is to compute the corresponding building footprints projection on the terrain. This projections of building footprint on the terrain are the TIC.

The TIC computation process is **Projecting Vertices of footprints on the Terrain (PVT)**. This practice ensures the number of points of the original footprints is preserved (Figure 6.9(b)). As expected, the shape of the projected footprint is unaltered as indicated from the top view, whereas the terrain is changed.

### 6.3.2 Set Height and Create Sides

After getting each counter-clockwise oriented projected footprint, sides are reconstructed by extruding them up along the  $Z$  – *direction* based on building heights ( $h$ ) (Figure 6.9(c)). In particular, a line segment of a projected footprint, which has the start and end vertices  $P_0(x_0, y_0, z_0)$  and  $P_1(x_1, y_1, z_1)$ , respectively.  $P_0$  and  $P_1$  will be extruded up along the  $Z$  – *direction* based on  $h$  to get  $P'_0(x_0, y_0, h)$  and  $P'_1(x_1, y_1, h)$ . Then, these four vertices can form a side, which can be represented as a *polygon*( $P_0, P_1, P'_1, P'_0, P_0$ ). It is worth noting that each composing polygon should follow counter-clockwise orientation to make sure the final 3D spaces are correct volumes (Figure 6.10).

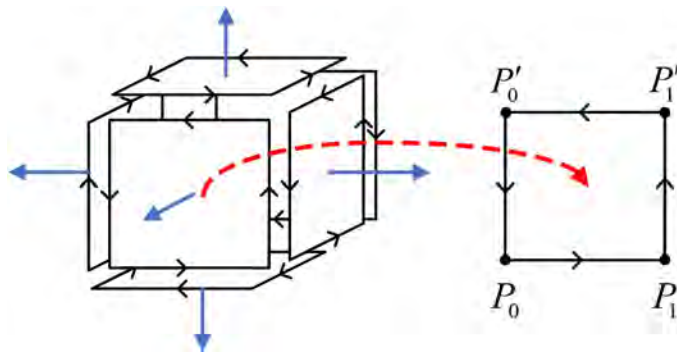


FIGURE 6.10: The outward-facing normal of boundaries of a 3D building shells.

### 6.3.3 Generate Top and Bottom to Reconstruct Building Shells

The third step is to generate the top(s) and bottom(s), and then join them with the reconstructed sides to make 3D volumes (Figure 6.9(d) and (e)). All tops are considered as planar surfaces and they are generated by making a polygon surface from a set of vertices. The bottom is slightly different from the top, because vertices used for the bottom(s) are not coplanar. Thus, after connecting the projected vertices, we can get an enclosed 3D polyline, and then it is patched as a bottom surface. After getting the top surfaces, bottom surfaces, and side surfaces, each 3D building shell can be reconstructed by joining them.

### 6.3.4 Rebuild Terrain Considering TIC as Constraints

The process of rebuilding terrain is taking the vertices of projected footprints as Points, and their edges as Breaklines (constraints) to calculate a Constrained Delaunay Triangulation (CDT), see Figure 6.9(f).

### 6.3.5 Illustration of the Building Shells Reconstruction

To illustrate and evaluate the entire process of the approach, a precinct example is employed, which includes 98 building footprints (Figure 6.11). The original building footprints are provided as a CAD file, in which all the footprints are polygons. The height of each buildings are also prepared. A DEM (5 metre) of the example area is used to construct Delaunay triangulation representing the terrain (DTM).

As the footprints and DTM are in the same coordinate system, they aligned automatically after importing. Then, the whole process starts from projecting the building footprints onto the terrain (Figure 6.12). From the top view, projected footprints (TIC) have the same shape as the original footprints, but they are 3D polylines rather than polygons.

Each line segment of a TIC will be extruded up to the same height along the  $Z$  – *direction* based on building heights to get a quadrilateral sides, i.e., a side is represented by one polygon. The bottom is made by patching the 3D polyline as a surface. The top is

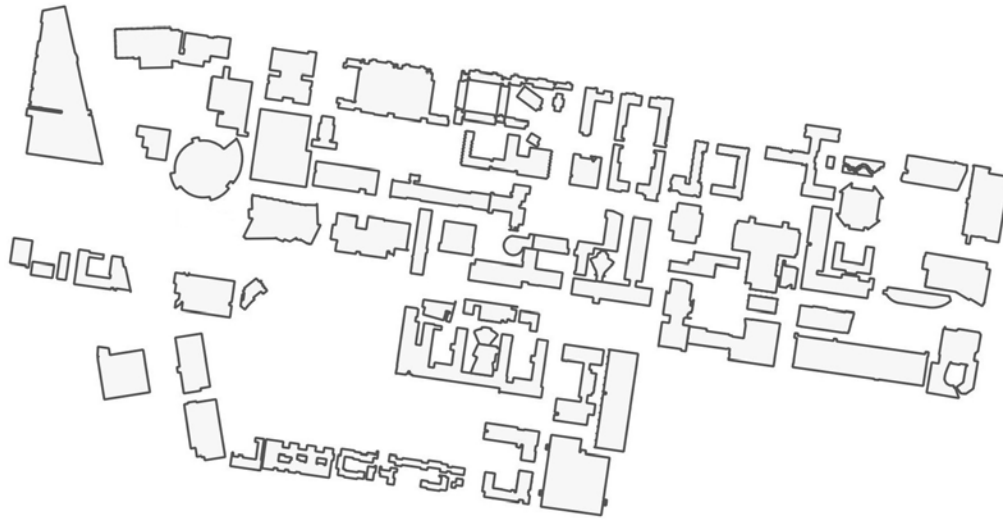


FIGURE 6.11: Building footprints for illustration.

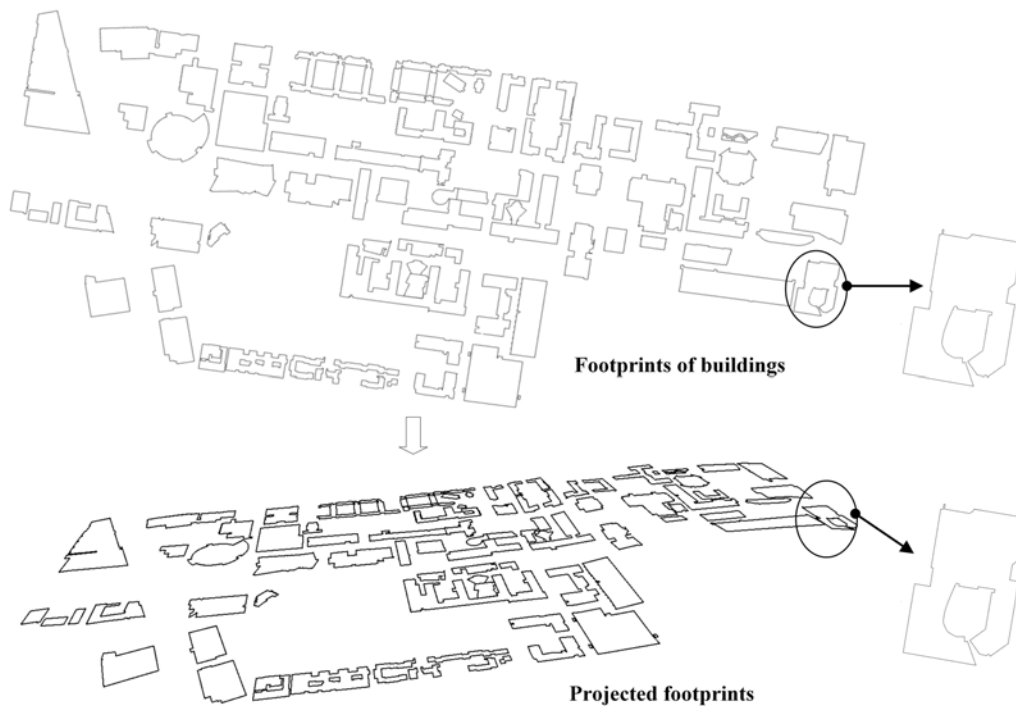
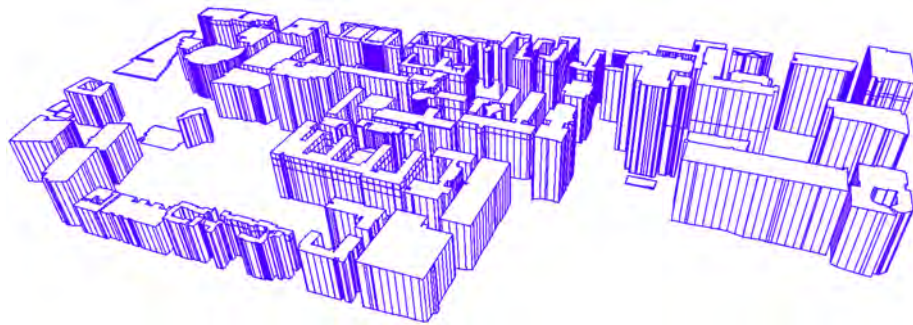


FIGURE 6.12: The projected footprints on the terrain.

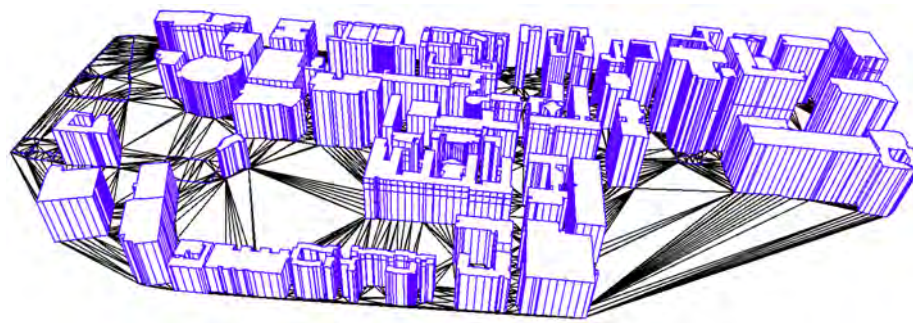
a planar surface constructed by ordered 3D points. Then, the building shells are enclosed by joining the tops(s), sides, and bottom(s) (Figure 6.13(a)).

The final step is to re-compute terrain using the vertices and edges of the projected

building footprints as constraints. The results of the re-triangulated terrain show that footprints are clearly recognisable within the triangulated surface. The principle of this method is changing the 3D I-spaces and terrain slightly to fit each other. The results show that the topological issue has been fixed and building shells are reconstructed successfully (Figure 6.13(b)).



(a) The reconstructed building shells.



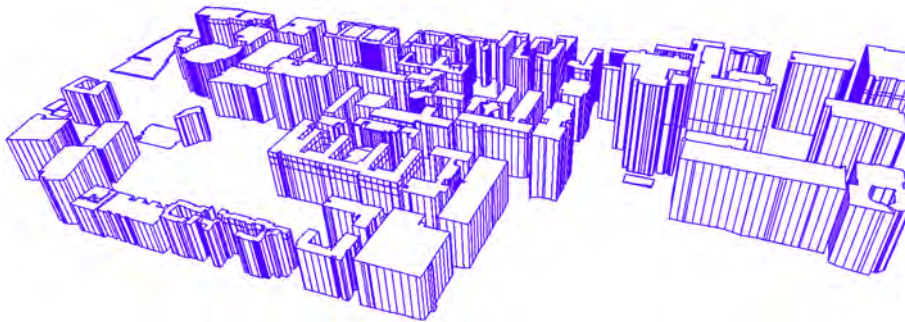
(b) The terrain combined with building shells.

FIGURE 6.13: The building shells and the terrain that are reconstructed based on PVT method.

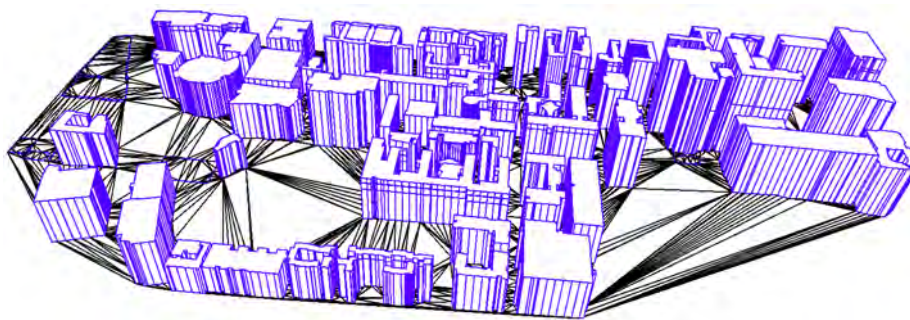
Except for the presented approach that project Vertices of footprints on the Terrain (PVT), another method is Projecting the whole footprint Polyline on the Terrain (PPT) (Figure 6.13(b)), the details can be seen in our paper (Yan et al., 2019). This method ensures the curvature of the terrain but might lead to unnecessarily complex walls, which differ from the reality (Figure 6.14(a)). Comparing terrain of the two methods, the result of PVT has less vertices and triangles in the terrain (Figure 6.13(b)), which means that the changes of terrain are more than in the PPT method.

The results of the two re-built DTM show that footprints are clearly recognisable

within the triangulated surface. That is, the topological consistency issue between the reconstructed 3D building shells and the terrain is successfully solved. The main point of the two methods are the reconstruction of building shells. The PVT method is more efficient in one aspect, having less vertices and façades, which is beneficial for a large precinct scale area. The PPT method complicates the building shells, but it preserves more details of TIC, which is good for estimating the areas of the building façades. (Figure 6.14(b)). It should be clarified that the terrain from PPT method has more triangles than the PVT method, but we cannot conclude that the terrain of the former is more precise than that of the latter method. Because the only difference comes from the TIC and only if there are more points in the empty spaces for terrain reconstruction, the rebuilt terrain will be more precise.



(a) The reconstructed building shells.



(b) The terrain combined with building shells.

FIGURE 6.14: The building shells and the terrain that are reconstructed based on PPT method.

In addition to the presented approach, other possible approaches of building shells reconstruction can be distinguished based on data source (Figure 6.15): (i) footprints +

Point cloud, (ii) 3D objects + DTM, (iii) 3D objects + 3D point clouds, and (iv) Point cloud only. The details of these four possible approaches can be found in our paper (Yan et al., 2019).

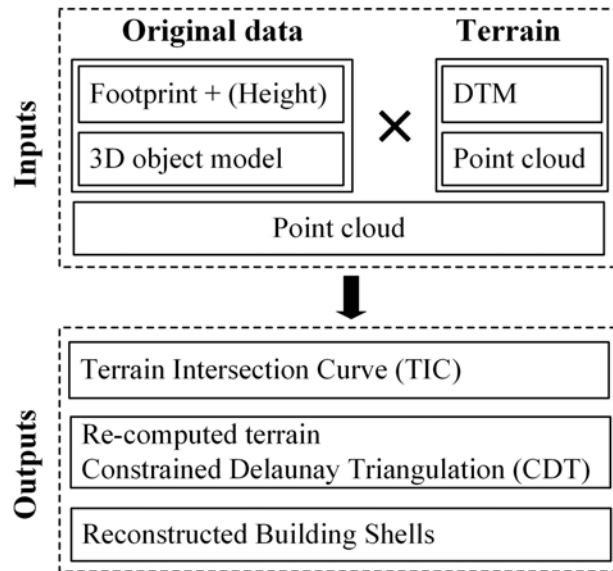


FIGURE 6.15: The other data sources for building shells reconstruction.

## 6.4 Summary

This chapter shows approaches that can automatically reconstruct sI-spaces, sO-spaces, O-spaces, and building shells as 3D spaces (volume). Thus, all types of spaces are able to mimic the indoor environments to derive a network based on 3D connectivity of spaces.

The sI-space reconstruction is an automatic method based on 3D models. The demonstration indicates that the reconstruction of sI-spaces (formed by built structures) is feasible on the basis of existing 3D standards such as CityGML or BIM. The reconstruction of sO-space and O-space is an automatic method based on a 2D map and DTM. However, considering the biggest limitation of the proposed approach is the data source, i.e., we generally do not have suitable data, such as detailed CityGML LoD 3 datasets or BIM

models. The approaches presented are only to demonstrate that these spaces can be created. We believe that the approaches can provide some inspirations for other researchers who need to reconstruct 3D spaces for navigations or other applications. The reconstruction procedure of the building shells is not a novel approach, but considering not always all the buildings exist as indoor models, therefore, the building shells still have to be reconstructed to provide better orientation. This research reconstructs the building shells to represent indoor spaces of the buildings that have no 3D models (e.g., BIM, CityGML LoD 4 models). But it does not mean that the 3D spaces within building shells are equal to indoor spaces as they have no interior.

In short, the sI-spaces formed by the building with 3D models are recommended to be reconstructed based on the projection-based method, while the reconstruction approach of the rests (data source is 2D maps) is extruding footprints of shelters along the z-direction with a contact height (2 meters). The procedures for sO-spaces and O-spaces reconstruction is also based on extrusion. Furthermore, all 3D space reconstructions in this research consider keeping the topological consistency between 3D spaces and terrain based on TIC (section 3.1.4). It is not true to assume that the reconstructed 3D spaces are standing on a plane surface and this surface is regarded as the default terrain. In fact, the natural terrain is irregular and uneven, rather than planar. It should be noted that the proposed approaches work fine within precinct areas (e.g., a campus or similar) where pedestrians can reach on foot. If the scenarios become a city level, abstraction/aggregation mechanisms will be needed. This research does not reach the complexity and optimization topics, but these topics will be investigated in-depth in future work (Section 8.3.4).

# CHAPTER 7

---

## IMPLEMENTATION & CASE STUDY

---

This chapter implements all the previously developed theories, models, and approaches for indoor-outdoor seamless navigation path planning. After introducing the data, software, and flowchart for implementation, the mapping of the UML model to Python classes, space classification, reconstruction, and selection are presented. Then, two path planning examples with five navigation paths are illustrated on the basis of the derived navigation networks. Finally, the uncertainties and limitations of the whole work are discussed in the summary. This chapter is based on my papers 1, 2 and 4 (see Section 1.6).

### **7.1 Data, Software, and Flowchart for Implementation**

The test area is part of the University of New South Wales (UNSW) campus in Kensington. There are seven types of objects, including buildings, shelters, roads, green areas,

hand railings, enclosing walls and fences (Figure 7.1). The buildings indicate I-spaces, hand railings, enclosing walls and fences serve as physical boundaries. Shelters represents areas of sI-spaces. Roads and green areas are sO-spaces and O-spaces.

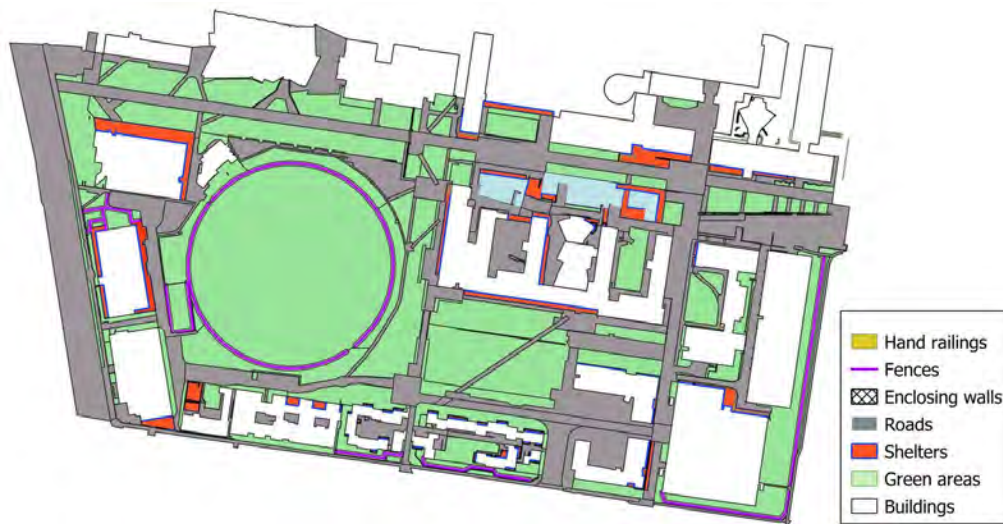
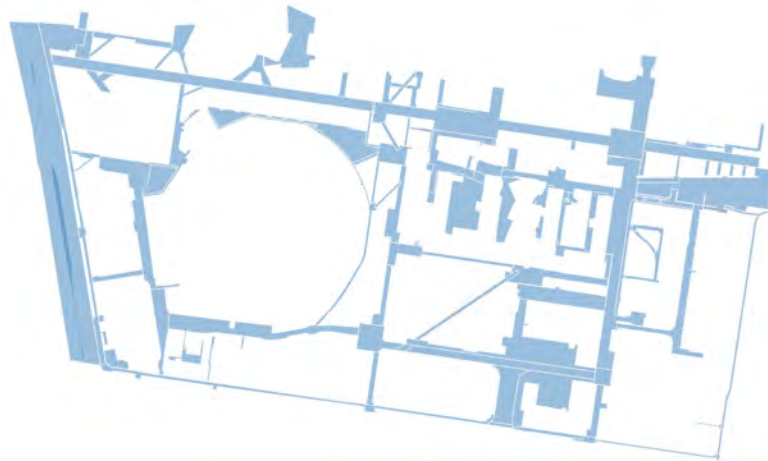


FIGURE 7.1: Footprints of spaces on the selected area of UNSW campus. The dot-filled footprint is the building that has BIM model.

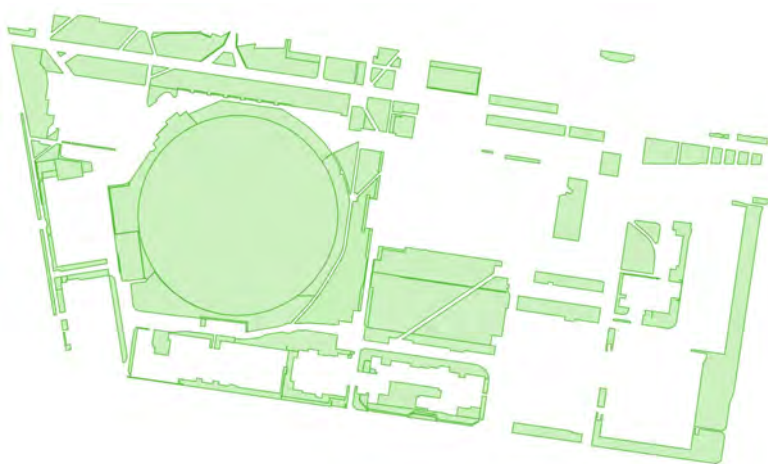
The initial data of the objects are footprints in a geo-referenced 2D map (the CRS is EPSG:28356). It is provided by the Estate Management (EM) of the UNSW as a CAD file, in which no attributes are attached to the geometry. General speaking, we can obtain such a 2D map with attributes from OSM, but in this implementation, geometry in the map provided by UNSW EM is used while the map from OSM is only utilized as the source of attributes. There are two reasons: by comparison, the footprints of the buildings in the map provided by EM have more details, and more importantly, this map contains footprints of unknown roads in the selected area.

There are four software packages are employed in this implementation: Quantum GIS (QGIS), Rhinoceros (with Grasshopper), the FME (Feature Manipulation Engine), and PostgreSQL with PostGIS extension. In the whole process, QGIS is used to add attributes, set the coordinate system, and edit the footprints. Rhinoceros (with Grasshopper) is used to process the entire workflow, and the whole data process is developed in *Python* script. FME is used for extracting point clouds from the DEM, and conducting

terrain re-computation and visualization. For instance, in the terrain rebuilt (Section 6.3), the transformer named *TINGenerator* from FME is utilized to constructs a Delaunay triangulation based on input points and breaklines. PostgreSQL is the data management tool of original BIM models.



(a) Road footprints

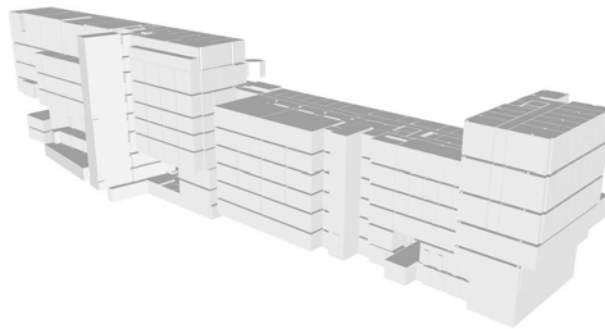


(b) Footprints of green areas

FIGURE 7.2: Footprints of road and green areas in the selected area of UNSW campus.

The data preparation includes three steps: (i) manage all the footprints as separate layers in QGIS; (ii) copy the attributes of footprints from OSM to the map provided from EM by utilizing the function named "Join attributes by location" in QGIS; (iii) manually correct all the footprints to be topologically correct. All the footprints of surface objects

are redrawn as closed polygons and they may share edges, but without any overlaps. The roads are connected, especially the footpaths for pedestrians (without names but connected to other roads), so does the green areas. Thus, the continuous roads/green areas are manually subdivided into small polygons (Figure 7.2), in which the following principle is followed: if the area has a name, it will be subdivided from other connected areas. Otherwise, we only consider subdividing the areas based on their attributes, such as if an area is a green area, this area will be redrawn as a closed polygon.



(a) The I-spaces come from the BIM model.

```

CRC_LCL on postgres@CRC_LCL
1 SELECT ifc_class, ifc_guid, ifc_name, ifc_description, ifc_containing_storey, ST_AsText(geom), color
2 FROM public."Red_Center_H13_IFC_color"
3 WHERE ifc_class = 'Spl_IfcDoor' or ifc_class = 'IfcSpace'

```

	ifc_class	ifc_guid	ifc_name	ifc_description	ifc_containing_st	st_astext	color
	character varying	character varying	character varying	character varying	character varying	text	character varying
1	IfcSpace	3Kq4JtKQj25QT895t...	B03B	Room	Basement	POLYHEDRALSURFACE Z (((16834...	rgb(130, 130, 130)
2	IfcSpace	3Kq4JtKQj25QT895t...	BQ05	Room	Basement	POLYHEDRALSURFACE Z (((16834...	rgb(130, 130, 130)
3	IfcSpace	3Kq4JtKQj25QT895t...	B03	Room	Basement	POLYHEDRALSURFACE Z (((16834...	rgb(130, 130, 130)
4	IfcSpace	3Kq4JtKQj25QT895t...	B05	Room	Basement	POLYHEDRALSURFACE Z (((16834...	rgb(130, 130, 130)
5	IfcSpace	3Kq4JtKQj25QT895t...	B01B	Room	Basement	POLYHEDRALSURFACE Z (((16834...	rgb(130, 130, 130)
6	IfcSpace	3Kq4JtKQj25QT895t...	B01A	Room	Basement	POLYHEDRALSURFACE Z (((16834...	rgb(130, 130, 130)
7	IfcSpace	3eaNOexAb4BxeyC4...	G022	Room	GroundFloorS...	POLYHEDRALSURFACE Z (((16834...	rgb(130, 130, 130)
8	IfcSpace	3Kq4JtKQj25QT895t...	B06	Room	Basement	POLYHEDRALSURFACE Z (((16834...	rgb(130, 130, 130)
9	IfcSpace	3Kq4JtKQj25QT895t...	B07	Room	Basement	POLYHEDRALSURFACE Z (((16834...	rgb(130, 130, 130)
10	IfcSpace	3Kq4JtKQj25QT895t...	B07A	Room	Basement	POLYHEDRALSURFACE Z (((16834...	rgb(130, 130, 130)
11	IfcSpace	3Kq4JtKQj25QT895t...	B08	Room	Basement	POLYHEDRALSURFACE Z (((16834...	rgb(130, 130, 130)

(b) The table of I-spaces in PostgreSQL.

FIGURE 7.3: The I-spaces and BIM model in PostgreSQL.

We employ a BIM model of a building (named as Red Center - H13) as the source of I-spaces (Figure 7.3(a)). In this model, only rooms and doors are utilized. The original model is stored in PostgreSQL, in which each room/door has seven attributes: {ifc\_class,

ifc\_guid, ifc\_name, ifc\_description, ifc\_containing\_storey, geom, color}. The geometry type of spaces is POLYHEDRALSURFACE Z (Figure 7.3(b)).

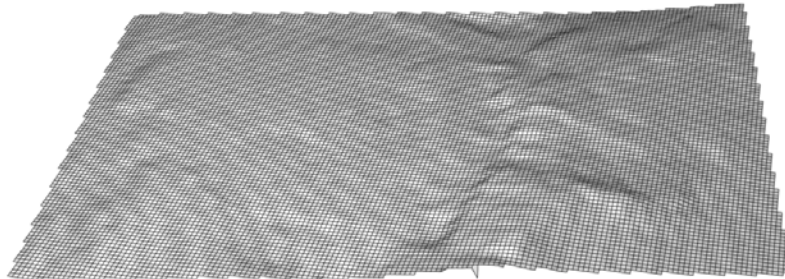


FIGURE 7.4: The terrain of the precinct.

Furthermore, a DEM (5 metre) of the test area is obtained from Elevation Foundation Spatial Data <sup>1</sup> that belongs to National Elevation Data Framework (NEDF), Geosciences Australia. The geometry of the DEM is coerced into point clouds, and then, they are used to construct Delaunay triangulation representing the bare terrain (DTM) (Figure 7.4).

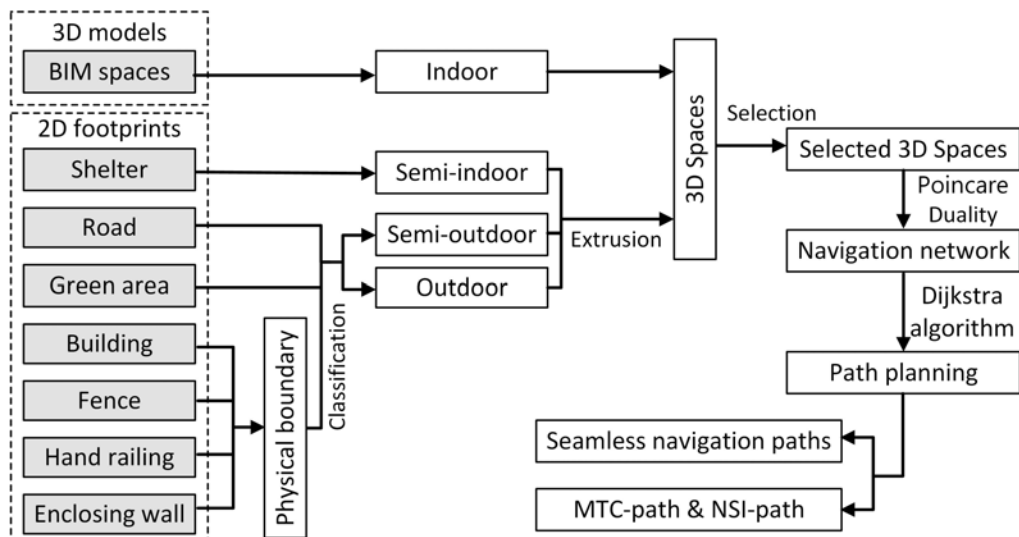


FIGURE 7.5: Flowchart of the implementation.

The flowchart for implementation is shown in Figure 7.5. The whole process consists of five steps:

<sup>1</sup><http://elevation.fsdf.org.au/>

- (i) Classify road and green spaces as semi-indoor and semi-outdoor by using footprints of building, fence, hand railing, and enclosing wall as physical boundaries;
- (ii) Reconstruct sI-spaces, sO-spaces, and O-spaces based on extrusion, in which footprints of shelters are used directly for the reconstruction of sI-spaces;
- (iii) Select spaces based on the size (see Section 7.4);
- (iv) Derive navigation network based on Poincaré duality (Section 2.2);
- (v) Plan navigation paths based on Dijkstra algorithm.

## 7.2 Mapping UML to Python Classes

The conceptual model (Figure 5.1) is partially implemented to demonstrate its use. In addition to the two classes (*IndoorCore::CellSpaceBoundary* and *IndoorCore::CellSpace*) themselves and their attributes, we implement the (association) link between them.

```
class CellSpace:
    def __init__(self, sType, topClosure, sideClosure, bottomClosure,
                containBoundary):
        self.sType = 'OSpace'
        self.topClosure = topClosure
        self.sideClosure = sideClosure
        self.bottomClosure = bottomClosure
        self.containBoundary = containBoundary
```

In the Python scripts, *IndoorCore::CellSpace* in the UML is mapped as another Python class named *CellSpace*. Its attributes *sType*, *topClosure*, *sideClosure*, *bottomClosure* are directly transformed as four attributes with the same names. The value of *sType* is one of four: 'ISpace', 'sISpace', 'sOSpace', and 'OSpace', which corresponding to I-space, sI-space, sO-space, and O-space respectively. The values of the closures are decimals between 0 and 1. The *IndoorCore::CellSpaceBoundary* and its two attributes are converted as a Python class named *CellSpaceBoundary* with two attributes *bType* and *category*. The value of *bType* is either 'Physical' or 'Virtual', and value of *category* is 'Top', 'Side', or 'Bottom'.

The (association) link is reflected by adding one more attribute named *containBoundary* to *CellSpace* and one attribute named *fromSpace* to the *CellSpaceBoundary*. The *containBoundary* contains the IDs of all *CellSpaceBoundary* that make up this *CellSpace*, while *fromSpace* records the ID of *CellSpace* where this *CellSpaceBoundary* comes from.

```
class CellSpaceBoundary:
def __init__(self, bType, category, fromSpace):
self.category = category
self.bType = bType
self.fromSpace = fromSpace
```

The following two tables shows the data structures of *CellSpace* and *CellSpaceBoundary* (Table 7.1 and Table 7.2) in the computer memory. The names of the columns are the same as the attribute names of the two classes. Each *CellSpace* is represented as a quintuple: *CellSpace* = {sType, topClosure, sideClosure, bottomClosure, boundary}, while each *CellSpaceBoundary* as a triples: *CellSpaceBoundary* = {category, bType, space}. In the Table 7.1, "bi" (e.g., "b0", "b3") are the IDs of *CellSpaceBoundary*, while "si" (e.g., "s1", "s2") in Table 7.2 are the IDs of *CellSpace*. Such IDs are not shown in the UML even the Python classes, but we consider each object will have an ID.

TABLE 7.1: Example of *CellSpace* table in the computer memory.

sType	topClosure	sideClosure	bottomClosure	containBoundary
ISpace	1	0.99	1	[b0, b4, ...]
sISpace	...	...	...	...
sOSpace	...	...	...	...
OSpace	...	...	...	...
...	...	...	...	...

It should be noted that the above python classes and tables are designed for internal data management in this research. The UML model can be implemented as a spatial schema in a database management system (DBMS) covering all classes, data types and code lists. Using a DBMS will ensure management of large urban areas and entire cities.

TABLE 7.2: Example of *CellSpaceBoundary* table in the computer memory.

category	bType	fromSpace
Top	Physical	s1
Top	Virtual	s2
Top	Physical	s2
Side	Virtual	s1
Side	Virtual	s4
...	...	...

### 7.3 Space Classification and Reconstruction

We consider the roads and green areas as the two sources of sO-spaces and O-spaces. This section classifies them into semi-outdoor and outdoor based on their *sideClosure* ( $C^S$ ), see Section 6.2.2. The footprints of buildings, hand railings, enclosing walls and fences are employed as physical boundaries (Figure 7.6).

The classified road and green spaces are shown in Figure 7.7. The results show that most roads and green areas are outdoor spaces, while yards and courtyards are sO-spaces. The classification of the footprints will be used as the semantic of the spaces reconstructed based on them, for instance, a semi-outdoor road footprint will be reconstructed into a sO-space in the following step.

Only the sI-spaces formed by the building with BIM model are reconstructed based on the approaches presented in Section 6.1. Other sI-spaces formed by shelters are reconstructed with an alternative way. The reconstructing process is extruding their projected footprints to 2 meters, which is similar to the reconstruction of building shells (Section 6.3). The reason why this alternative way is utilized is that the data source for most sI-spaces generation in this implementation is footprints on a 2D map, in which proper components of 3D built structure (such as *OuterCeilingSurface*, *OuterFloorSurface*) do not exist.

The sO-spaces and O-spaces are reconstructed on the basis of the procedures presented in Section 6.2. It should be noted that, in this implementation, the height of sO-spaces and O-spaces is set as 2 meters. However, height is variable. The reason why 2

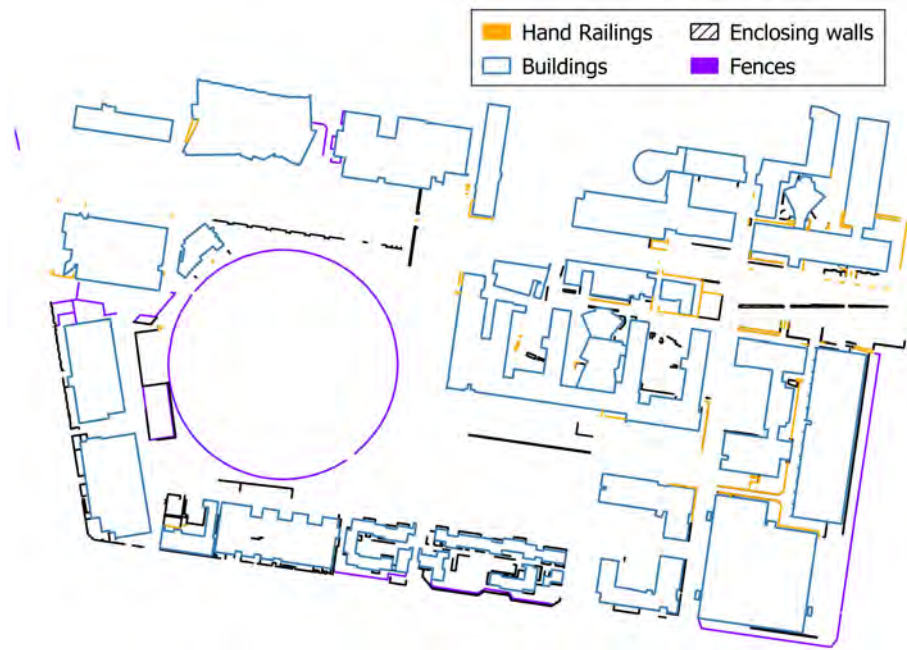


FIGURE 7.6: Physical boundaries used for space classification.

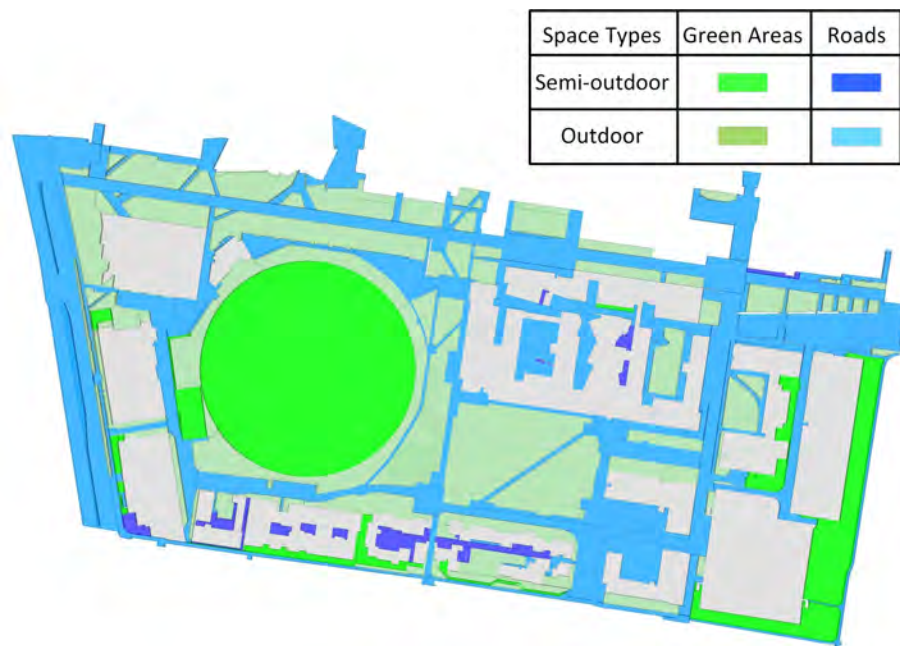


FIGURE 7.7: Classified road and green area footprints. The darker white polygons are building footprints.

meters is used is that we consider this height sufficient for pedestrian navigation. Furthermore, the purpose of setting height is enclosing spaces as 3D volumes. The tops of the spaces do not offer vertical constraints, for instance, if the height of a person is 2.5

meters, the spaces are still qualified for navigation.

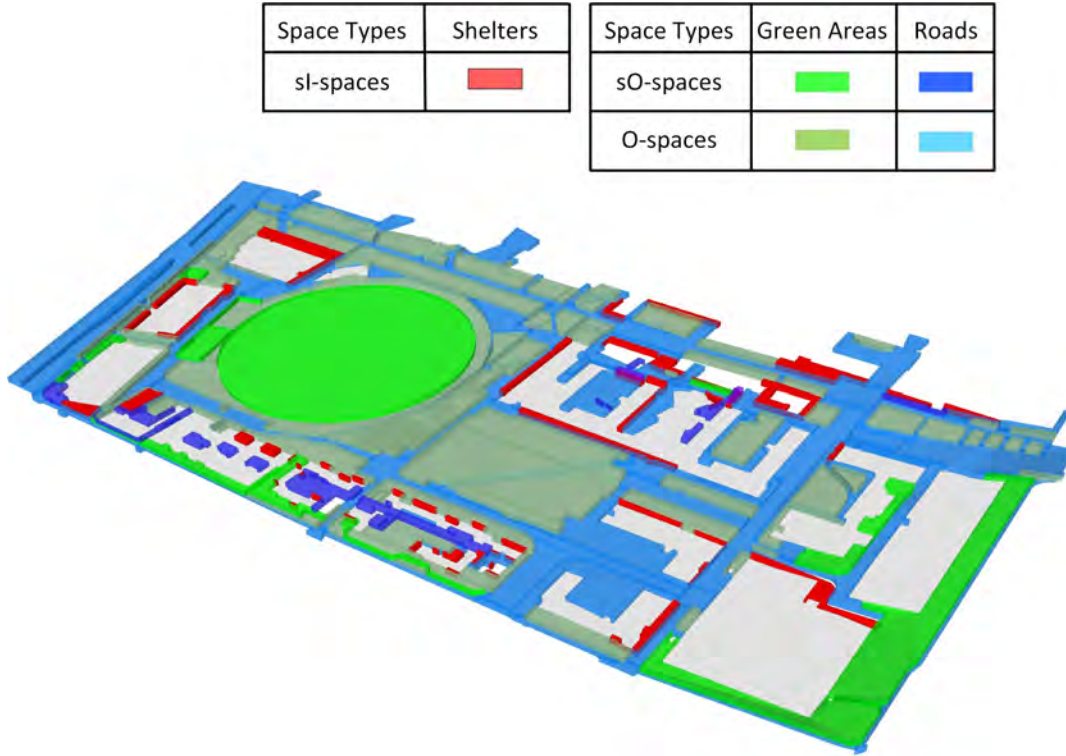


FIGURE 7.8: Reconstructed sl-spaces, sO-spaces, and O-spaces. The darker white polygons are building footprints.

The reconstructed spaces (Figure 7.8) show that all environments where pedestrian navigation can happen are filled by spaces, except the physical boundaries. The data structures and classes used in this step are exactly the same as those presented in Section 7.2, but the *bottomClosure* of all spaces are assigned as 1.

## 7.4 Space Selection and Navigation Network Derivation

As mentioned in Section 3.1.1, agents in this research are pedestrians who are 3D objects that have certain requirements for spaces. Thus, considering if spaces are large enough to accommodate pedestrians, the reconstructed spaces are selected based on their size. The minimum space needed by a pedestrian is estimated by Equation 3.3, i.e.,  $\{l', w', h'\} = \{750, 550, 1949.3\}$ . Then, the space selection criteria for pedestrian navigation are:  $r_s \geq 465.0mm$  and  $h_s \geq 1949.3mm$ . Only the qualified spaces are selected to

participate in the navigation network derivation and navigation path planning. Nevertheless, it should be noted that the two criteria ( $r_s$  and  $h_s$ ) only focus on the size of the space, which are the most basic criteria for space selection. Other than that, the space selection can consider the specific navigation purposes by adding other criteria, for example, utilizing *topClosure* ( $C^T$ ) as a criterion to select the spaces for the pedestrians who prefer to MTC-path or NSI-path during their navigation.

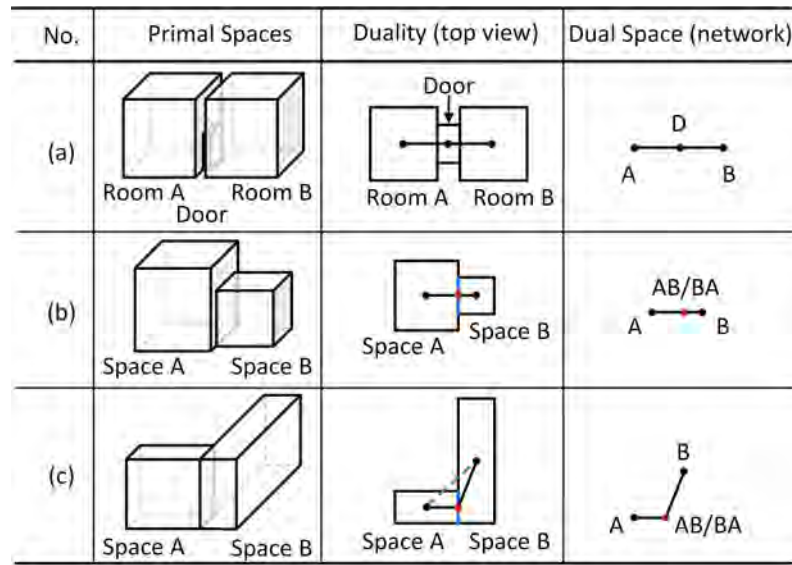


FIGURE 7.9: The duality used in this implementation. The red dots are extra vertices extracted from shared virtual boundaries.

Indoor spaces are generally connected by doors (Figure 7.9(a)). Thus, theoretically, a navigation network can be derived from 3D spaces on the basis of Poincaré duality (Section 2.2). However, sI-spaces, sO-spaces, and O-spaces are naturally connected by virtual boundaries rather than doors (Figure 7.9(b)). Therefore, we use additional vertex on the face where two spaces meet to indicate how to traverse the spaces. Even if the path does not intersect the spaces, the vertices are still needed, see the abstracted example (the green line in Figure 7.9(c)). Thus, curve edges and extra vertices are employed to force the navigation links to pass through the sharing of virtual boundaries. It should be mentioned that the computation of the additional vertices includes two steps: (i) evaluate if two spaces are sharing a virtual boundary surface based on 3D space intersection and

(ii) extract the centroid of the intersection surface as the additional vertex. If there is more than one virtual boundary shared by two spaces, the vertex that ensures the shortest distance between the two spaces will be selected.

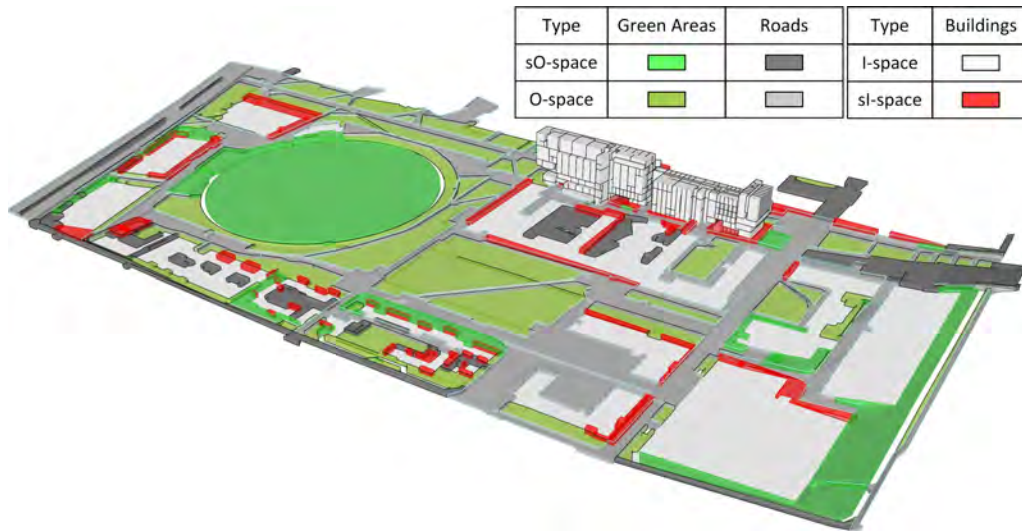


FIGURE 7.10: All the spaces in the selected area on the UNSW campus. The darker white polygons are building footprints.

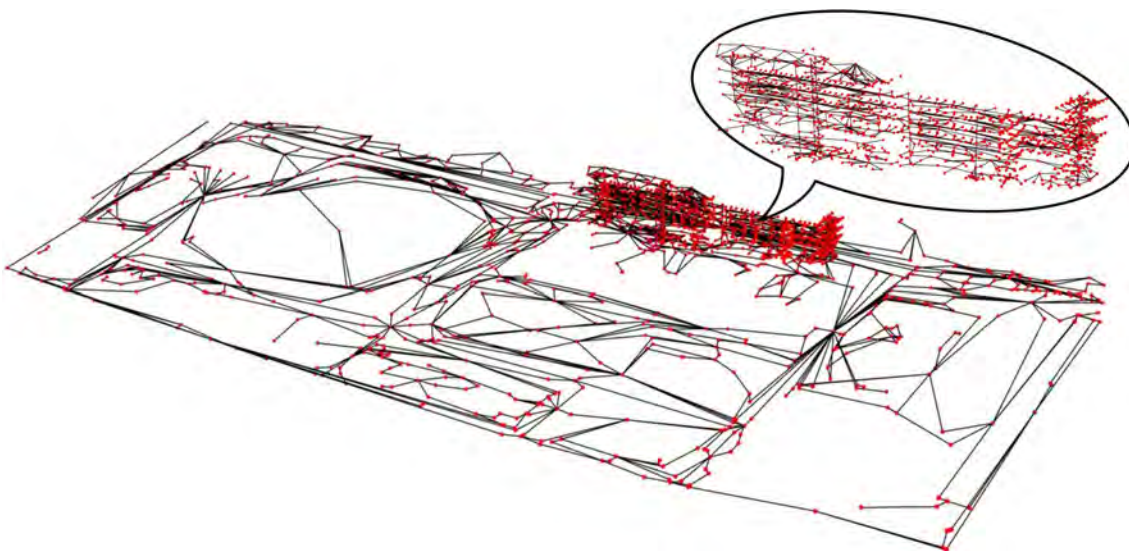


FIGURE 7.11: Derived unified navigation network in the test area. Black lines are edges and red dots are nodes.

Furthermore, we integrated the I-spaces from geo-referenced BIM models based

on the approach presented in (Diakit  and Zlatanova, 2020) with all the reconstructed spaces. The integrated 3D spaces are shown in Figure 7.10. The data structure of the I-spaces is slightly different from other spaces, because we do not split the POLYHEDRALSURFACE of each I-space into top(s), side(s), and bottom(s). That is to say, the geometry of each space remains a solid. But, the *topClosure*, *sideClosure*, and *bottomClosure* of all I-spaces are assigned the value as 1. The name of each space corresponds to the "Ifc\_name" column of the BIM model stored in an SQL database.

Utilizing all the selected I-spaces, sI-spaces, sO-space, and O-spaces, we derived the unified navigation network on the basis of Poincar  duality (Figure 7.11).

## 7.5 Path Planning

This section presents path planning, which includes two examples with five navigation paths. For comparison, OSM and Google Maps are also used for path planning.

### 7.5.1 Examples of Seamless Navigation

Three navigation paths are performed to demonstrate the seamless navigation cases (Figure 7.12, 7.13 and 7.14). In the planned paths, black points are navigation nodes while the red are extra vertices. Blue curves indicate the navigation paths. Information about 3D spaces in the Figure is linked to the table by number.

The first case is a path planning from an O-space (Road16) to a sO-space (Village green), see Figure 7.12, which is used to demonstrate the sO-spaces and the spaces without clear paths can be included in navigation path planning. The paths planned by OSM and Google Maps try to guide pedestrians to walk around the spaces without clear paths (such as green areas), which we call as detour issues since obviously pedestrians can walk through green areas directly to the destination. The path in our approach shows the detour issues are avoided by involving sO-spaces and O-spaces (greenArea25 and greenArea29) in the navigation map. We noticed that the detour issues are avoided, but some new detour issues occur. For instance, it has undesirable zigzags between

greenArea25 (node 4) to destination (node 7). Another issue is that partial segments of the navigation path are exposed to the outside of spaces. The reason why the two issues occur is the road space (road34 - node 5) and green area space (greenArea25 - node 6) are not convex polygons. The undesirable zigzags result from non-convex spaces. The undesirable zigzags are caused by non-convex spaces. One way to ensure that all spaces are convex polygons is space division (Zlatanova et al., 2014). But, this topic is not included in this research, but it has been listed in the future work, see Section 8.3.2 Apply Space Subdivision.

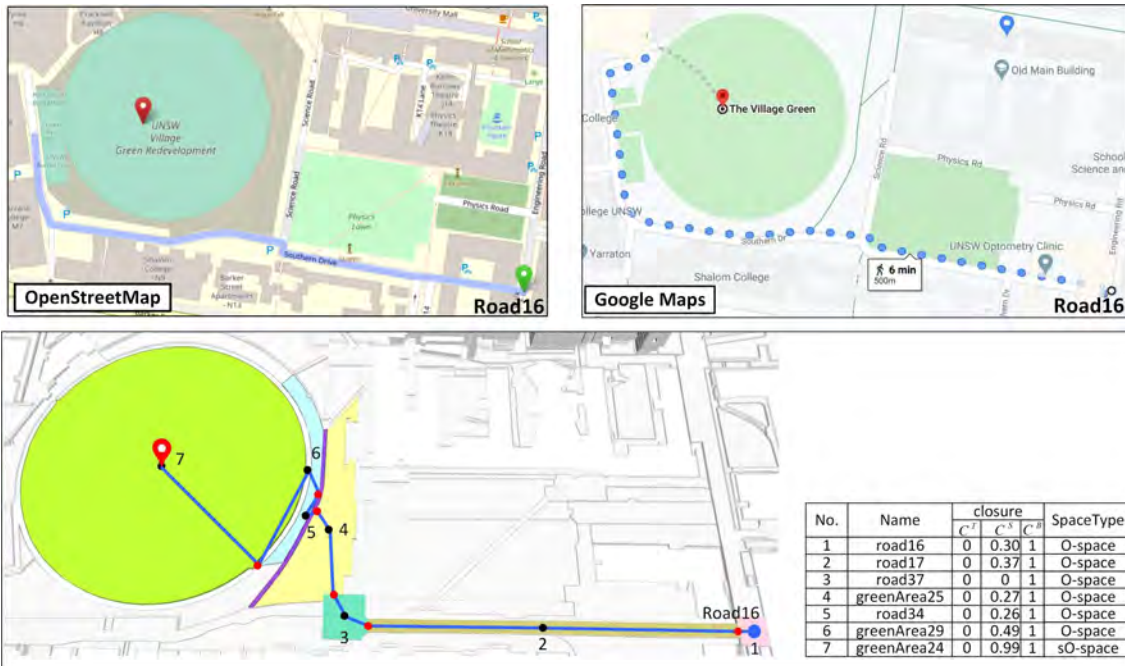


FIGURE 7.12: From O-space to sO-space (Road16  $\rightsquigarrow$  Village green).

The second path planning is taking an O-space (Road19) as the departure while an I-spaces (sI-space47) as destination (Figure 7.13), which is designed to show that the sI-space can be departure/destination/transition in a navigation path. In the OSM and Google Maps, we cannot choose a sI-space as the destination since no clues show that somewhere is a sI-space. Our approach can indicate sI-spaces and includes them as departure, destination, or transition in the navigation map. Furthermore, the path shows the possibility to consider the vertical constraint (height bottleneck) in navigation. For

instance, the sI-space (sI60), which formed by a building bridge. The accurate height of this bridge has a decisive effect on the navigation, specifically, if the height of a user is larger than this height, this path will be unavailable.

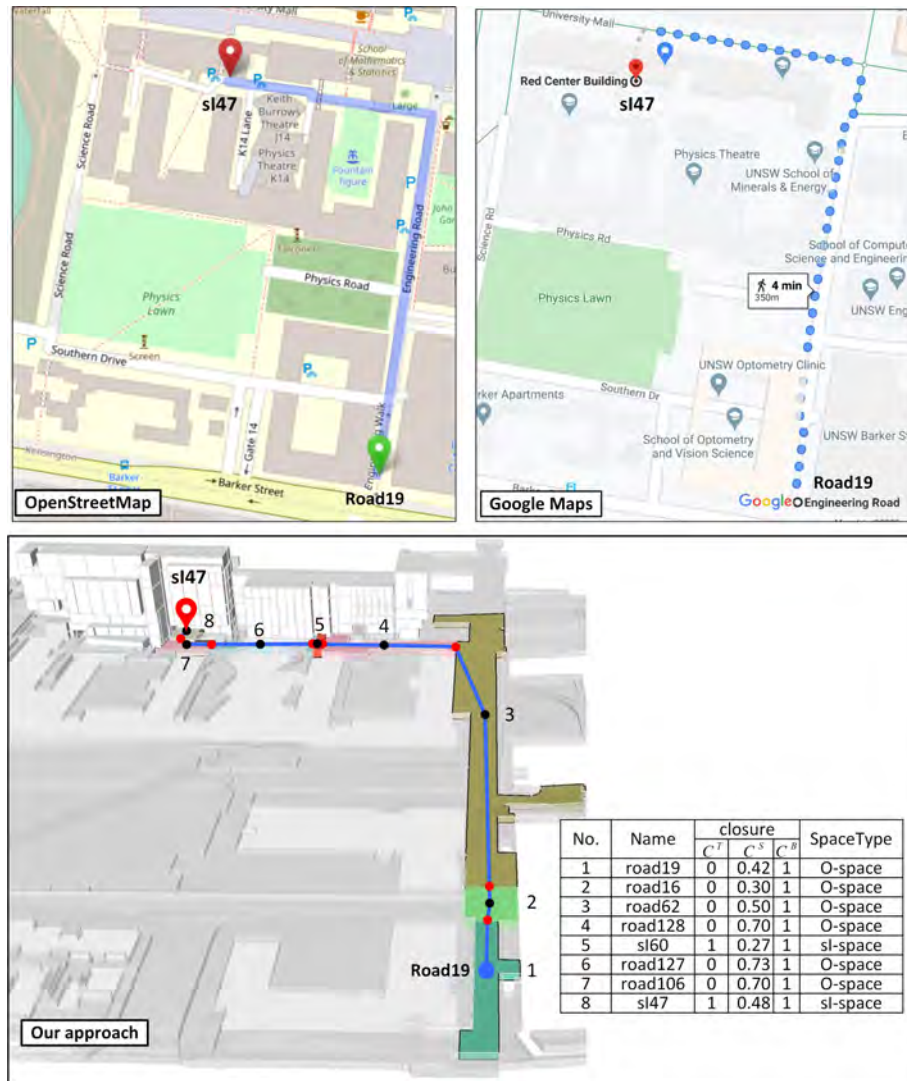


FIGURE 7.13: From O-space to sI-space (Road19  $\rightsquigarrow$  sI-space47).

The third case is a path from a sO-space (Road80) to an I-space (Room 4036), see Figure 7.14, which is designed to demonstrate the seamless navigation. Considering we have only one BIM building that has I-spaces, if both departure and destination are located within this building, the navigation becomes indoor navigation. Thus, to demonstrate the seamless navigation, we chose a place out of the building as the departure while a

place as the destination inside of the building. In OSM and Google Maps, the navigation is limited in outdoor and there are no details of I-spaces. Thus, an I-space (room) cannot be chosen as the destination, and pedestrians are failed to get navigation paths in indoor parts. Our approach overcomes such kinds of shortcomings. On one hand, indoor spaces are able to be set as departures, destinations or transitions, and on the other hand, the navigation path includes the indoor parts. The path shows that seamless navigation is possible and there is no difference between indoor and outdoor from a navigation point of view.

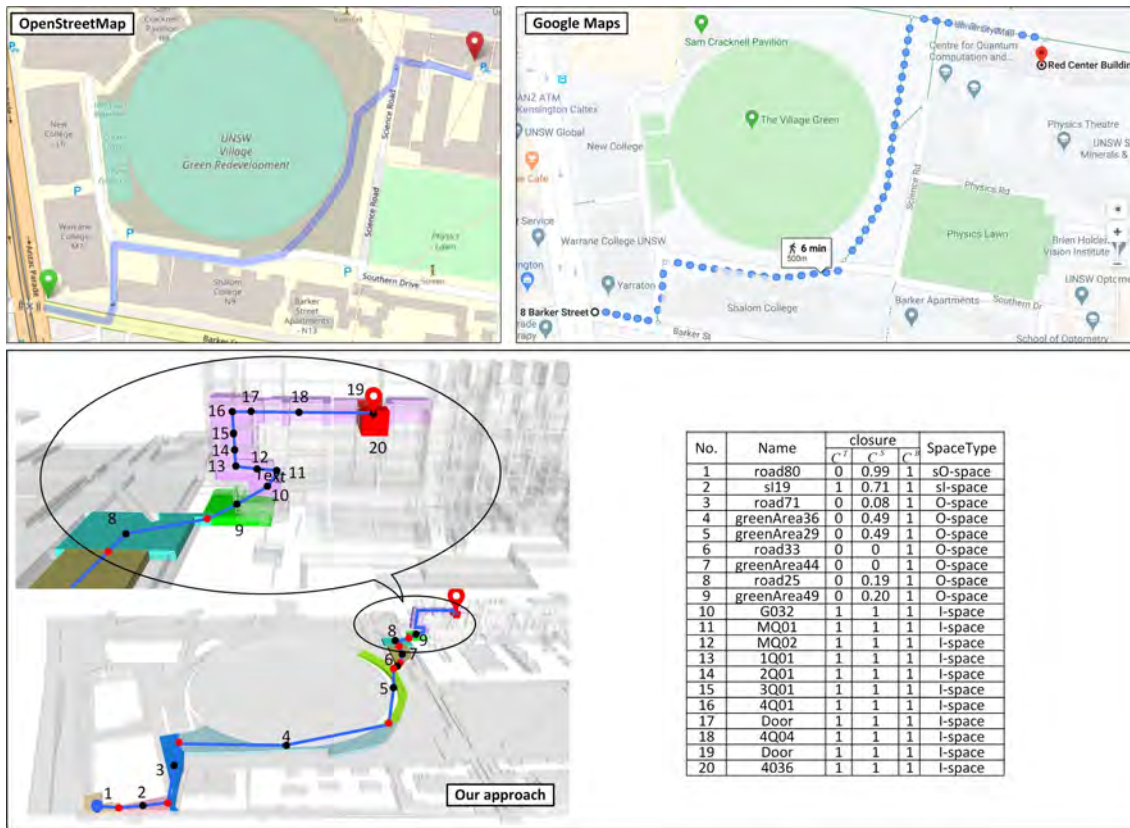


FIGURE 7.14: From sO-space to I-space (Road80 ~> Room 4036).

### 7.5.2 Example of MTC-path & NSI-path

As mentioned in Chapter 5, the MTC-path (Section 5.2.2) and NSI-path (Section 5.2.3) are two new path options developed based on sl-space. Both their first step is the sl-space

selection. Then, a new navigation network can be derived based on selected spaces. In this paths planning test, the navigation network derived in the last section is used as we assume that all the sI-spaces have a qualified *topClosure* ( $C^T \geq 0.8$ ). The reason why we have such an assumption is that most sI-spaces are reconstructed from footprints of shelters, which makes us cannot estimate exact values of *topClosure* for them. The MTC-path and NSI-path are implemented with two navigation cases:  $A \rightsquigarrow B$  (Figure 7.15),  $C \rightsquigarrow D$  (Figure 7.16).

The first navigation case takes A as departure and B as the destination. The shortest path and MTC-path can be seen in Figure 7.15. All different approaches can offer the shortest path, but only our approach can offer the MTC-path and NSI-path. The navigation path computed by Google Maps obviously shows this system tries to guide pedestrians to go along the roads. Furthermore, the third dimension (vertical constraint) of outdoor spaces in OSM and Google Maps is neglected, but which can be considered in our approach, because the navigation network of our approach is derived from 3D spaces.

Our approach not only can offer the shortest path and MTC-path but also more detailed information of the path, such as covered/uncovered distance as well as the top-coverage-ratio. As shown in the figure at the bottom right, the navigation path includes as many sI-spaces as possible can increase the top-coverage-ratio of the path, see the black circled part in the MTC-path of Figure 7.15.

The second navigation case is from C (departure) to D (destination) (Figure 7.16). The path planning results of this case vary greatly. Path offered by OSM shows the pedestrians can go through a building. Navigation in Google Maps still tried to guide pedestrians to follow the roads. We expect our approach to have a similar shortest path to the result from OSM, but with the reason that this building does not have BIM model and therefore is excluded, the shortest path of our approach slightly changes. In the MTC-path, it clearly shows that the path tries to include as many sI-spaces as possible to increase the covered distance and top-coverage-ratio of the path.

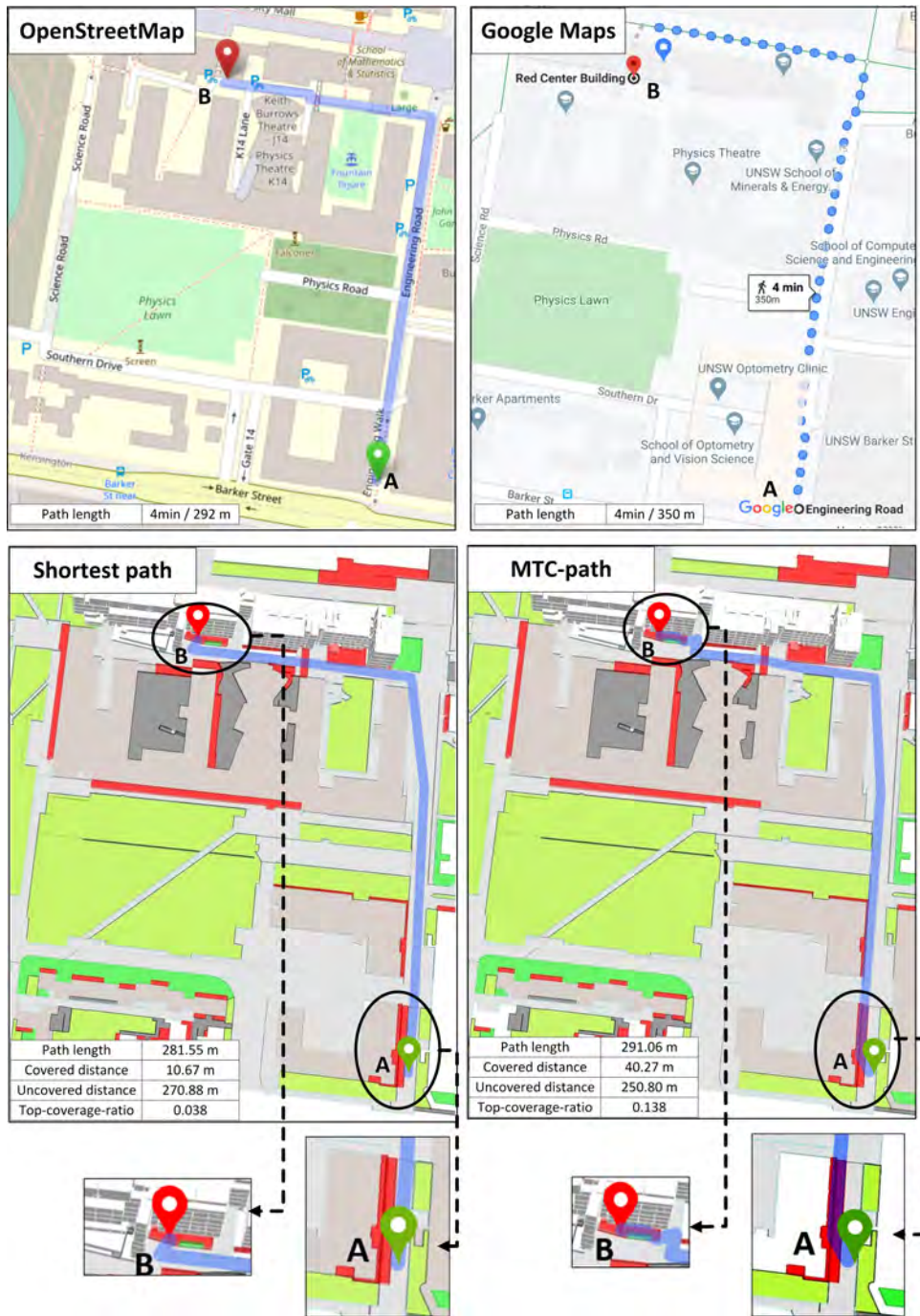


FIGURE 7.15: Navigation paths of A  $\rightsquigarrow$  B. Differences between shortest path and MTC-path are marked by black ellipses, which shows where the sl-spaces are involved.

Based on the path selection strategy, both MTC-path in the two cases is recommended, since their uncovered distances are shorter than that of the corresponding shortest path (250.80 vs 270.88, and 270.48 vs 347.91) and the coverage ratio of the two MTC-paths is larger than that of the shortest paths (0.138 vs 0.038, and 0.226 vs 0). As mentioned above, the NSI-path is a compromise option when neither the shortest path nor

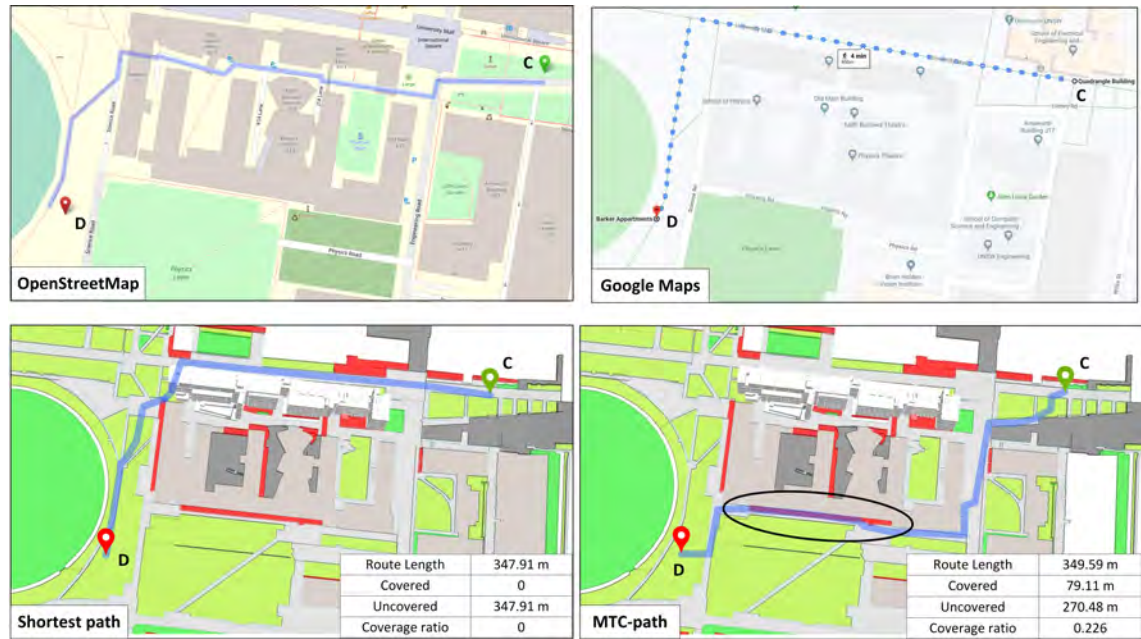


FIGURE 7.16: Navigation paths of  $C \rightsquigarrow D$ . The part marked by black ellipse shows where the sI-spaces are involved in MTC-path.

MTC-path is recommended. Considering both MTC-path of two cases are recommended, this implementation does not further to compute the NSI-path. But, the NSI-path surely can be computed with our approach.

## 7.6 Comparison of Results

We compare the path planning results of OSM, Google Maps, and our approach from six aspects (Table 7.3): (i) if the sI-/sO-spaces are considered in the navigation map, (ii) it performs navigation in 2D or 3D, (iii) if it can compute the shortest path, (iv) if it can offer the seamless indoor/outdoor navigation path, (v) if it is able to offer the MTC-path, and (vi) if it can provide a NSI-path.

TABLE 7.3: Comparisons of three navigation systems.  $\times$  means no while  $\checkmark$  means yes.

Approach	sI-/sO-space	2D/3D	Shortest path	Seamless path	MTC-path	NSI-path
OSM	$\times$	2D	$\checkmark$	$\times$	$\times$	$\times$
Google Maps	$\times$	2D	$\checkmark$	$\times$	$\times$	$\times$
Our approach	$\checkmark$	3D	$\checkmark$	$\checkmark$	$\checkmark$	$\checkmark$

The results show that current navigation applications do not consider sI-spaces and sO-spaces in navigation map, perform navigation in 2D, and offer the shortest path as the only path option. However, thanks to the developed generic space definition framework, the unified 3D space-based navigation model, and reconstruction approach for 3D spaces, we can classify, define, manage, structure, and reconstruct all types of spaces (especially sI-/sO-spaces) as 3D spaces and include them in the navigation map for seamless path planning. The navigation path shows that our approach performs navigation in 3D. More importantly, it not only can offer the shortest path but also the seamless navigation path, MTC-path, and NSI-path.

## 7.7 Summary

This chapter illustrates how to utilize all developed theories, models and approaches to perform indoor-outdoor seamless navigation path planning, including reconstruction of 3D spaces, implementation of the unified 3D space-based navigation model, derivation of navigation networks and path planning. There are several aspects should be further elaborated:

The height of sI-space should be strictly defined by the height of physical structures (e.g., roof, shelter, bridge). In this implementation, a contact height (2 meters) was employed, because (i) the input data for sI-space reconstruction are 2D footprints, thus information of physical tops of sI-spaces are not available and (ii) 2 meters are sufficient for the pedestrian navigation. For the similar reason, this contact height is also used in reconstruction of sO-spaces and O-spaces. But, it should be noted that the purpose of setting height is only enclosing sO-spaces and O-spaces as 3D volumes. In other words, this height of sO-spaces and O-spaces will not be used as the basis to determine whether such a space can meet the requirements of vertical constraints in navigation.

This unified model is based on 3D spaces, but it gives the impression that except for the I-spaces, the sI-spaces, sO-spaces, and O-spaces in the implementation are 2.5D. The reasons why we still regard the model as 3D are: (i) I-spaces employed in the model are

3D; (ii) sI-spaces should be 3D spaces generated from 3D models (e.g., CityGML LoD3). Due to lack of appropriate 3D models, sI-spaces are created by extruding 2D footprints up to a certain height; and (iii) all kinds of 3D space constructions take terrain into consideration to keep the topological consistency, which makes the navigation nodes are not on the same plane.

Space identification and subdivision is a pre-step of the navigation network derivation. A refined space subdivision would yield a smoother path. If the spaces are not subdivided properly, the navigation path will be undesirable. However, in the data preparation, only a rough space subdivision is conducted manually, which brings in some issues. For instance, because the spaces are not convex, partial zigzag, or navigation paths are exposed to the outside of spaces (Figure 7.12).

Another aspect is that the navigation network looks still very rough (one space is abstracted as a node) and gives the wrong impression that the developed model only can be based on 3D spaces for navigation network construction. The navigation network in this experiment shows that it has the same structures with existing networks (i.e., NRG). Thence, although the unified model is based on 3D spaces, it remains valid if the environments are represented as 2D spaces. The information on the third dimension will be lost, but the navigation network will still be derived under unified rules and will, therefore, can combine with existing navigation networks and further provide seamless navigation.



# CHAPTER 8

---

## CONCLUSION AND FUTURE WORK

---

This final chapter summarizes the key findings of this PhD research and presents future work to continue the topics. After providing our answers to the research questions posed in this PhD study, we list ten topics that can be investigated in future research.

### **8.1 Conclusion**

Contemporary public buildings are becoming conglomerates of open, semi-open and closed spaces, with indoor and outdoor sections, posing a set of challenges for humans to navigate seamlessly through such environments. Navigation systems generally rely on a network (nodes and edges) as an abstraction of underlying space connectivity. However, (i) indoor and outdoor networks are currently built differently. While indoor systems rely on indoor space subdivision approaches, current outdoor systems utilize

road-based network approaches. (ii) Linking such networks via particular nodes is a possible but restrictive way to make a unified navigation model. (iii) Semi-bounded spaces in the built environment are not strictly indoor or outdoor spaces and are thus often omitted from navigation networks, further limiting navigation options. (iv) Current navigation networks are derived based on 2D-connectivity and the path planning assumes agents are points. Thus, vertical constraints during the navigation are not considered.

To overcome these challenges, based existing knowledge, this thesis developed new theories, models, and approaches to support seamless navigation path planning in all kinds of environments, which include a novel generic space definition framework, a unified 3D space-based navigation model, approaches for automatically reconstructing 3D spaces, and two new path options (MTC-path and NSI-path). The introduced novel generic space definition framework can categorise and define the entire space formed by built structures as indoor outdoor, semi-indoor, and semi-outdoor spaces. The developed 3D space-based model illustrates that a same navigation network derivation and management approach for all types of spaces are possible. This elaborated procedures and algorithms demonstrate that all introduced spaces are able to be automatically derived as 3D volumes. The MTC-path and NSI-path prove that using the introduced spaces to define new navigation path options is feasible.

In short, this thesis has contributed to the development of solutions for seamless navigation path planning in the entire space formed by built structures. The contributions of this research on the seamless navigation path planning can be summarized as the following four aspects: (i) semi-bounded spaces are systematically and parametrically categorised as semi-indoor and semi-outdoor, thereby allowing to include them in navigation maps; (ii) all types of environments are uniformly modelled and managed as 3D spaces, which allows they can share the same derivation approaches for navigation networks, thereby overcoming the difficulties of exchange and maintain the integrated navigation network; (iii) path planning base on 3D spaces makes vertical constraints during navigation are considered; and (iv) new navigation path options are developed based on the semantics of introduced spaces.

With the developed theories, models, and approaches, the spaces are enriched with attributes and linked to supplementary data to derive user dedicated information. Such extended information can be used in many applications for navigation: shopping, facility management, guidance at airports and hospitals, etc. We also believe this research is important for location-based services (LBS) applications, urban data management, and urban analytics. Furthermore, through the spaces, environmental conditions (high temperatures, rain, pollution) can be taken into consideration and studies could be completed on mobility and human activities. As mentioned previously, people can use sI-spaces in case of rain or high temperatures. Such studies can motivate urban planners and designers to consider more transitional spaces.

### 8.1.1 Answers to the Research Questions

The main research question that I seek to answer in this thesis is:

*What a (3D) spatial model can include all types of living environments for supporting seamless navigation path planning?*

This research has elaborated on the issues related to the spatial model in depth. It has shown that spatial models require an extended definition of environmental spaces, their attributes, and relationships. This thesis concluded that a unified 3D space-based model can be defined as an extension of presently well-known space-based model for indoor, i.e., IndoorGML. Such a solution has the following advantage that all types of living environments are modelled as 3D spaces and included in the navigation map to support seamless navigation path planning.

### 8.1.2 Environments

**Q1: Which environments (spaces) should be considered in seamless navigation activities?**

This research found that the semi-enclosed spaces that are generally located between indoor (I-space) and outdoor (O-space) but cannot be strictly defined as indoor or outdoor should be considered in seamless navigation (Section 2.4.2). The specific way of

including such kind of spaces in the navigation map is classifying and defining them into two new types of spaces, semi-indoor (sI-space) and semi-outdoor (sO-space). This thesis provided formal definitions of the four spaces: I-space, O-space, sI-space and sO-space. We have demonstrated that with the four strictly defined spaces, all types of living environments can be covered for supporting seamless navigation path planning. The spaces ensure the automatic derivation of robust seamless networks for navigation path planning. Furthermore, including the sI-spaces and sO-spaces into the navigation opens new directions for further tailoring of the navigation path with respect to environmental factors, such as the MTC-path (Section 5.2.2).

**Q2: Is it possible to classify and define all the complex environments as 3D spaces for seamless navigation?**

This thesis investigated the definition of spaces in the literature and adopted the term "space", which is utilized to represent the 3D hollow parts in the environment that are bounded by physical or imaginary (non-existing) elements (Section 2.4). That is, for the purpose of navigation, our living environments can be defined in a formal way - 3D spaces, although they are contemporarily getting more and more complex, combining structures indoor and outdoor. Chapter 4 has presented a generic space definition framework, which uniquely classifies and formally defines any space into one of the four categories: I-space, O-space, sI-space, and sO-space. Using this framework, all types of spaces are able to be included in the navigation map with the same management structures, thereby any spatial model can rely on it to use the same network extraction approaches across the built environments for providing a seamless navigation solution.

### 8.1.3 Spaces Representation

**Q3: Can we introduce unified names and terminology to define all kinds of spaces?**

We introduced three terms, *Top*, *Side*, and *Bottom*, to extend the basic building elements, roof, wall, floor respectively for an indoor space to other structures in non-indoor spaces, such as the shelter, fence, and ground. That is, the three terms generalized the elements/structures in all types of spaces with generic notions, for instance, both roof

and shelter can act as upper boundary of a space, but they are different. The former is mostly for I-space, while the latter for sI-space. Similarly, both wall and fence can be the surrounding boundary, and floor and ground can be the lower boundary (Section 3.2.1). The three terms allow all complex boundary configurations to be considered, although the materials, shapes, and dimensions of the structures that form the spaces are diverse. With the three terms, all spaces have unified definitions (Section 4.1.1) and they are modelled as 3D volumes composed of *Top*, *Side*, and *Bottom*. This approach provides the basis for defining and developing a unified 3D space-based navigation model, i.e., network (Chapter 5).

**Q4: What kind of terminology should be introduced to quantitatively define all kinds of spaces?**

In addition to the three terms (*Top*, *Side*, and *Bottom*), we introduced six more terms to quantitatively define all kinds of spaces (Section 3.2), including *topClosure* ( $C^T$ ), *bottomClosure* ( $C^B$ ) and *sideClosure* ( $C^S$ ), *Gradient* ( $G$ ), *Physical boundary*, *Virtual boundary*. Furthermore, three threshold values ( $\alpha$ ,  $\beta$  and  $\eta$ ) are introduced for  $C^T$  and two ( $\gamma$  and  $\delta$ ) for  $C^S$  to control their definitions (Section 4.1.2). As shown in implementation (Chapter 7), these terms are able to help with classifying and identifying spaces for navigation uniquely and group them parametrically. In addition, spaces can be selected based on their closure for developing new path options. For example, the sI-spaces are selected based on their  $C^T$  for the path planning of MTC-path (Section 5.2.2) and NSI-path (Section 5.2.3).

#### 8.1.4 Unified Navigation Model and Path Options

**Q5: Is it possible to develop a 3D unified spatial model for seamless navigation?**

The core of this thesis is a spatial model that can integrate all the defined parameters in a structured way to be able to be queried and modified with respect to changed environment and user needs. We developed a spatial model that can integrate the 3D spaces and their characteristics by extending the the concept of *CellSpace* and *CellSpace-Boundary* in IndoorGML (Chapter 5). The proposed modifications are relatively small

and can be easily adopted by the standard, because all the classes remain the same as that in IndoorGML, and only several attributes are added. In particular, the modification for *CellSpace* is adding four attributes (*sType*, *topClosure*, *sideClosure*, and *bottomClosure*) (Section 5.1.1), while that of *CellSpaceBoundary* is two new attributes: *category* and *bType* (Section 5.1.2).

With this unified 3D space-based model, we are able to (i) maintain all types of environments (indoor, outdoor, semi-indoor, and semi-outdoor) as 3D spaces, (ii) manage all types of spaces in a uniform way, such as management methods and network construction approach, and (iii) develop new seamless navigation path options based on the semantics of spaces.

**Q6: Is it possible to develop new path options by considering the semantics of spaces?**

Having defined all spaces formally, this thesis demonstrated that new path options, which differ from the commonly shortest/fastest can be defined. We put forward two roofed/sheltered navigation path options (MTC-path (Section 5.2.2) and NSI-path (Section 5.2.3)) based on the sI-spaces in the navigation map. This enriches the traditional navigation options (the shortest distance/time paths) and opens new directions for path options, which can bring in a new navigation experience for humans. With similar ideas, we can investigate new paths with I-spaces, even sO-spaces or O-spaces for other navigation preferences.

In simple terms, the new path options bring in three contributions to indoor-outdoor seamless navigation path planning: (i) people can have point-to-point navigation path with less undesirable detour issues; (ii) MTC-path and NSI-path are computed and suggested for users who need the shortest path with as many covers from the top as possible and (iii) the navigation performs in 3D, which aligns to the real situation that navigation is a process of pedestrians moving from one 3D space to another.

## 8.2 Discussion

Aiming at considering all types of spaces into navigation map to support seamless navigation path planning, our research developed theories, models and approaches. Although the results show that seamless navigation path planning can successfully be achieved, there are still some limitations that may affect the use of them in real navigation systems and need to be considered in further developments.

First of all, this research presented a generic definition framework, which is strictly based on parameters and thresholds. We attempted to assign values to them, such as the five thresholds ( $\alpha = 0.05$ ,  $\beta = 0.95$ ,  $\gamma = 0.75$ ,  $\delta = 0.95$ , and  $\eta = 0.6$ ) for the  $C^T$  and  $C^S$  in the generic definition framework. The threshold ( $C^T \geq 0.8$ ) was utilized to select sI-spaces for the MTC-path and NSI-path. Theoretically, these parameters, thresholds and their suggested values are enough for the seamless navigation path planning, because they can fully control classifications, definitions, and usages of the spaces. However, they are not verified by pedestrians in real scenarios. Thence, we cannot convincingly conclude that the values of them are well accepted by users. Therefore, to further verify this research, a set of tests should be conducted by deploying them in a navigation system or application. And then, improve them based on the feedbacks collected from pedestrians.

Secondly, a unified 3D space-based navigation model is developed for supporting space management. This model extends the two classes (*CellSpace* and *CellSpaceBoundary*) in IndoorGML, which ensures all types of spaces for navigation (indoor, semi-indoor, semi-outdoor, and outdoor) have the same representation, management methods, and network construction approach. But it is necessary to mention that there are still three limitations: (i) obstacles shall be represented and included in the model as non-navigable spaces. In particular, they shall be semantically categorised as static (e.g., pillar, tree), semi-mobile (e.g., small table, car), and mobile (e.g., fire) (Diakit  and Zlatanova, 2018). But, the model only focuses on the navigable spaces, thus the obstacles are overlooked; (ii) we presume all the spaces are available for navigation. However, although some spaces are there, they might be not accessible. For instance, pedestrians are forbidden

to visit some spaces, because they are private, occupied, not allowed, or closed. The accessibility may be a critical one in indoor and outdoor mixed contexts, but the model has currently no attribute that deals with this information; (iii) the model is based on 3D spaces, but the 3D spaces might not be always available or needed to be created. Although if the spaces are merely represented as 2D, navigation networks still can be derived under unified rules and will provide seamless navigation, the information in the third dimension will be lost. Thus, the reliance on 3D space will also reduce the usability of the model to a certain extent. These three limitations shall be further investigated in the future work.

Thirdly, we mainly focus on the definition, classification, and reconstruction of the spaces formed by built structures. Agents may also be interested in the spaces from other structures, such as the underground (e.g., tunnels), landscape spaces, mines, caves, even desert during their navigation. For instance, partial landscape spaces are formed by trees, in which trees themselves can form non-navigable spaces but their treetops are able to form SI-spaces. Theoretically, such kind of spaces could be also classified and included in the unified navigation model and employed to enhance the MTC-path or NSI-path. But, because such kind of structures is different from building structures, the estimation approaches of parameters and thresholds in the generic space definition framework, approaches of 3D space reconstruction, and data sources should be further investigated.

Last but not the least, a pedestrian was utilized as the agent for implementations, which allows us to determine that if a space is qualified for navigation as long as (i) it is big enough to hold a pedestrian and (ii) its *topClosure* ( $C^T$ ) is good enough for MTC-path and NSI-path planning purposes. However, a pedestrian is only one specific type of agent. Pedestrians often can walk with extra devices, such as trailers, child buggies. Besides, other types of agents such as drones and robots also need seamless navigation path planning. These agents could have different requirements for space in size,  $C^T$ , as well as other aspects, such as the gradient of bottom. We expect the developed theories, models and approaches to be usable for these different types of agents. Therefore, extensions of agent types could help to better test the whole research.

## 8.3 Recommendations for Further Research

This section introduces future work to this PhD research. As discussed, several aspects still need to be investigated deeply to enhance the developed theories, models and approaches for indoor-outdoor seamless navigation path planning. Future work can be categorized into eight aspects, in which the first four directions are to strengthen and supplement the current results, while the remaining four are further sublimation of this research.

- Extend the definition of spaces;
- Apply space subdivision;
- Include obstacles in the path planning;
- Evaluate the navigation performance;
- Popularize the results to other applications;
- Reconstruct space based on other data sources;
- Investigate space accessibility;
- Develop and evaluate new navigation path options.

### 8.3.1 Extend the Definition of Spaces

The generic definition framework developed by this research can systematically classify and define the built environment spaces into I-space, O-space, sI-space, and sO-space. Nevertheless, other than the spaces formed by built structures, pedestrians or other types of agents may also need navigation in the spaces formed by underground (e.g., caves), landscape spaces, mines, even desert. Therefore, it is essential to extend the generic space definition framework to cover such kind of spaces.

For extensions, the terms introduced by this research (Section 3.2), including *Top*, *Side*, *Bottom*, *topClosure*, *sideClosure*, *bottomClosure*, *Gradient*, *Physical/Virtual boundary*, still

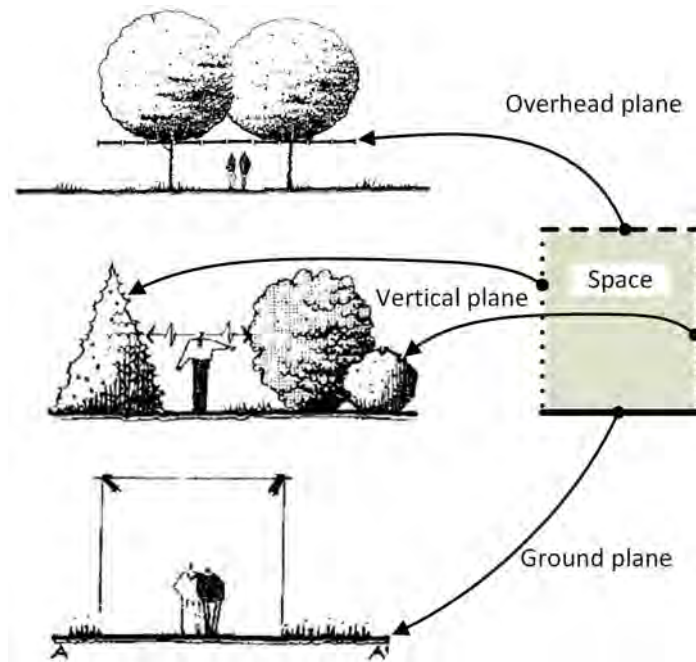


FIGURE 8.1: Example of the space modelling in landscape. Adapted from the figures in (Zlatanova et al., 2020).

can be utilized, but the three threshold values ( $\alpha$ ,  $\beta$  and  $\eta$ ) for  $C^T$  and the two ( $\gamma$  and  $\delta$ ) for  $C^S$  need to be re-estimated. For instance, landscape spaces are represented by boundaries with geometric representations, in which boundaries are called as surrounding planes, including ground plane, vertical plane, and overhead plane (Zlatanova et al., 2020; Wang et al., 2020). As seen in Figure 8.1, treetops of arbours act as overhead planes, bushes as vertical planes, and ground/terrain as the ground plane. It means that the ground plane, vertical plane and overhead plane can correspond to Bottom, Side, and Top respectively. But the  $C^T$  and  $C^S$  of the spaces formed by trees cannot be computed based on the elaborated approaches (Section 3.2.2), because it is very complex to estimate the physically enclosed areas and entire areas. Therefore, currently, it is hard to say how spaces formed by trees can be classified. For trees themselves, they are non-navigable while the spaces formed by them could be some of these four classified spaces, for instance, the spaces formed by treetops could be sI-spaces. That is, after additional investigation, the expectation is that forests can be included in *CellSpace* and *CellSpaceBoundary*.

### 8.3.2 Apply Space Subdivision

Space subdivision is expected to bring in two benefits to path planning. One is to accurately subdivide the areas of outdoor to make sure spaces have the correct attributes, such as roads, streets, green areas, water bodies. Another is to help with deriving a refined navigation network, such as subdividing spaces into convex can make sure the navigation nodes stay within the spaces. In this thesis, we only have manually split roads/streets into closed polygons on the basis of their attributes, in which only buildings, shelters, roads, green areas, hand railings, enclosing walls, and fences are used as the borders. In the navigation network derivation, a road/street space is abstracted as a node without considering its convexity.



FIGURE 8.2: Example of outdoor borders.

Thence, space subdivision rules or algorithms for automatically subdividing outdoor spaces based on different borders should be investigated. Particularly, drawing on the methods originally designed for indoor spaces can offer possibilities for extensions to outdoor, such as 3D indoor space subdivision based on the convex (Diakit  and

Zlatanova, 2018) or visibility (Jiang and Liu, 2010). Furthermore, consider more types of borders in outdoor spaces, because besides the borders mentioned above, outdoor spaces may have other natural borders, such as water (Figure 8.2(a)), cliff (Figure 8.2(b)), and traffic markers (Figure 8.2(c)). If the agent becomes a vehicle, traffic markers especially should be considered as the borders, for example, the street in Figure 8.2(d). There are road signs ("DO NOT ENTER") that indicate no cars are allowed to enter the street.

### 8.3.3 Include Obstacles in the Path Planning

All parts in this research assume that the spaces are freely walkable and empty, i.e., there is no furniture/facilities. However, it is over idealistic, because this assumption fails to reflect the complexity of real indoor and outdoor environments thereby missing to consider the possibility that obstacles may change the navigation paths. Therefore, in future work, obstacles shall be included in the unified navigation model and further used for seamless navigation path planning. For instance, we can use the Flexible Space Subdivision framework (FSS) introduced by (Diakit  and Zlatanova, 2018) to categories indoor obstacle spaces as static (e.g., pillar), semi-mobile (e.g., small table), and mobile (e.g., fire). As for the obstacles in sI-spaces, sO-spaces, and O-spaces, further investigations should be carried out on adapting the FSS framework or proposing new theories/approaches.

### 8.3.4 Evaluate the Navigation Performance

It is appropriate to say that the presented approach is suitable for precinct areas (e.g., a campus or similar) where pedestrians can reach on foot. However, navigation does not always only happen within such areas and the travel mode is not always limited to walk. For instance, someone may need a navigation path from an office at one end of the city to a friend's home at the other end. For such a case, a lot of spaces should be included and multiple locomotion modes may be needed. Due to the current implementations are performed based on files, once the scenario becomes a city level, without any abstraction/aggregation mechanisms, we may have great trouble to reconstruct the spaces, derive navigation networks, and plan the seamless navigation paths. More importantly,

navigation paths are generally required to be planned in real-time and path planning becomes unacceptable if it takes too much time. Therefore, in the future work, two aspects should be conducted to cope with computing problems: (i) evaluate navigation path computational performance and involve multiple locomotion modes, and (ii) investigate abstraction/aggregation mechanisms for computing the spaces and deriving a network in large areas.

### 8.3.5 Popularize the Results to Other Applications

As mentioned in Section 3.1.1, agents can be broadly categorised as humans and robots, which have different locomotion modes and can vary in size and height, such as walking (pedestrians), rolling (trolleys, wheelchairs), flying objects (e.g., drones) or combinations of these. Therefore, other than pedestrian, research should be conducted on other types of agents, such as trolleys, wheelchairs, drones, or robots. Theoretically, the developed space classification, definition, the unified 3D space-based model, and space reconstruction approaches are still capable, but more parameters and criteria should be added to reflect the agents. For instance, compared to a pedestrian, a wheelchair user needs larger spaces in length and width but less space in the height, and he/she would require to be navigated with spaces that have no stairs and no undue bottom gradient.

Furthermore, this research developed the internal memory data structures (Section 7.2) by using the UML of the unified 3D space-based navigation model (Figure 5.1). This model is extended from IndoorGML and intended for representation indoor, semi-indoor, semi-outdoor and outdoor spatial information based on 3D spaces and network/-graph. To make this model for multiple and multi-purpose uses, in the future, it is necessary to learn from IndoorGML, for example, develop an XML-based schema of this model for the exchange of information. Other than that, another way to popularize this model is to utilize it as a data model for the persistent storage of data in the DBMS for different purposes.

### 8.3.6 Reconstruct Spaces based on Other Data Source

Space reconstruction is a key step of the presented unified model and path planning based on 3D spaces, because the 3D spaces might not be always available or needed to be created. No one currently knows if existing data sources can provide these four navigation spaces at the same time. For instance, map providers or agencies generally cannot provide information of indoor and semi-indoor spaces. BIM models and footprints (2D maps) used in this research have been available from different sources, such as Estate Management, mapping agencies or OSM. If BIM models or 2D maps are not available, other algorithms could be the options, such as from point clouds (Rodenberg, Verbree, and Zlatanova, 2016). Furthermore, with the development of 3D space modelling, we can access more 3D models, such as CityGML models. The on-going version of CityGML 3.0 is planning to model the outdoor as 3D spaces (Kutzner, Chaturvedi, and Kolbe, 2020), which includes driving lane, sidewalks, even waterway (Labetski et al., 2018).

Therefore, exploring 3D models as inputs to support the better 3D reconstruction of semi-outdoor and outdoor spaces can be a future direction. Other than 3D models, point clouds from airborne laser scans (Haala and Brenner, 1997; Verma, Kumar, and Hsu, 2006; Rodenberg, Verbree, and Zlatanova, 2016), or aerial photographs and terrestrial laser scans (Fruh and Zakhor, 2001), or images from UAV (Xie et al., 2012) can also be the data sources for 3D reconstruction of spaces, although these kind of data currently are mainly for 3D (building) models generation (Nikoohemat et al., 2020).

### 8.3.7 Investigate Space Accessibility

Currently, this research presumes that all the spaces are available for navigation. However, although the spaces are there, they might not be accessible. For instance, pedestrians are forbidden to visit some spaces because they are private, occupied, not allowed, or closed (Figure 8.3). Specifically, the space accessibility issues can be classified into property, object, legal, and time. The property issue means that spaces are private (e.g., the building with balconies in Figure 8.3(a)). There are two sI-spaces: one is formed by the roof and outer floor (balcony space), and the other is formed by the ground and the

outer ceiling (space under the balcony). Generally speaking, the former cannot be used in the navigation model/system, as this space is private and only the house owner can use it, while the latter can be public. The object issue is that some spaces may be occupied by some objects. For instance, the spaces are occupied by plants (Figure 8.3(a)) or a car (Figure 8.3(b)). The legal issue usually arises in some public spaces, such as areas where pedestrians are not allowed to cross some zones considering the security (Figure 8.3(c)). The time issue means the spaces are available for pedestrians during certain time slots (Figure 8.3(d)).

The Land Administration Domain Model (LADM) (Lemmen et al., 2010; Lemmen, Van Oosterom, and Bennett, 2015; Zlatanova et al., 2016a; Zlatanova et al., 2016b; Alattas et al., 2018b; Alattas, Oosterom, and Zlatanova, 2018; Alattas et al., 2018a) can provide an option to solve the property issue, and the object issue can be addressed by considering the locations of objects. Based on the combined use of LADM models (Lemmen, Van Oosterom, and Bennett, 2015) with IndoorGML, indoor navigation can be performed with the accessibility of the indoor spaces based on user rights (Alattas et al., 2017). This practice is capable to make the navigation process more appropriate and simpler because the navigation path will avoid all of the non-accessible spaces based on the rights of the agents, which further can save computation resources for path planning in a large area. Therefore, in the future work, it is necessary to investigate how to add accessibility attribute to spaces by using the LADM.

### 8.3.8 Develop and Evaluate New Navigation Path Options

This thesis developed two new navigation path options, MTC-path and NSI-path, in which the top-coverage-ratio of a path ( $P_{c_r}$ ) is used as a metric for the optimal path determination. However, besides this, other metrics may also be interesting for some agent, such as the number of turns (Vanclouster et al., 2019), safety (Wang and Zlatanova, 2019), specific level of calories burn (Sharker, Karimi, and Zgibor, 2012), minimum traffic related air pollution exposure (Alam, Perugu, and McNabola, 2018), etc. Moreover, this research only attempted to develop new path options based on sI-space. It means that



(a) Property and object issue



(b) Object issue



(c) Legal issue



(d) Time issue

FIGURE 8.3: Example of space accessibility issues.

one of the future work is to develop new models that can consider more metrics, and another work can be developing new path options based on all types of spaces for further tailoring of the navigation path with respect to environmental factors. For instance, a path with as many I-spaces as possible, which could be very attractive in hot summer, since the I-spaces are generally equipped with air conditioners.

The experiences and feedbacks are critical for the research of seamless path planning, because the ultimate goal of developing new path options is to better navigate agents.

---

However, currently, the new path options are merely devised by observations of human behaviours and needs in routing. Therefore, in future work, it is necessary to deploy the developed new path options in navigation systems, and then, evaluate and improve them based on the feedbacks of agents. For instance, by collecting questionnaires, investigating the acceptable  $C^T$  of space for selecting sI-spaces and I-spaces in MTC-path planning.



---

## BIBLIOGRAPHY

---

- Afyouni, Imad, Cyril Ray, and Christophe Claramunt (2010). "A fine-grained context-dependent model for indoor spaces". In: *Proceedings of the 2nd acm sigspatial international workshop on indoor spatial awareness*. ACM, pp. 33–38.
- Alam, MS, H Perugu, and A McNabola (2018). "A comparison of route-choice navigation across air pollution exposure, CO2 emission and traditional travel cost factors". In: *Transportation Research Part D: Transport and Environment* 65, pp. 82–100.
- Alattas, A. et al. (2018a). "USING THE COMBINED LADM-INDOORGML MODEL TO SUPPORT BUIILDING EVACUATION". In: *ISPRS - International Archives of the Photogrammetry, Remote Sensing and Spatial Information Sciences XLII-4*, pp. 11–23.
- Alattas, Abdullah, Peter van Oosterom, and Sisi Zlatanova (2018). "Deriving the Technical Model for the Indoor Navigation Prototype based on the Integration of IndoorGML and LADM Conceptual Model". In: *Proceedings of the 7th Land Administration Domain Model Workshop, Zagreb*, p. 24.

- Alattas, Abdullah et al. (2017). "Supporting Indoor Navigation Using Access Rights to Spaces Based on Combined Use of IndoorGML and LADM Models". In: *ISPRS international journal of geo-information* 6.12, p. 384.
- Alattas, Abdullah et al. (2018b). "Developing a database for the LADM-IndoorGML model". In: *Proceedings of the 6th International FIG 3D Cadastre Workshop, 2-4 October 2018, Delft, The Netherlands*, pp. 261–278.
- Alattas, Abdullah et al. (2018c). "Improved and more complete conceptual model for the revision of IndoorGML". In: *Proceedings of the 10th International Conference on Geographic Information Science (GIScience 2018)*. Vol. 114. Leibniz International Proceedings in Informatics, 21:1–21:12.
- Aleksandrov, M et al. (2019). "Voxel-Based Visibility Analysis for Safety Assessment of Urban Environments". In: *ISPRS Annals of Photogrammetry, Remote Sensing and Spatial Information Sciences*, pp. 11–17.
- Amutha, B and Karthick Nanmaran (2014). "Development of a ZigBee based virtual eye for visually impaired persons". In: *2014 International Conference on Indoor Positioning and Indoor Navigation (IPIN)*. IEEE, pp. 564–574.
- Andreev, Simeon et al. (2015). "Towards Realistic Pedestrian Route Planning". In: *15th Workshop on Algorithmic Approaches for Transportation Modelling, Optimization, and Systems (ATMOS 2015)*. Schloss Dagstuhl-Leibniz-Zentrum fuer Informatik, pp. 1–15.
- Ashihara, Yoshinobu (1981). *Exterior design in architecture*. Van Nostrand Reinhold Company.
- Balata, Jan, Jakub Berka, and Zdenek Mikovec (2018). "Indoor-Outdoor Intermodal Sidewalk-Based Navigation Instructions for Pedestrians with Visual Impairments". In: *International Conference on Computers Helping People with Special Needs*. Springer, pp. 292–301.
- Ballester, Miquel Ginard, Maurici Ruiz Pérez, and HJ Stuiiver (2011). "Automatic pedestrian network generation". In: *14th AGILE International Conference on GIS*, pp. 1–13.
- Becker, Thomas, Claus Nagel, and Thomas H Kolbe (2009). "A multilayered space-event model for navigation in indoor spaces". In: *3D geo-information sciences*. Springer, pp. 61–77.

- Beil, Christof and Thomas H Kolbe (2017). "CityGML and the streets of New York-A proposal for detailed street space modelling:(accepted)". In: *Proceedings of the 12th International 3D GeoInfo Conference 2017*, pp. 9–16.
- Beirão, José Nuno, André Chaszar, and Ljiljana Čavić (2015). "Analysis and Classification of Public Spaces Using Convex and Solid-Void Models". In: *Future City Architecture for Optimal Living*. Springer, pp. 241–270.
- Beirão, José Nuno, André Chaszar, et al. (2014). "Convex-and Solid-Void Models for Analysis and Classification of Public Spaces". In: *Proceedings of the 19th CAADRIA International Conference, Kyoto*. CUMINCAD, pp. 253–262.
- Bodgan, J and Volker Coors (2009). "Using 3d urban models for pedestrian navigation support". In: *Proceedings of the ISPRS working group III/4, IV/8, IV/5: GeoWeb*, pp. 9–15.
- Boguslawski, Pawel and Christopher Gold (2009). "Construction operators for modelling 3D objects and dual navigation structures". In: *3D Geo-Information Sciences*, pp. 47–59.
- Bosina, Ernst et al. (2016). "Avoiding Walls: What Distance Do Pedestrians Keep from Walls and Obstacles?" In: *Traffic and Granular Flow'15*. Springer, pp. 19–26.
- Bouyer, J et al. (2007). "Thermal comfort assessment in semi-outdoor environments: Application to comfort study in stadia". In: *Journal of Wind Engineering and Industrial Aerodynamics* 95.9, pp. 963–976.
- Bowyer, Adrian (1996). *Chapter 2: Boundary-representation Models*. [http://homepages.inf.ed.ac.uk/rbf/CVonline/LOCAL\\_COPIES/BOWYER1/c2.htm](http://homepages.inf.ed.ac.uk/rbf/CVonline/LOCAL_COPIES/BOWYER1/c2.htm). Accessed March 2, 2020.
- Boysen, Mikkel et al. (2014). "A journey from ifc files to indoor navigation". In: *International Symposium on Web and Wireless Geographical Information Systems*. Springer, pp. 148–165.
- Brandli, MARTIN (1996). "Hierarchical Models for the Definition and Extraction of Terrain". In: *Geographic objects with indeterminate boundaries 2*, p. 257.

- Brédif, Mathieu et al. (2013). "Extracting polygonal building footprints from digital surface models: A fully-automatic global optimization framework". In: *ISPRS journal of photogrammetry and remote sensing* 77, pp. 57–65.
- Budroni, Angela and J Boehm (2010). "Automated 3D Reconstruction of Interiors from Point Clouds". In: *International Journal of Architectural Computing* 8.1, pp. 55–73.
- buildingSMART International Ltd. (1996-2019). *Industry Foundation Classes Version 4.2 bSI Draft Standard IFC Bridge proposed extension*. [https://standards.buildingsmart.org/IFC/DEV/IFC4\\_2/FINAL/HTML/](https://standards.buildingsmart.org/IFC/DEV/IFC4_2/FINAL/HTML/). Accessed December 17, 2019.
- Cambra, Paulo Jorge, Alexandre Gonçalves, and Filipe Moura (2019). "The Digital Pedestrian Network in Complex Urban Contexts: A Primer Discussion on Typological Specifications". In: *Finisterra* 54.110, pp. 155–170.
- Cambridge University Press 2019 (2019). *Cambridge Dictionary*. <http://dictionary.cambridge.org>. Accessed December 17, 2019.
- Cao, Bin et al. (2017). "Thermal comfort in semi-outdoor spaces within an office building in Shenzhen: A case study in a hot climate region of China". In: *Indoor and Built Environment* 27.10, pp. 1431–1444.
- Center, Permit (2002). *BUILDING HEIGHT CALCULATION INSTRUCTIONS*. <https://www.cob.org/documents/planning/applications-forms/building-height-calculation.pdf>. Accessed December 17, 2019.
- Chen, Jorge and Keith C Clarke (2019). "Indoor cartography". In: *Cartography and Geographic Information Science*, pp. 1–15.
- Cheng, Jiantong et al. (2014). "Seamless outdoor/indoor navigation with WIFI/GPS aided low cost Inertial Navigation System". In: *Physical Communication* 13, pp. 31–43.
- Chengappa, Chaya et al. (2007). "Impact of improved cookstoves on indoor air quality in the Bundelkhand region in India". In: *Energy for Sustainable Development* 11.2, pp. 33–44.
- Collins (2019). *Collins Dictionary*. <https://www.collinsdictionary.com/>. Accessed December 17, 2019.

- Diakit , Abdoulaye and Sisi Zlatanova (2020). "Automatic geo-referencing of BIM in GIS environments using building footprints". In: *Computers, Environment and Urban Systems* 80.
- Diakit , Abdoulaye A and Sisi Zlatanova (2018). "Spatial subdivision of complex indoor environments for 3D indoor navigation". In: *International Journal of Geographical Information Science* 32.2, pp. 213–235.
- Dijkstra, E.W. (1959). "A note on two problems in connexion with graphs". In: *Numerische Mathematik* 1, pp. 269–271.
- Du, Xiaoyu, Regina Bokel, and Andy van den Dobbelsteen (2014). "Building microclimate and summer thermal comfort in free-running buildings with diverse spaces: A Chinese vernacular house case". In: *Building and Environment* 82, pp. 215–227.
- Duckham, Matt and Lars Kulik (2003). " "Simplest" paths: automated route selection for navigation". In: *International Conference on Spatial Information Theory*. Springer, pp. 169–185.
- Dudas, Patrick M, Mahsa Ghafourian, and Hassan A Karimi (2009). "ONALIN: Ontology and algorithm for indoor routing". In: *2009 Tenth International Conference on Mobile Data Management: Systems, Services and Middleware*. IEEE, pp. 720–725.
- Fan, Hongchao et al. (2014). "Quality assessment for building footprints data on OpenStreetMap". In: *International Journal of Geographical Information Science* 28.4, pp. 700–719.
- Farlex, Inc (2003-2019). *THE FREE DICTIONARY BY FARLEX*. <http://www.thefreedictionary.com/>. Accessed December 17, 2019.
- Fruh, Christian and Avideh Zakhor (2001). "3D model generation for cities using aerial photographs and ground level laser scans". In: *Proceedings of the 2001 IEEE Computer Society Conference on Computer Vision and Pattern Recognition. CVPR 2001*. Vol. 2. IEEE, pp. II–II.
- Ghafourian, Mahsa and Hassan A Karimi (2009). "CAD/GIS Integration Issues for Seamless Navigation between Indoor and Outdoor Environments". In: *CAD and GIS Integration*. Auerbach Publications, pp. 141–154.

- Gorte, B, M Aleksandrov, and S Zlatanova (2019). "Towards Egress Modelling in Voxel Building Models". In: *ISPRS Annals of Photogrammetry, Remote Sensing and Spatial Information Sciences*, pp. 43–47.
- Gorte, B., S. Zlatanova, and F. Fadli (2019). "NAVIGATION IN INDOOR VOXEL MODELS". In: *ISPRS Annals of Photogrammetry, Remote Sensing and Spatial Information Sciences IV-2/W5*, pp. 279–283.
- Goshayeshi, Danial et al. (2013). "A review of researches about human thermal comfort in semi-outdoor spaces". In: *European Online Journal of Natural and Social Sciences* 2.4, p. 516.
- Graser, Anita (2016). "Integrating Open Spaces into OpenStreetMap Routing Graphs for Realistic Crossing Behaviour in Pedestrian Navigation". In: *GI\_Forum—Journal for Geographic Information Science, Salzburg, Österreich, July*, pp. 5–8.
- Gröger, Gerhard et al. (2012). *OGC City Geography Markup Language (CityGML) encoding standard*. [https://portal.opengeospatial.org/files/?artifact\\_id=47842](https://portal.opengeospatial.org/files/?artifact_id=47842). Accessed June 10, 2020.
- Haala, Norbert and Claus Brenner (1997). "Generation of 3D city models from airborne laser scanning data". In: *3rd EARSEL Workshop on LIDAR remote sensing on land and sea, Tallinn/Estonia*, pp. 105–112.
- Hammoudi, Karim, Fadi Dornaika, and Nicolas Paparoditis (2009). "Extracting building footprints from 3D point clouds using terrestrial laser scanning at street level". In: *ISPRS/CMRT09* 38, pp. 65–70.
- Hannah, Charlotte, Irena Spasić, and Pdraig Corcoran (2018). "A computational model of pedestrian road safety: the long way round is the safe way home". In: *Accident Analysis & Prevention* 121, pp. 347–357.
- He, Jiang and Akira Hoyano (2010). "Measurement and evaluation of the summer microclimate in the semi-enclosed space under a membrane structure". In: *Building and Environment* 45.1, pp. 230–242.
- Hillier, Bill and Julienne Hanson (1984). *The social logic of space*. Cambridge university press.

- Hooff, Twan Antonius Johannes van and Bert Blocken (2009). "Computational analysis of natural ventilation in a large semi-enclosed stadium". In: *Proceedings of the 5th European and African Conference on Wind Engineering*. Firenze University Press., pp. 1–11.
- Howard, Charlene and Elizabeth K Burns (2001). "Cycling to work in Phoenix: Route choice, travel behavior, and commuter characteristics". In: *Transportation Research Record* 1773.1, pp. 39–46.
- Hwang, Ruey-Lung and Tzu-Ping Lin (2007). "Thermal comfort requirements for occupants of semi-outdoor and outdoor environments in hot-humid regions". In: *Architectural Science Review* 50.4, pp. 357–364.
- Indraganti, Madhavi (2010). "Adaptive use of natural ventilation for thermal comfort in Indian apartments". In: *Building and environment* 45.6, pp. 1490–1507.
- Ishaque, Muhammad Moazzam and Robert B Noland (2008). "Behavioural issues in pedestrian speed choice and street crossing behaviour: a review". In: *Transport Reviews* 28.1, pp. 61–85.
- Isikdag, Umit, Sisi Zlatanova, and Jason Underwood (2013). "A BIM-Oriented Model for supporting indoor navigation requirements". In: *Computers, Environment and Urban Systems* 41, pp. 112–123.
- Jiang, Bin and Xintao Liu (2010). "Automatic generation of the axial lines of urban environments to capture what we perceive". In: *International Journal of Geographical Information Science* 24.4, pp. 545–558.
- Kara, Abdullah et al. (2018). "Towards harmonizing property measurement standards". In: *Journal of Spatial Information Science* 2018.17, pp. 87–119.
- Karimi, Hassan A, Ming Jiang, and Rui Zhu (2013). "Pedestrian navigation services: challenges and current trends". In: *Geomatica* 67.4, pp. 259–271.
- Kim, Jiyoeng, Taeyeon Kim, and Seung-Bok Leigh (2011). "Double window system with ventilation slits to prevent window surface condensation in residential buildings". In: *Energy and Buildings* 43.11, pp. 3120–3130.

- Kim, Kwangho, Sanghyun Park, and Byungseon Sean Kim (2008). "Survey and numerical effect analyses of the market structure and arcade form on the indoor environment of enclosed-arcade markets during summer". In: *Solar Energy* 82.10, pp. 940–955.
- Kim, KyoHyouk and John P Wilson (2015). "Planning and visualising 3D routes for indoor and outdoor spaces using CityEngine". In: *Journal of Spatial Science* 60.1, pp. 179–193.
- Kim, Taehoon, Kyoung-Sook Kim, and Jiyeong Lee (2019). "How to Extend IndoorGML for Seamless Navigation Between Indoor and Outdoor Space". In: *International Symposium on Web and Wireless Geographical Information Systems*. Springer, pp. 46–62.
- Kim, Taeyeon, Shinsuke Kato, and Shuzo Murakami (2001). "Indoor cooling/heating load analysis based on coupled simulation of convection, radiation and HVAC control". In: *Building and Environment* 36.7, pp. 901–908.
- Kimmel, Ron, Arnon Amir, and Alfred M. Bruckstein (1995). "Finding shortest paths on surfaces using level sets propagation". In: *IEEE Transactions on Pattern Analysis and Machine Intelligence* 17.6, pp. 635–640.
- Klochkova, Olena et al. (2017). "Pedestrian Route Planning based on an Enhanced Representation of Pedestrian Network and Probabilistic Estimate of Signal Delays". In: *GIS Research UK (GISRUK)*, pp. 1–6.
- Kolavali, Sudha Rani and Shalabh Bhatnagar (2008). "Ant colony optimization algorithms for shortest path problems". In: *International Conference on Network Control and Optimization*. Springer, pp. 37–44.
- Kouroggi, Masakatsu et al. (2006). "Indoor/outdoor pedestrian navigation with an embedded GPS/RFID/self-contained sensor system". In: *Advances in Artificial Reality and Tele-Existence*, pp. 1310–1321.
- Kray, Christian et al. (2013). "Transitional spaces: between indoor and outdoor spaces". In: *International Conference on Spatial Information Theory*. Springer, pp. 14–32.
- Krūminaitė, Marija (2014). "Space Subdivision for Indoor Navigation". MA thesis. Dissertação (Mestrado em Geomática). Delft University of Technology.

- Krūminaitė, Marija and Sisi Zlatanova (2014). "Indoor space subdivision for indoor navigation". In: *Proceedings of the Sixth ACM SIGSPATIAL International Workshop on Indoor Spatial Awareness*. ACM, pp. 25–31.
- Kutzner, Tatjana, Kanishk Chaturvedi, and Thomas H Kolbe (2020). "CityGML 3.0: New Functions Open Up New Applications". In: *PFG—Journal of Photogrammetry, Remote Sensing and Geoinformation Science*, pp. 1–19.
- Labetski, Anna et al. (2018). "A proposal for an improved transportation model in CityGML". In: *ISPRS - International Archives of the Photogrammetry, Remote Sensing and Spatial Information Sciences*, pp. 89–96.
- Ledoux, Hugo and Martijn Meijers (2009). "Extruding building footprints to create topologically consistent 3D city models". In: *Urban and Regional Data Management*. CRC Press, pp. 51–60.
- Lee, J et al. (2015). *OGC IndoorGML, Document No. 14-005r4*. <http://docs.opengeo-spatial.org/is/14-005r5/14-005r5.html>. Accessed February 03, 2020.
- Lee, Jay (1991). "Comparison of existing methods for building triangular irregular network, models of terrain from grid digital elevation models". In: *International Journal of Geographical Information System* 5.3, pp. 267–285.
- Lee, Jiyeong (2004a). "A Spatial Access-Oriented Implementation of a 3-D GIS Topological Data Model for Urban Entities". In: *Geoinformatica* 8.3, pp. 237–264.
- (2004b). "A spatial access-oriented implementation of a 3-D GIS topological data model for urban entities". In: *GeoInformatica* 8.3, pp. 237–264.
- Lemmen, CHJ et al. (2010). "The modelling of spatial units (parcels) in the Land Administration Domain Model (LADM)". In: *Proceedings of the XXIV FIG International Congress 2010: Facing the Challenges - Building the Capacity*. International Federation of Surveyors (FIG), pp. 1–21.
- Lemmen, Christiaan, Peter Van Oosterom, and Rohan Bennett (2015). "The land administration domain model". In: *Land use policy* 49, pp. 535–545.
- Lexico.com, 2019 (2019). *OXFORD DICTIONARY*. <https://en.oxforddictionaries.com>. Accessed December 17, 2019.

- Li, Fangyu et al. (2018). "Universal path planning for an indoor drone". In: *Automation in Construction* 95, pp. 275–283.
- Li, Ki-Joune et al. (2019). "Survey on Indoor Map Standards and Formats". In: *2019 International Conference on Indoor Positioning and Indoor Navigation (IPIN)*. IEEE, pp. 1–8.
- Li, Shaogang (1994). "Users' behaviour of small urban spaces in winter and marginal seasons". In: *Architecture and Behaviour* 10.1, pp. 95–109.
- Lin, Tzu-Ping (2009). "Thermal perception, adaptation and attendance in a public square in hot and humid regions". In: *Building and environment* 44.10, pp. 2017–2026.
- Lin, Tzu-Ping, Andreas Matzarakis, and Jia-Jian Huang (2006). "Thermal comfort and passive design strategy of bus shelters". In: *The 23rd Conference on Passive and Low Energy Architecture, Geneva, Switzerland, 6-8 September 2006*. Citeseer.
- Lin, Tzu-Ping et al. (2008). "The comparison of thermal sensation and acceptable range for outdoor occupants between Mediterranean and subtropical climates". In: *Proceedings 18th International Congress on Biometeorology, Urban Climate*.
- Lin, Ya-Hong et al. (2013). "The IFC-based path planning for 3D indoor spaces". In: *Advanced Engineering Informatics* 27.2, pp. 189–205.
- Liu, Liu (2017). "Indoor semantic modelling for routing: The two-level routing approach for indoor navigation". PhD thesis, pp. 1–252.
- Liu, Liu and Sisi Zlatanova (2013). "A two-level path-finding strategy for indoor navigation". In: *Intelligent systems for crisis management*. Springer, pp. 31–42.
- Liu, Xiao Hu et al. (Mar. 2013). "Urban Solar Updraft Tower Integrated with Hi-Rise Building – Case Study of Wuhan New Energy Institute Headquarter". In: *Solar Updraft Tower Power Technology*. Trans Tech Publications, pp. 67–71.
- Lorenz, Bernhard, Hans Jürgen Ohlbach, and Edgar Philipp Stoffel (2006). "A Hybrid Spatial Model for Representing Indoor Environments". In: *Web & Wireless Geographical Information Systems, International Symposium, W2gis, Hong Kong, China, December*, pp. 1–11.

- Macher, H, Tania Landes, and Pierre Grussenmeyer (2017). "From Point Clouds to Building Information Models: 3D Semi-Automatic Reconstruction of Indoors of Existing Buildings". In: *Applied Sciences* 7.10, p. 1030.
- May, Andrew J et al. (2003). "Pedestrian navigation aids: information requirements and design implications". In: *Personal and Ubiquitous Computing* 7.6, pp. 331–338.
- Meijers, Martijn, Sisi Zlatanova, and Norbert Pfeifer (2005). "3D geoinformation indoors: structuring for evacuation". In: *Proceedings of Next generation 3D city models*. Vol. 6. Germany Bonn, pp. 11–16.
- Merriam-Webster, Incorporated (2019). *Merriam-Webster DICTIONARY*. <https://www.merriam-webster.com/dictionary>. Accessed December 17, 2019.
- Miller, George A (1995). "WordNet: a lexical database for English". In: *Communications of the ACM* 38.11, pp. 39–41.
- Millonig, Alexandra and K Schechtner (2007a). "Decision loads and route qualities for pedestrians—Key requirements for the design of pedestrian navigation services". In: *Pedestrian and evacuation dynamics 2005*. Springer, pp. 109–118.
- Millonig, Alexandra and Katja Schechtner (2007b). "Developing landmark-based pedestrian-navigation systems". In: *IEEE Transactions on Intelligent Transportation Systems* 8.1, pp. 43–49.
- Monteiro, Leonardo M and Marcia P Alucci (2007). "Transitional spaces in São Paulo, Brazil: mathematical modeling and empirical calibration for thermal comfort assessment". In: *Building Simulation 2007*, pp. 737–744.
- Mortari, Filippo et al. (2014). "'Improved geometric network model' (IGNM): A novel approach for deriving connectivity graphs for indoor navigation". In: *ISPRS Annals of the Photogrammetry, Remote Sensing and Spatial Information Sciences* 2.4, p. 45.
- Munkres, James R (1984). *Elements of algebraic topology*. Vol. 2. Addison-Wesley Menlo Park.
- Nagel, Claus et al. (2010). "Requirements and Space-Event Modeling for Indoor Navigation - How to simultaneously address route planning, multiple localization methods,

- navigation contexts, and different locomotion types". In: *Open Geospatial Consortium*, pp. 1–54.
- Nasir, Nazliyah Hani Mohd, Farha Salim, and Maheran Yaman (Apr. 2014). "The Potential of Outdoor Space Utilization for Learning Interaction". In: *Kulliyah of Architecture and Environmental Design*, pp. 1–17.
- Neufert, Ernst et al. (1980). *Architects' data*. Granada St Albans, Herts.
- Nikander, Jussi et al. (2013). "Indoor and outdoor mobile navigation by using a combination of floor plans and street maps". In: *Progress in Location-Based Services*. Springer, pp. 233–249.
- Nikooohemat, S et al. (2020). "Indoor 3D reconstruction from point clouds for optimal routing in complex buildings to support disaster management". In: *Automation in Construction* 113, p. 103109.
- Nourian, Pirouz et al. (2016). "Voxelization algorithms for geospatial applications: Computational methods for voxelating spatial datasets of 3D city models containing 3D surface, curve and point data models". In: *MethodsX* 3, pp. 69–86.
- Ortiz, Alberto et al. (2015). "Saliency-driven Visual Inspection of Vessels by means of a Multicopter". In: *The Workshop on Vision-Based Control & Navigation of Small*, pp. 20–46.
- Pagliarini, G and S Rainieri (2011a). "Dynamic thermal simulation of a glass-covered semi-outdoor space with roof evaporative cooling". In: *Energy and Buildings* 43.2, pp. 592–598.
- (2011b). "Thermal environment characterisation of a glass-covered semi-outdoor space subjected to natural climate mitigation". In: *Energy and Buildings* 43.7, pp. 1609–1617.
- Park, Junho, Dasol Ahn, and Jiyeong Lee (2018). "Development of data fusion method based on topological relationships using IndoorGML core module". In: *Journal of Sensors* 2018, pp. 1–14.
- Peltola, Pekka and Terry Moore (2017). "Towards Seamless Navigation". In: *Multi-Technology Positioning*. Springer International Publishing, pp. 125–147.

- Philokyrou, Maria et al. (2017). "Thermal performance assessment of vernacular residential semi-open spaces in Mediterranean climate". In: *Indoor and Built Environment* 27.8, pp. 1050–1068.
- Powers, Edward J, Doug Gray, and Richard C Green (1996). *Artificial Vision: Image Description, Recognition, and Communication*. Academic Press.
- Previtali, M. et al. (2014). "A flexible methodology for outdoor/indoor building reconstruction from occluded point clouds". In: *ISPRS Annals of Photogrammetry, Remote Sensing and Spatial Information Sciences* II-3, pp. 119–126.
- Princeton University (2010). *Princeton WorldNetWeb*. <http://wordnetweb.princeton.edu/perl/webwn>. Accessed December 17, 2019.
- Raghothama, Srinivas and Vadim Shapiro (1998). "Boundary representation deformation in parametric solid modeling". In: *ACM Transactions on Graphics (TOG)* 17.4, pp. 259–286.
- Ramakrishnan, CV et al. (1992). "An integrated approach for automated generation of two/three dimensional finite element grids using spatial occupancy enumeration and Delaunay triangulation". In: *International journal for numerical methods in engineering* 34.3, pp. 1035–1050.
- Rodenberg, OBPM, E Verbree, and S Zlatanova (2016). "Indoor A\* pathfinding through an octree representation of a point cloud". In: *ISPRS Annals of the Photogrammetry, Remote Sensing and Spatial Information Sciences* 4, p. 249.
- Rossignac, Jaroslaw R (1987). "Constraints in constructive solid geometry". In: *Proceedings of the 1986 workshop on Interactive 3D graphics*. ACM, pp. 93–110.
- Rüetschi, Urs-Jakob (2007). "Wayfinding in scene space: Modelling Transfers in public transport". PhD thesis. University of Zurich.
- Rüetschi, Urs-Jakob and Sabine Timpf (2004). "Modelling wayfinding in public transport: Network space and scene space". In: *International Conference on Spatial Cognition*. Springer, pp. 24–41.

- Sharker, Monir H, Hassan A Karimi, and Janice C Zgibor (2012). "Health-optimal routing in pedestrian navigation services". In: *Proceedings of the First ACM SIGSPATIAL International Workshop on Use of GIS in Public Health*. ACM, pp. 1–10.
- Shelke, SN et al. (2016). "Autonomous Campus Driver Assistant for Indoor and Outdoor Navigation". In: *Imperial Journal of Interdisciplinary Research* 2.7.
- Shiode, Narushige (2000). "3D urban models: Recent developments in the digital modelling of urban environments in three-dimensions". In: *GeoJournal* 52.3, pp. 263–269.
- Sileryte, Rusne, Ljiljana Cavic, and José Nuno Beirão (2017). "Automated generation of versatile data model for analyzing urban architectural void". In: *Computers, Environment and Urban Systems* 66, pp. 130–144.
- Slingsby, Aidan and Jonathan Raper (2008). "Navigable space in 3D city models for pedestrians". In: Springer, pp. 49–64.
- Spagnolo, Jennifer and Richard De Dear (2003). "A field study of thermal comfort in outdoor and semi-outdoor environments in subtropical Sydney Australia". In: *Building and environment* 38.5, pp. 721–738.
- Tang, SJ et al. (2015). "Automatic topology derivation from IFC building model for indoor intelligent navigation". In: *The International Archives of Photogrammetry, Remote Sensing and Spatial Information Sciences* 40.4, p. 7.
- Teo, Tee-Ann and Kuan-Hsun Cho (2016). "BIM-oriented indoor network model for indoor and outdoor combined route planning". In: *Advanced Engineering Informatics* 30.3, pp. 268–282.
- Thill, Jean-Claude, Thi Hong Diep Dao, and Yuhong Zhou (2011). "Traveling in the three-dimensional city: applications in route planning, accessibility assessment, location analysis and beyond". In: *Journal of Transport Geography* 19.3, pp. 405–421.
- Torres-Sospedra, Joaquín et al. (2015). "Enhancing integrated indoor/outdoor mobility in a smart campus". In: *International Journal of Geographical Information Science* 29.11, pp. 1955–1968.

- Trubka, Roman et al. (2016). "A web-based 3D visualisation and assessment system for urban precinct scenario modelling". In: *ISPRS Journal of Photogrammetry and Remote Sensing* 117, pp. 175–186.
- Turrin, Michela et al. (2009). "Digital design exploration of structural morphologies integrating adaptable modules". In: *A design process based on parametric modeling. in: Proceedings of Caad Futures 2009 International Conference. Joining languages, cultures and visions. Montreal, Canada. CUMINCAD*, pp. 17–19.
- Turrin, Michela et al. (2012). "Performative skins for passive climatic comfort: A parametric design process". In: *Automation in Construction* 22, pp. 36–50.
- Van Timmeren, A and M Turrin (2009). "Case study 'the Vela Roof–UNIPOL', Bologna: use of on-site climate and energy resources". In: *WIT Transactions on Ecology and the Environment* 121, pp. 333–342.
- Vanclouster, Ann and Philippe De Maeyer (2012). "Combining indoor and outdoor navigation: the current approach of route planners". In: *Advances in Location-Based Services*. Springer, pp. 283–303.
- Vanclouster, Ann, Nico Van de Weghe, and Philippe De Maeyer (2016). "Integrating indoor and outdoor spaces for pedestrian navigation guidance: A review". In: *Transactions in GIS* 20.4, pp. 491–525.
- Vanclouster, Ann et al. (2019). "Turn calculations for the indoor application of the fewest turns path algorithm". In: *International Journal of Geographical Information Science* 33.11, pp. 2284–2304.
- Verma, Vivek, Rakesh Kumar, and Stephen Hsu (2006). "3D building detection and modeling from aerial LIDAR data". In: *2006 IEEE Computer Society Conference on Computer Vision and Pattern Recognition (CVPR'06)*. Vol. 2. IEEE, pp. 2213–2220.
- Wallgrün, Jan Oliver (2004). "Autonomous construction of hierarchical voronoi-based route graph representations". In: *International Conference on Spatial Cognition*. Springer, pp. 413–433.
- Wang, Weiping et al. (2016). "Indoor-Outdoor Detection Using a Smart Phone Sensor". In: *Sensors* 16.10, p. 1563.

- Wang, Yijing et al. (2020). "Identification of physical and visual enclosure of landscape space units with the help of point clouds". In: *Spatial Cognition & Computation* 0.0, pp. 1–23.
- Wang, Z. and S Zlatanova (2019). "Safe Route Determination for First Responders in the Presence of Moving Obstacles". In: *IEEE Transactions on Intelligent Transportation Systems*, pp. 1–19.
- Wang, Zhiyong and Lei Niu (2018). "A Data Model for Using OpenStreetMap to Integrate Indoor and Outdoor Route Planning". In: *Sensors* 18.7, p. 2100.
- Winter, Stephan (2012). "Indoor spatial information". In: *International Journal of 3-D Information Modeling (IJ3DIM)* 1.1, pp. 25–42.
- Worboys, Michael (2011). "Modeling indoor space". In: *Proceedings of the 3rd ACM SIGSPATIAL International Workshop on Indoor Spatial Awareness*. ACM, pp. 1–6.
- Xie, Feifei et al. (2012). "Study on construction of 3D building based on UAV images". In: *The International Archives of the Photogrammetry, Remote Sensing and Spatial Information Sciences* 39, B1.
- Yan, J. et al. (2017). "CHALLENGES IN FLYING QUADROTOR UNMANNED AERIAL VEHICLE FOR 3D INDOOR RECONSTRUCTION". In: *ISPRS - International Archives of the Photogrammetry, Remote Sensing and Spatial Information Sciences XLII-2/W7*, pp. 423–430.
- Yan, Jinjin et al. (2019). "INTEGRATION OF 3D OBJECTS AND TERRAIN FOR 3D MODELLING SUPPORTING THE DIGITAL TWIN". In: *ISPRS Annals of the Photogrammetry, Remote Sensing and Spatial Information Sciences*, pp. 147–154.
- Yang, Liping and Michael Worboys (2011a). "A navigation ontology for outdoor-indoor space:(work-in-progress)". In: *Proceedings of the 3rd ACM SIGSPATIAL international workshop on indoor spatial awareness*. ACM, pp. 31–34.
- (2011b). "Similarities and differences between outdoor and indoor space from the perspective of navigation". In: COSIT 2011.
- (2015). "Generation of navigation graphs for indoor space". In: *International Journal of Geographical Information Science* 29.10, pp. 1737–1756.

- Yang, Wei, Nyuk Hien Wong, and Steve Kardinal Jusuf (2013). "Thermal comfort in outdoor urban spaces in Singapore". In: *Building and Environment* 59, pp. 426–435.
- Yuan, Wenjie and Markus Schneider (2010). "Supporting 3D route planning in indoor space based on the LEGO representation". In: *Proceedings of the 2nd ACM SIGSPATIAL International Workshop on Indoor Spatial Awareness*. ACM, pp. 16–23.
- Zar, Myat Thu and Myint Myint Sein (2016). "Finding shortest path and transit nodes in public transportation system". In: *Genetic and Evolutionary Computing*. Springer, pp. 339–348.
- Zeng, Wei and Richard L Church (2009). "Finding shortest paths on real road networks: the case for A". In: *International journal of geographical information science* 23.4, pp. 531–543.
- Zhang, Keqi, Jianhua Yan, and S-C Chen (2006). "Automatic construction of building footprints from airborne LIDAR data". In: *IEEE Transactions on Geoscience and Remote Sensing* 44.9, pp. 2523–2533.
- Zhou, Pengfei et al. (2012). "Iodetector: A generic service for indoor outdoor detection". In: *Proceedings of the 10th acm conference on embedded network sensor systems*. ACM, pp. 113–126.
- Zhu, Qing et al. (2016). "Indoor multi-dimensional location gml and its application for ubiquitous indoor location services". In: *ISPRS International Journal of Geo-Information* 5.12, p. 220.
- Zlatanova, Sisi, Liu Liu, and George Sithole (2013). "A conceptual framework of space subdivision for indoor navigation". In: *Proceedings of the Fifth ACM SIGSPATIAL International Workshop on Indoor Spatial Awareness*. ACM, pp. 37–41.
- Zlatanova, Sisi et al. (2014). "Space subdivision for indoor applications". In: *GIS Report No. 66*. Delft University of Technology, OTB Research Institute for the Built Environment.
- Zlatanova, Sisi et al. (2016a). "Indoor abstract spaces: linking IndoorGML and LADM". In: *Proceedings of the 5th international FIG workshop on 3D cadastres, 18-20 October 2016, Athens, Greece*. Delft: FIG, 2016, pp. 317–328.

- Zlatanova, Sisi et al. (2016b). "LADM and IndoorGML for support of Indoor Space Identification". In: *ISPRS Annals of the Photogrammetry, Remote Sensing and Spatial Information Sciences* 4, pp. 257–263.
- Zlatanova, Sisi et al. (2020). "Spaces in Spatial Science and Urban Applications—State of the Art Review". In: *ISPRS international journal of geo-information* 9.1, p. 58.
- Zverovich, Vadim et al. (2016). "Emergency response in complex buildings: Automated selection of safest and balanced routes". In: *Computer-Aided Civil and Infrastructure Engineering* 31.8, pp. 617–632.

# APPENDIX A

---

## CURRICULUM VITAE

---

Jinjin Yan was born in Lvliang, Shanxi, China, on 3rd February, 1990. He finished his master's degree (2013-2016) and bachelor's degree (2009-2013) in the Faculty of Information Engineering, China University of Geosciences in Wuhan. Afterwards he started his PhD project (seamless indoor and outdoor navigation) in the 3D GeoInformation group at the Department of Urbanism, Delft University of Technology (TU Delft), where his supervisors were Prof. Sisi Zlatanova and Prof. Jantien Stoter. His project was funded by the China Scholarship Council (CSC). Since June 2018, he transferred to Geospatial Research Innovation and Development (GRID) in Faculty of Built Environment, University of New South Wales (UNSW), where his supervisors became Prof. Sisi Zlatanova and Dr. Abdoulaye Diakité.

The research interests of Jinjin include 3D modelling (indoor, outdoor, semi-indoor, and semi-outdoor), space-based navigation, 3D analysis, 3D space subdivision, seamless indoor and outdoor navigation, BIM and GIS integration. Now he is continuing the

research of 3D space modelling, seamless navigation and analysis.